UNIVERSITY OF CALIFORNIA
SANTA CRUZ

PERFORMANCE ANALYSIS OF WIRELESS NETWORKS

A dissertation submitted in partial satisfaction of the
requirements for the degree of

DOCTOR OF PHILOSOPHY

in

ELECTRICAL ENGINEERING

by

Renato Mariz de Moraes

December 2005

The Dissertation of Renato Mariz de Moraes
is approved:

_____
Professor J.J. Garcia-Luna-Aceves, Chair

_____
Professor Hamid R. Sadjadpour, Co-Chair

_____
Professor John Vesecky

_____
Professor Patrick Mantey

_____
Lisa C. Sloan
Vice Provost and Dean of Graduate Studies

Report Documentation Page

Form Approved
OMB No. 0704-0188

1. REPORT DATE	2. REPORT TYPE	3. DATES COVERED
DEC 2005		**00-12-2005 to 00-12-2005**

4. TITLE AND SUBTITLE	5a. CONTRACT NUMBER
Performance Analysis of Wireless Networks	5b. GRANT NUMBER
	5c. PROGRAM ELEMENT NUMBER
6. AUTHOR(S)	5d. PROJECT NUMBER
	5e. TASK NUMBER
	5f. WORK UNIT NUMBER
7. PERFORMING ORGANIZATION NAME(S) AND ADDRESS(ES) **University of California at Santa Cruz,Department of Computer Engineering,Santa Cruz,CA,95064**	8. PERFORMING ORGANIZATION REPORT NUMBER
9. SPONSORING/MONITORING AGENCY NAME(S) AND ADDRESS(ES)	10. SPONSOR/MONITOR'S ACRONYM(S)
	11. SPONSOR/MONITOR'S REPORT NUMBER(S)

12. DISTRIBUTION/AVAILABILITY STATEMENT
Approved for public release; distribution unlimited

13. SUPPLEMENTARY NOTES
The original document contains color images.

14. ABSTRACT

15. SUBJECT TERMS

16. SECURITY CLASSIFICATION OF:			17. LIMITATION OF ABSTRACT	18. NUMBER OF PAGES	19a. NAME OF RESPONSIBLE PERSON
a. REPORT	b. ABSTRACT	c. THIS PAGE			
unclassified	**unclassified**	**unclassified**		**167**	

Contents

List of Figures

List of Tables

Abstract

Performance Analysis of Wireless Networks

by

Renato Mariz de Moraes

In this thesis, we investigate the performance of wireless ad hoc networks. First, we propose a multi-copy relaying scheme for packets in mobile ad hoc networks (MANETs), which reduces the delivery delay without changing the throughput order. We also present a method for computing the interference caused from other nodes.

Second, we study the trade-off among mobility, capacity, and delay for wireless ad hoc networks. By considering nodes that are subject to restrained movements, we found that mobility is an entity that can be exchanged with capacity and delay. Furthermore, the throughput-delay trade-off is investigated for nodes employing directional antennas and the results are compared with previous work.

Third, we propose a new communication scheme based on collaboration among nodes where the transmission (exchange) of packets is concurrently possible by employing a many-to-many communication framework. We present the principles of operation for such a technique, followed by two practical examples of implementation using FDMA/CDMA, and FDMA/MIMO systems. Shannon capacity, throughput and delay are computed and compared with related works.

To my beloved wife, Cynara, and my adorable son, Danilo.

Acknowledgements

First of all, I would like to thank my wife, Cynara, for her love, dedication and patience, whose support was fundamental for the success of my doctoral studies. For my adorable son, Danilo, who brought to my family the sense of completeness.

I want to express my deep gratitude to my advisors, Professor Hamid R. Sadjadpour and Professor Jose Joaquin Garcia-Luna-Aceves (or simply JJ), for their continuing support, guidance, friendship and mentorship. Their optimism and positive attitude always motivated me during my graduate studies.

I thank the members of my committee, Professors John Vesecky and Patrick Mantey. I also want to thank Carol Mullane, Tracie Tucker and Jodi Rieger for their help and advice.

My thankfulness to my fellow *cocos* (Marcelo, Dr. Marco, Hari, Ravindra, Rolando, Zhenjiang and Wenyi) in the *computer communication research group* (CCRG), and my lab mates (Christophe, Roger, Dyng, Xianren and Kyungmin) in the *UCSC broadband communication (UCBC) research group*. In addition, I want to thank Professor Katia Obraczka and her students Cintia and Ignacio (Nacho) in the *inter-networking research group* (i-NRG) for their friendship and help.

Of course, I also want to thank my parents, Agildo and Yara, and my brothers and sisters, Armando, Adilson, Jacyara and Ana, for their love, friendship and support.

Finally, I would like to thank the financial support from CAPES (*Coordenação de Aperfeiçoamento de Pessoal de Nível Superior*, Brazil). This work was also supported by the US Army Research Office under grants W911NF-04-1-0224 and W911NF-05-1-0246, by the Baskin Chair of Computer Engineering, and by UCOP CLC under grant SC-05-33.

Chapter 1

Introduction

There are many different scenarios for wireless networks. In a traditional cellular wireless network, the nodes (or users) communicate with each other through base stations (or access points). These stations provide access control in the network and play a central role, such as frequency management, power control, etc. The base stations are fixed and form a network infrastructure while the nodes are either mobile or stationary. We can find such networks in the common cellular phone systems, for example.

Wireless ad hoc networks require no base station and all the control and access tasks are distributed among nodes acting as peers. This makes them attractive in situations where there is no fixed infrastructure, such as battle fields or catastrophe-relief efforts. However, the lack of centralized control imposes significant challenges for ad hoc network designers and there are many open problems, questions like throughput-delay trade-offs, and capacity bounds need clarification. Also, the network modeling issue is a research challenge, and more complete and real models are necessary to help the network analysis. Therefore, the perfor-

mance analysis of wireless networks is a key issue in the field of network communications and requires careful modeling and attention. In addition, the demand for higher data rates in fixed or mobile wireless ad hoc networks offer challenging scalability issues. Consequently, there have been considerable efforts [26], [70], [55] [37], [72], [56], [5] to increase the performance of wireless ad hoc networks since Gupta and Kumar [28] showed that the capacity of a fixed wireless network decreases as the number of nodes increases when all the nodes share a common wireless channel. More precisely, they showed that the node throughput [1] of a fixed wireless network scales [2] as $\Theta\Big(1/\sqrt{n\log(n)}\Big)$ for n total users (or nodes) in the network, while the associated packet delivery delay grows as $\Theta\Big(\sqrt{n/\log(n)}\Big)$ [23]. This is a disappointing result, because both the capacity and delay degrade as the number of nodes in the network increases. On the other hand, Grossglauser and Tse [26], [27] demonstrated that the capacity and delay of wireless mobile ad hoc networks (MANETs) scale as $\Theta(1)$ and $\Theta(n)$ [23], respectively, by utilizing mobility and a multiuser diversity scheme [35] together with a two-phase relaying strategy. The importance of this result is that it proves that trade-offs can be made to substantially improve the capacity of wireless networks.

Accordingly, the performance analysis and enhancement of wireless ad hoc networks is the main contribution of this dissertation. The scope of our thesis is to provide analytical methods for computing the Shannon capacity, throughput and delay of wireless ad hoc networks. We revise the main models that are used for the analysis of such networks, and use the Information Theory tools for computation of capacity in network communication

[1] The precise definitions for node throughput and delivery delay will be given in the next section.

[2] Here we use the notation: (a) $b(n) = O(h(n))$ means there are positive constants c and m, such that $0 \leq b(n) \leq c\,h(n)\ \forall\ n > m$. (b) $b(n) = \Omega(h(n))$ means there are positive constants c_1, and m_1, such that $0 \leq c_1\,h(n) \leq b(n)\ \forall\ n > m_1$. (c) $b(n) = \Theta(h(n))$ means there are positive constants c_2, c_3, and m_2, such that $0 \leq c_2\,h(n) \leq b(n) \leq c_3\,h(n)\ \forall\ n > m_2$. Also, $\log(\cdot)$ stands for the natural logarithm.

systems. Moreover, we propose different schemes to improve the overall behavior of wireless networks. Multi-copy forwarding of packets is presented to reduce delay of MANETs without changing the $\Theta(1)$ capacity scalability order where an exact mathematical model of interference computation is obtained. Also, we provide a mathematical formula for the throughput as a function of the network parameters. In addition, the capacity-delay trade-off of ad hoc wireless networks is investigated, where we found that mobility can be exchanged with capacity and delay, in which the multi-copy forward scheme is also applied. Furthermore, we observe that by changing the physical layer properties of the ad hoc network (e.g., considering restrained mobility or directional antennas for the nodes), the capacity or delay behavior can be significantly improved. These findings leaded us to design a new cooperation scheme for mobile ad hoc networks where nodes are allowed to concurrently communicate with many other nodes without causing interference among each other. Upon collaboration, multi-copy forwarding of packets helps to reduce delay and high capacity is attained.

Fig. 1.1 illustrates the roadmap of our thesis. Here in the Introduction, we present a summary of our results along with the contributions of our research. After, the related work is presented which introduces the previous research associated to our studies. The multi-copy relaying (forwarding) scheme is analyzed next. The remaining chapters also include the multi-copy relaying strategy as indicated in the roadmap. After this, the mobility-capacity-delay trade-off is presented. The opportunistic cooperation scheme is the following topic introduced. Then, two implementations for opportunistic cooperation are considered using FDMA/CDMA and FDMA/MIMO respectively. Finally, the conclusion summarizes the main ideas presented in the thesis with the the possible future unfold that our work allows.

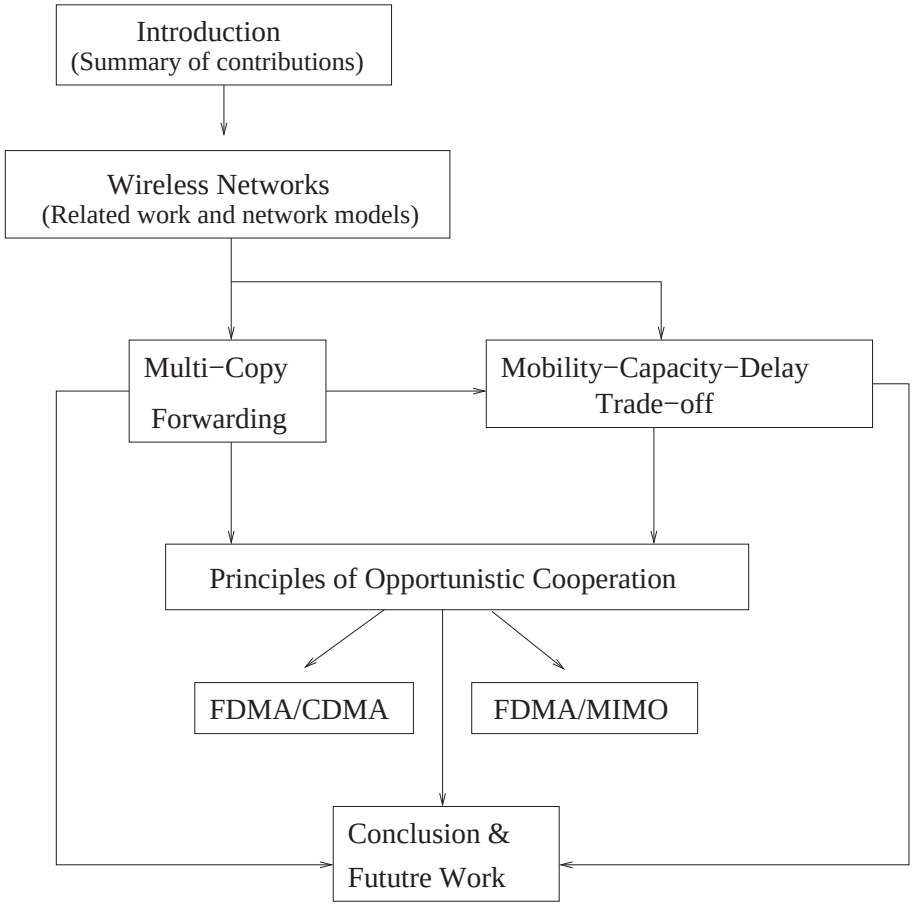

Figure 1.1: Roadmap of the thesis topics.

1.1 Basic Definitions

Because our work investigates capacity and delay of wireless networks, we present the following definitions that are used throughout the text.

Link's Shannon capacity is the maximum transmission rate (in units of bits/sec) achievable by a physical link of communication [15]. Therefore, this definition is related to the physical layer of a network employing links of communication. Accordingly, if a node i transmits to a node j through a frequency bandwidth (or sub-spectrum) W of units of Hertz

(Hz), the capacity of this link is given (in units of nats/sec) [3] by [15]

$$R_{ij} \quad = \quad W \log\left(1 + SNIR\right), \tag{1.1}$$

where SNIR stands for signal-to-noise and interference ratio measured at the receiver node j.

A *node throughput* (or per source-destination throughput, or simply throughput) of $\lambda(n)$ bits per second is feasible if every node can send information at an average rate of $\lambda(n)$ bits per second to its chosen destination [28], [23].

The *delivery delay* (or simply delay, or latency) of a packet in a network is the time it takes the packet to reach the destination after it leaves the source, where queuing delay at the source is not considered. The average packet delay for a network with n nodes is obtained by averaging over all packets, all source-destination pairs, and all random network configurations [23].

The *interference* at a node j, when node i transmits to node j through a frequency bandwidth W Hz, is defined as the power of the signals (in units of Watts) from all transmitting nodes in the network in the sub-spectrum W, except node i.

The term *half-duplex* means that a node cannot transmit and receive data simultaneously through the same frequency bandwidth.

We use the term *cell* to denote the set of nodes located inside a defined area of the network.

[3] $bits = \frac{nats}{\log(2)}$.

1.2 Research Contributions and Summary of Results

In Chapter 2, we summarize the works that are directly related to our research and introduce the network models used throughout the text.

Our first contribution, as described in Chapter 3, is a multiuser diversity strategy for packet relaying in MANETs that permits more than one-copy (multi-copies) of a packet being received by relay nodes [39], [41], [43], which attain an exponential reduction in delivery delay. We also demonstrate that the $\Theta(1)$ throughput is preserved by our multi-copy technique when n goes to infinity, where we provide a mathematical formula for computation of the throughput as a function of the network parameters. The reason behind achieving such asymptotic throughput is the fact that interference for communication among closest neighbors is bounded for different channel path losses even when n goes to infinity. In addition, we find that the average delay and variance scale like $\Theta(n)$ and $\Theta(n^2)$, respectively, for both one-copy and multi-copies techniques. We also show that a reduction of more than 69% in average delay is obtained for a finite n, while a maximum bounded delay value can be guaranteed. Surprisingly, because the basic principle of our idea is that each copy of a packet follows different random routes in the search for the destination, our result of delay reduction is related to those obtained by Azar et al [4] and Mitzenmacher [38] who found an exponential reduction of waiting time for the problem of loading balancing, by having a task the ability to chose among different servers. That is, we find an analogous qualitative behavior for a problem from a distinct research field. Another contribution of this work consists of an analytical model for interference calculation, which permits us to obtain the signal-to-interference ratio (SIR) measured by a receiver node at any point in the network. We show that the receiver SIR

tends to a constant if it communicates with close neighbors when the path loss parameter α is greater than two, regardless of the position of the node in the network. These results are consistent with all previous works, except that earlier works have only considered the receiver node located at the center of the network [36], [61], [30].

In Chapter 4, we quantitatively show that there is a trade off among mobility, capacity, and delay in ad hoc networks [40], [42], [44]. More specifically, we consider two schemes for node mobility in ad hoc networks. In the first scheme, the size of the cells varies with the total number of nodes n. The associated throughput and delay as functions of n are given by $\Theta\left(\sqrt{\frac{\log(n)}{n}}\right)$ and $\Theta(\sqrt{n})$, respectively. Compared to the static network model [28], this scheme attains a gain of $\Theta(\log(n))$ by using restrained mobility. In the second scheme, the size of a cell is not a function of n. For a given constant number of cells l, the size of each cell is $1/l$, and the corresponding throughput and delay are $\frac{1}{\sqrt{l}}\,\Theta(1)$ and $\Theta\left(\frac{n}{l}\right)$. These derivations are generalization of the results by Grossglauser and Tse [26] and represent a reduction of $1/\sqrt{l}$ in throughput, while the delivery delay is decreased. This result indicates that mobility, capacity, and delay should be treated as exchangeable entities. The multi-copy relaying strategy is added to this scheme and it is shown that the order of magnitude of the throughput is preserved, but lower delivery delay is attained. The last scheme analyzed presents the throughput-delay analysis for a fixed network in which nodes are endowed with directional antennas. We find that the throughput and delay for this scheme are $\Theta\left(\sqrt{\frac{\log(n)}{n}}\right)$ and $\Theta\left(\sqrt{\frac{n}{\log(n)}}\right)$, respectively. This result is important, because it represents a capacity gain of $\Theta(\log(n))$ compared to the results in Gupta and Kumar [28], and Yi et al [70]. However, this capacity gain is not associated with a decrease in delay, as one would expect due to the

capacity-delay trade-off, because we have changed the physical layer properties of the wireless network analyzed. The overall results suggest that using mobility or enhanced physical layer properties (for example, directional antennas) can improve capacity or delay. This result guided us to the topic covered in the Chapter 5 where we change the physical layer properties of the wireless ad hoc network such that the nodes can collaborate among each other in order to improve the performance of the network.

A novel collaboration-driven approach to the sharing of the available bandwidth in wireless ad hoc networks, which we call *opportunistic cooperation* is introduced in Chapter 5. Contrasting with traditional ad hoc network schemes where communication among nodes is one-to-one, one-to-many, or many-to-one, we propose a many-to-many framework in which nodes simultaneously communicate with each other overcoming interference. This scheme is based on the integration of multi-user detection and position-location information with frequency division in MANETs. By having concurrent transmission and reception of multiple packets among close neighbors, multi-copy forwarding of packets is employed such that the nodes collaborates among each other by looking for one another destinations. Also, we provide a simple channel access scheme for neighbor discovery and the relationship between the probability of collision and the parameters of the network.

In Chapter 6, we present an example of opportunistic cooperation with frequency division multiple access (FDMA), code division multiple access (CDMA) and successive interference cancelation (SIC) [45], [46]. In this scheme, transmissions are divided in frequency and codes according to nodal locations, and SIC is used at receivers to allow them to decode and use all transmissions from strongly interfering sources. Consequently, the interference

is divided into constructive interference (COI) and destructive interference (DEI). We show that, if each node is allowed to expand its bandwidth, both the link's Shannon capacity and the per source-destination throughput scale like $O(n^{\frac{\alpha}{2}})$ (upper-bound) and $\Omega[f(n)]$ (lower-bound), for a path loss parameter $\alpha > 2$ and $1 \leq f(n) < n^{\frac{\alpha}{2}}$. The upper-bound is the highest throughput reported in the literature for ad hoc networks. Opportunistic cooperation allows multi-copy relaying of the same packet, which reduces the packet delivery delay significantly compared to single-copy relaying without any penalty in capacity.

Another example of opportunistic cooperation using multiple-input multiple-output (MIMO) systems is presented in Chapter 7. We compute the capacity of MANETS when all the nodes in the network are endowed with M antennas. More specifically, we obtain the upper-bound ergodic capacity of each node. We show that this approach significantly reduces the destructive effects of interference, and we demonstrate that this capacity grows when the transmit power of the nodes in the network increases up to a point, where no gain in capacity is possible by increasing power. In addition, the capacity upper-bound does not decrease with the increase in the number of nodes in the network. The numerical results obtained are compared with Monte-Carlo simulations.

Chapter 2

Related Work and Network Models

This chapter summarizes the main results reported in the literature on the field of capacity analysis for ad hoc networks that are related to our studies. The network models and fundamental assumptions employed throughout the thesis are also described here.

Basically, the wireless ad hoc networks can be classified in either static, or mobile, or even hybrid, according to the properties of the nodes. In general, the mobile networks present more complexity than the static ones, because with mobility the arrangement of network is constantly changing, which imposes control challenges for communication. In either case, the capacity and delay behavior can result quite different as it is discussed in the next sections and chapters.

2.1 Static Wireless Networks

The first kind of wireless network considered in our study is the fixed (or static). The nodes are fixed and can be deployed arbitrarily, or randomly, or regularly spaced (like in

a grid) in the network.

2.1.1 The Fundamental Scalability Results

In 2000, Gupta and Kumar [28] analyzed the capacity of static wireless networks when the number of total nodes in the network scale to infinite. The network model consisted of a sphere of unit area containing n total fixed nodes with identical properties. Nodes were placed either arbitrarily or randomly in the area. Communication among nodes was obtained through a single wireless channel shared among all nodes, and therefore subject to interference. Packets were sent from source to destination in a multihop fashion following the path close to the straight line that links the source to its destination. Therefore, each node could function as source, relay and destination of packets. They showed that there exists a Voronoi tessellation $\mathcal{V}_n$ on the unit sphere surface satisfying the following properties:

- Every Voronoi cell V contains a disk of area $100\ \log(n)/n$ and corresponding radius $\epsilon(n) = c_4\sqrt{\log(n)/n}$, for some positive constant c_4.
- Every Voronoi cell is contained within a circle of radius $2\epsilon(n)$.

Each Voronoi cell $V \in \mathcal{V}_n$ is simply a cell of the network, and the cells do not have a regular shape because the network is arbitrary or random. With this tessellation, each cell contains at least one node with high probability (whp) [1] which meets the connectivity requirement [28]. Furthermore, by choosing the transmission range equal to $8\epsilon(n)$ for each node, it allows direct communication within a cell and between adjacent cells. Accordingly, two cells are interfering neighbors if there is a point in one cell that is within a distance $(2+\Delta)8\epsilon(n)$ of some point

[1] With high probability means with probability $\geq 1 - \frac{c_5}{n}$, for some positive constant c_5 [47].

in the other cell, in which $\Delta > 0$ is a given constant modeling condition where a guard zone is required to prevent a neighboring node from transmitting on the same channel at the same time [28]. They described two models for successful communication among nodes. Let X_i denote the location of a node i in the network. The *Protocol Model* establishes that node i transmits successfully to node j if the following condition is satisfied [28]

$$|X_k - X_j| \geq (1 + \Delta)|X_i - X_j|, \tag{2.1}$$

so that transmit node X_k will not impede X_i and X_j communication. In the *Physical Model* node i transmits successfully to node j if the signal to noise and interference ratio ($SNIR$) at node j satisfies [28]

$$SNIR = \frac{\dfrac{P_i}{|X_i - X_j|^\alpha}}{N_0 + \displaystyle\sum_{k \neq i} \dfrac{P_k}{|X_k - X_j|^\alpha}} \geq \beta, \tag{2.2}$$

where P_i is the transmit power of node i, α is the path loss parameter, N_0 is the noise power, and β is the minimum value of $SNIR$ necessary for successful reception. It is known that if $\alpha > 2$ and each node transmits at same power, then the *Protocol* and *Physical* models are equivalent [23].

Gupta and Kumar showed that, by using the previous two communication models, the node throughput of fixed wireless networks scale as $\Theta\left(1/\sqrt{n}\right)$ for the arbitrary placement of nodes, and as $\Theta\left(1/\sqrt{n\log(n)}\right)$ for the random placement of nodes. In either case, the capacity of each node decreases as the number of total nodes n in the network increases. This poor performance is mainly due to interference among nodes.

2.1.2 Wireless Backbone Approach

Franceschetti et al [22] proved that a node throughput of $\Theta(1/\sqrt{n})$ can be achieved in a static random network, if a wireless backbone is rich enough in crossing paths such that it transports all traffic of the static network, although it does not cover all the nodes.

2.1.3 The Minimum Power Routing

Shepard [61] was the first to note that if the minimum power route for packets is considered along with an efficient distributed channel access technique, then a scalable static wireless network is feasible. Later, Negi and Rajeswaran [51] provided an ultra wide band multiple access technique, using the minimum power routing idea, and they proved that a wireless network can indeed have a capacity that grows with the total number of nodes. They showed that appropriate change in the physical layer assumptions can improve the throughput of wireless ad hoc and sensor networks significantly.

2.1.4 Directional Antennas

Channel access techniques for directional antennas has been proposed for ad hoc wireless networks [6], [14]. Yi et al [70] investigated the capacity scalability for an extended model from Gupta and Kumar [28] where the nodes are endowed with directional antennas. They found that a constant gain in capacity is possible when compared to [28]. However, Peraki and Servetto [55] employed a network flow analysis to study the capacity of wireless networks implementing directional antennas and they showed that it is indeed possible to obtain gains of $\Theta(\log(n))$ compared to Gupta and Kumar's results [28]. This result is in

agreement to our findings presented in Chapter 4.

2.2 Mobile Wireless Networks

The second type of wireless network is formed by mobile nodes. The movement of the nodes are function of their velocity and direction. There are many models for movements. In our work, we are going to consider the *uniform mobility model* [5] and the *random waypoint model* [12], [9].

In the *uniform mobility model* [5], the nodes are initially uniformly distributed, and move at a constant speed v and the directions of motion are independent and identically distributed (iid) with uniform distribution in the range $[0, 2\pi)$. As time passes, each node chooses a direction uniformly from $[0, 2\pi)$ and moves in that direction at speed v for a distance z, where z is an exponential random variable with mean μ. After reaching z the process repeats. This model satisfies the following properties [5]:

- At any time t, the position of the nodes are independent of each other.
- The steady-state distribution of the mobile nodes is uniform.
- Conditional on the position of a node, the direction of the node movement is uniformly distributed in $[0, 2\pi)$.

The uniform mobility is the theoretical model implemented in our analysis for MANETs.

In the *random waypoint mobility model* [12], [9], the nodes are initially randomly distributed in the network area. A node begins its movement by remaining in a certain position for some fixed time, called *pause time*, distributed according to some random variable, and

when it expires the node chooses a random destination point in the network area and begins to move toward that point with a constant speed uniformly distributed over $[v_{min}, v_{max}]$, where v_{min} and v_{max} stands for minimum and maximum velocity respectively. Upon arrival at the destination, the node pauses again according to the pause time random variable and the process repeats. Nodes move independently of each other. This is the model implemented in our simulations for MANETs. This idea can also be used for ad hoc networks.

2.2.1 Multiuser Diversity

Knopp and Humblet [35] established a new communication scheme for wireless systems called *multiuser diversity* which was shown to maximize the capacity of a single-cell multiuser communication. Their basic idea is that the base station reserves the communication link to the user which presents the best channel. Because in a mobile wireless network the communication channel to each user is governed by independent fading, multiuser diversity provides a form of randomization of the channel access which one can take advantage of.

2.2.2 Mobility Increases the Capacity of Wireless Networks

In 2001, Grossglauser and Tse [26], [27] presented a two-phase packet relaying technique for mobile ad hoc networks that attains $\Theta(1)$ per source-destination throughput when n tends to infinity.

The scheme is based on *multiuser diversity* [35] where each source node transmits a packet to the nearest neighbor; that is, using the simple path propagation model, the source reserves its channel for a receiver that can best exploit it. This neighbor node functions as

a relay and delivers the packet to the destination when this destination becomes the closest neighbor of the relay.

The network model consists of a normalized unit area disk containing n mobile nodes. They considered a time-slotted operation to simplify the analysis. The position of node i at time t is indicated by $X_i(t)$. The process $\{X_i(\cdot)\}$ is stationary and ergodic with stationary uniform distribution on the disk, which yields node trajectories that are iid.

At each time step, a scheduler decides which nodes are senders, relays, or destinations, in such a manner that the source-destination association does not change with time. Each node can be a source for one session and a destination for another session. Packets are assumed to have header information for scheduling and identification purposes.

Suppose that a source i has data for a certain destination $d(i)$ at time t. Because nodes i and $d(i)$ can have direct communication only $1/n$ of the time on the average, a relay strategy is proposed to deliver data to $d(i)$ via relay nodes. They assume that each packet can be relayed at most once.

According to the *Physical Model*, at time t, node j is capable of receiving at a given rate of $W\ bits/sec$ from i if

$$SNIR = \frac{P_i(t)g_{ij}(t)}{N_0 + \frac{1}{M}\underbrace{\sum_{k\neq i} P_k(t)g_{kj}(t)}_{I}} = \frac{P_i(t)g_{ij}(t)}{N_0 + \frac{1}{M}I} \geq \beta, \tag{2.3}$$

where $P_i(t)$ is the transmitting power of node i, $g_{ij}(t)$ is the channel path gain from node i to j, β is the signal to noise and interference ratio level necessary for reliable communication, N_0 is the noise power, M is the processing gain of the system, and I is the total interference at node

j. The channel path gain is assumed to be a function of the distance only, so that [26], [28]

$$g_{ij}(t) = \frac{1}{|X_i(t) - X_j(t)|^\alpha} = \frac{1}{r_{ij}^\alpha(t)}, \tag{2.4}$$

where α is the path loss parameter, and $r_{ij}(t)$ is the distance between i and j.

Therefore, according to the above communication scheme, each node sends data to its destination in a two phase process (see Fig. 2.1). Packet transmissions from sources to relays (or destinations) occur during *Phase 1*, and packet transmissions from relays (or sources) to destinations happen during *Phase 2*. Both phases occur concurrently, but *Phase 2* has absolute priority in all scheduled sender-receiver pairs.

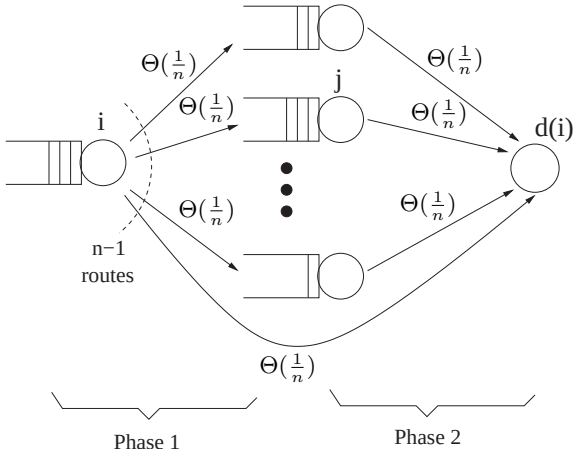

Figure 2.1: Two-phase process for packet delivery.

Because node trajectories are iid and the system is in steady-state, the long-term throughput between any two nodes equals the probability that these two nodes are selected by the scheduler as a feasible sender-receiver pair. According to [26] this probability is $\Theta(\frac{1}{n})$. Also, there is one direct route and $n-2$ two-hop routes passing through one relay node for a randomly chosen source-destination pair. Thus, the service rate is $\lambda_j = \Theta(\frac{1}{n})$ through each actual relay node, as well as the direct route. Accordingly, the total throughput per source-

destination pair λ_T is

$$\lambda_T = \sum_{j=1, j\neq i}^{n} \lambda_j = \sum_{j=1, j\neq i}^{n} \Theta\left(\frac{1}{n}\right) = \Theta\left(\frac{n-1}{n}\right) \overset{n\to\infty}{\longrightarrow} \Theta(1). \tag{2.5}$$

Thus, this scheme attains $\Theta(1)$ per source-destination throughput when n tends to infinity. However, the delay experienced by packets under this strategy was shown to be large and it can be even infinite for a fixed number of nodes (n) in the system, which has prompted more recent work presenting analysis of capacity and delay tradeoffs [56], [5], [50], [23], [66]. Given that the number of nodes in real MANETs is finite, delay is an important performance issue.

2.3 Random Loading Balancing

The works by Azar et al [4] and Mitzenmacher [38] develop a powerful idea in the field of computer performance. They showed that an small amount of choice can lead to drastically different results in random load balancing. More specifically, if n balls are randomly placed into n bins, the size of the maximum bin is given approximately by $\frac{\log(n)}{\log(\log(n))}$ whp. However, if each ball is placed sequentially into the least full of K bins chosen uniformly and independently at random, the maximum load is then only $\frac{\log(\log(n))}{\log(K)} + O(1)$ whp, which represents an exponential reduction in maximum load. This principle seems to be related to the delay reduction we found in Chapter 3 by using multiple copies of same packet following distinct random routes to the destination.

2.4 Trade-off Analysis

In wireless ad hoc networks, the capacity-delay trade-off is a key issue. The assumptions for attaining a given capacity is always associated with the delivery delay of packets. Perevalov and Blum [56] presented an analysis for delay limited capacity of ad hoc networks in which they computed the ensemble average of the probability that two nodes come close to each other. We use their approach to obtain delay for our multi-copy forwarding scheme proposed in this thesis. Neely and Modiano [50] provided an interesting study on capacity and delay trade-off for mobile ad hoc networks using the theory of queues. By assuming that the network has a cell partitioned structure, that the nodes move according to an iid model, and using a modified two-hop relaying strategy, they found that there the throughput and delay must satisfy $delay/rate \geq O(n)$. El Gamal et al [23] provided a detailed trade-off analysis for throughput and delay in wireless networks, where they recover the results by Gupta and Kumar [28], as well as Grossglauser and Tse [26], using simpler techniques. However, because a node is not always allowed to move around the entire network for some practical applications of ad hoc networks, we present a study on mobility-capacity-delay trade-off in Chapter 4, and we comment on the impact of the results for the scalability of such networks.

2.5 Hybrid Networks

Another possible scenario arises when there are nodes and base stations in a wireless network [17]. Liu et al [37] study the capacity scalability for these types of networks. They considered that some static nodes are represented by base stations which are interconnected

by a broadband wired infrastructure. These base stations can forward the messages from the user nodes across the network. They showed that the number of base stations should grows faster than $\sqrt{n}$, where n is the number of mobile nodes, in order to obtain a capacity that scale linearly with the number of base stations. Otherwise, the benefit of adding base stations on capacity is insignificant. In another hybrid scenario, Agarwal and Kumar [2] emphasized that by choosing appropriate transmission power levels and communicating with the closest node or base station in a multihop fashion can provide good capacity performance for static ad hoc wireless network.

2.6 MIMO Systems

The capacity of MIMO systems has received considerable attention [21], [62], [25]; however, all these studies concentrate on the concept of one-to-one communication among nodes. Even the work by Jovičić et al [34] studies the capacity of wireless ad hoc networks by assuming that the entire network is a single MIMO system in which some nodes are part of the transmitter and the remaining nodes in the network are part of the receiver, and where all the nodes have only one antenna. A random line is used to cut the network into two parts for senders and receivers. While this work [34] was the first attempt to compute the capacity of networks based on MIMO systems, the results are rather optimistic by assuming all the receiving nodes in the network are capable of cooperating with each other to decode the data. Furthermore, Chen and Gans [13] showed that the node capacity of a MIMO ad hoc network goes to zero as n increases. In Chapter 7, we will show different result for such networks using a distinct model and the opportunistic cooperation scheme introduced in Chapter 5.

Chapter 3

Throughput-Delay Analysis of MANETs with Multi-Copy Forwarding

This chapter introduces and analyzes an improved two-phase packet forwarding strategy for MANETs [39], [41], [43] that attains the $\Theta(1)$ capacity of the basic scheme by Grossglauser and Tse [26] (see Section 2.2), but provides better delay behavior than the single-copy technique. Our main objective is to decrease the delay incurred by the packet to reach its destination in steady-state[1] while maintaining the capacity of the network at the same order of magnitude as that attained in [26]. Our basic idea is to give a copy of the packet to multiple one-time relay nodes that are within the transmission range of the sender. By doing so, the

[1] That is, after averaging over all possible starting random network topologies so that transient behaviors are removed.

time within which a copy of the packet reaches its destination can be decreased. The first one-time relay node that is close enough to the destination delivers the packet.

We find an enormous reduction in delay by having a packet more than one possible random route to the destination. This result is analogous to the problem in which Azar et al [4] and Mitzenmacher [38] showed that a small amount of choices can lead to drastically different result in randomized load balancing. More specifically, having just two random choices yields an exponential reduction in maximum loading over having one choice, while each additional choice beyond two decreases the maximum load by just a constant factor. In our case, by multi-copy forwarding a packet and having only the fastest copy being delivered, it is analogous to having the packet taking one of the shortest random path to the destination from multiple random routes (or choices).

An interesting feature of the multi-copy relaying approach is that the additional relaying nodes carrying that same copy of the packet can be used as backups to protect against node failures which improves the reliability of the network [49].

Furthermore, we provide an analytical method to compute the exact effect of interference in ad hoc networks.

The remaining of the chapter is organized as follows. Section 3.1 summarizes the basic assumptions used to analyze the capacity of MANETs [26]. Section 3.2 explains our multi-copy packet forwarding strategy. Section 3.3 presents the average number of feasible receiving nodes around a sender. Section 3.4 presents the interference analysis. Section 3.5 shows that the new relaying scheme attains the same capacity order of magnitude as the original two-phase scheme proposed by Grossglauser and Tse [26]. Section 3.6 shows the delay

reduction resulting from our forwarding strategy and presents theoretical and simulation results. Section 3.7 concludes the chapter summarizing our main ideas.

3.1 Basic Assumptions

The network model we assume is the one introduced by Grossglauser and Tse [26] (see also Section 2.2), and consists of a normalized unit area disk containing n mobile nodes. We consider a time-slotted operation to simplify the analysis, and we assume that communication occurs only among those nodes that are close enough, so that interference caused by other nodes is low, allowing reliable communication. The position of node i at time t is indicated by $X_i(t)$. The nodes are assumed to be uniformly distributed on the disk at the beginning, and there is no preferential direction of movement.

Nodes are assumed to move according to the *uniform mobility model* [5], in which the steady-state distribution of the mobile nodes in the network is uniform (see Section 2.2).

At each time step, a scheduler decides which nodes are senders, relays, or destinations, in such a manner that the source-destination association does not change with time. Each node can be a source for one session and a destination for another session. Packets are assumed to have header information for scheduling and identification purposes, and a time-to-live threshold field as well.

Suppose that a source i has data for a certain destination $d(i)$ at time t. Because nodes i and $d(i)$ can have direct communication only $1/n$ of the time on the average, a relay strategy is required to deliver data to $d(i)$ via relay nodes. We assume that each packet can be relayed at most once.

Using the physical model as described in Eq. (2.3) and given that the interference coming from other nodes generally is much greater than the noise power for narrowband communication, the denominator in Eq. (2.3) is dominated by the interference factor, i.e., $\sum_{k \neq i} P_k(t) g_{kj}(t) = I >> N_0$. In addition, we assume that no processing gain is used, i.e., $M = 1$, and that $P_i = P \ \forall i$. Then, combining Eqs. (2.3) and (2.4) yields the Signal-to-Interference Ratio (SIR)

$$SIR = \frac{\frac{P}{r_{ij}^{\alpha}}}{I} = \frac{P}{r_{ij}^{\alpha} \cdot I} \geq \beta \,. \tag{3.1}$$

We will determine an equation relating the total interference measured by a receiver communicating with a neighbor node as a function of the number of total nodes n in the network. More precisely, we want to obtain an expression for Eq. (3.1) as a function of n, calculate the asymptotic value of the SIR as n goes to infinity, and verify that communication among close neighbors is still feasible.

3.2 Multi-Copy One-time Relaying

As discussed in Section 2.2, Grossglauser and Tse [26] consider a single-copy forwarding scheme consisting of two phases. Packet transmissions from sources to relays (or destinations) occur during *Phase 1*, and packet transmissions from relays (or sources) to destinations happen during *Phase 2*. Both phases occur concurrently, but *Phase 2* has absolute priority in all scheduled sender-receiver pairs. We extend this scheme to allow multiple copies of the same packet during *Phase 1*, as described below.

3.2.1 Packet Forwarding Scheme

We allow more than one relay node to receive a copy of the same packet during *Phase 1*. Thus, the chance that a copy of this packet reaches its destination in a shorter time is increased, compared to using only one relay node as in [26]. Also, if for some reason a relaying node fails to deliver the packet when it is within the transmission range of the destination, the packet can be delivered when another relaying node carrying a copy of the same packet approaches the destination.

In Fig. 3.1(a), three copies of the same packet are received by adjacent relay nodes j, p, and k during *Phase 1*. All such relays are located within a distance r_o from sender i. At a future time t, in *Phase 2*, node j reaches the destination before the other relays and delivers the packet. Note that relay node j need not be the closest node to the source during *Phase 1*.

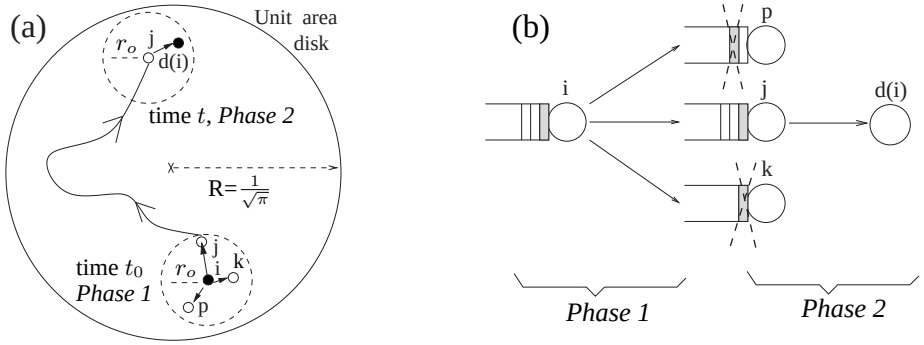

Figure 3.1: (a) Three copies of the same packet are transmitted to different receivers at *Phase 1*. *Node* j is the first to find the destination, and delivers the packet at *Phase 2*. The movement of all the remaining nodes in the disk is not shown for simplicity. (b) Time-to-live threshold timeout for three copies transmission (from (a)).

3.2.2 Enforcing One-Copy Delivery

There are several ways in which the delivery of more than one copy of the same packet to a destination can be prevented. For example, each packet can be assigned a sequence number (SN) and time-to-live (TTL) threshold. Before a packet is delivered to its destination, a relay-destination handshake can be established to verify that the destination has not received a copy of the same packet. All relays delete the packet copies from their queues after the TTL expires for the packet, and the destination of the packet remembers the SN of a packet it receives for a period of time that is much larger than the TTL of the packet to ensure that any handshake for the packet is correct in practice.

Fig. 3.1(b) depicts the situation in which node j finds the destination node $d(i)$ first and delivers the packet before the TTL expires. The other copies are dropped from the queues at p and k, and only one node out of the three potential relays actually delivers the packet to the destination.

To ascertain if this multi-copy relaying strategy provides any advantages over the single-copy strategy proposed by Grossglauser and Tse [26], we need to answer two questions.

- How many nodes around a sender can successfully receive copies of the same packet?
- What is the delay d_K (for K copies) for the new packet transmission scheme compared to the delay d in the single-copy strategy [26] when the network is in steady-state?

Because we address the network capacity for any embodiment of the multi-copy relaying strategy, we assume in the rest of this paper that the overhead of the relay-destination handshake is negligible.

3.3 Feasible Number of Receivers in *Phase 1* and Cell Definition

A fraction of the total number of nodes n in the network, n_S, is chosen randomly by the scheduler as senders, while the remaining nodes, n_R, operate as possible receiving nodes [26]. A sender density parameter θ is defined as $n_S = \theta n$, where $\theta \in$ (0,1), and $n_R = (1-\theta)n$. In the proposed multi-copy relay strategy each sender transmits to all the nodes in the feasible transmission range, these additional copies follow different random routes and find the destination earlier compared to the single-copy strategy of Grossglauser and Tse [26].

If the density of nodes in the disk is

$$\rho = \frac{n}{total \;\; area} = \frac{n}{1} = n, \tag{3.2}$$

then, for a uniform distribution of nodes, the radius for one sender node is given by

$$1 = \theta\rho\pi r_o^2 = \theta n\pi r_o^2 \Longrightarrow r_o = \frac{1}{\sqrt{\theta n\pi}}. \tag{3.3}$$

Thus, the radius r_o defines a cell (radius range) around a sender.

Assuming a uniform node distribution, the average number of receiving nodes within r_o, called $\overline{K}$, is

$$\overline{K} = n_R\pi r_o^2 = \frac{1}{\theta} - 1, \tag{3.4}$$

which is a function of θ and does not depend on n. The main idea behind multi-copy scheme stems from the fact that θ can be smaller than 0.5 and consequently, for any sender node, on average there is more than one relay available for many senders. Grossglauser and Tse [26] showed that the maximum capacity is obtained for $\theta < 0.5$ (for $\alpha \leq 4$), so that we can have $\overline{K} > 1$ and be very close to the maximum capacity, as shown later. Note that Eq. (3.4)

provides a benchmark to choose a value for $\overline{K}$ based on θ. However, the actual number of receiving nodes, called K, for each sender node varies.

Referring to the recent work by El Gamal et al [23], each cell in our strategy has area $a(n) = \frac{1}{n_S} = \frac{1}{\theta n}$. By applying random occupancy theory [47, Chapter 3], the fraction of cells containing L senders and K receivers is obtained by

$$\begin{aligned}
&\mathbb{P}\{\text{senders = } L,\ \text{receivers = } K\} \\
&= \mathbb{P}\{\text{senders = } L\}\mathbb{P}\{\text{receivers = } K \mid \text{senders = } L\} \\
&= \begin{pmatrix} n \\ L \end{pmatrix} \left(\frac{1}{n_S}\right)^L \left(1 - \frac{1}{n_S}\right)^{n-L} \begin{pmatrix} n-L \\ k \end{pmatrix} \left(\frac{1}{n_S}\right)^K \left(1 - \frac{1}{n_S}\right)^{n-L-K} \\
&= \begin{pmatrix} n \\ L \end{pmatrix} \left(\frac{1}{\theta\, n}\right)^L \left(1 - \frac{1}{\theta\, n}\right)^{n-L} \begin{pmatrix} n-L \\ K \end{pmatrix} \left(\frac{1}{\theta\, n}\right)^K \left(1 - \frac{1}{\theta\, n}\right)^{n-L-K}. \qquad (3.5)
\end{aligned}$$

Given that we are interested in very large values for n, and using the limit $\left(1 - \frac{1}{x}\right)^x \longrightarrow e^{-1}$ as $x \to \infty$, we have the following result for $n >> L, K$

$$\begin{aligned}
\mathbb{P}\{\text{senders = } L,\ \text{receivers = } K\} &\approx \frac{n^L}{L!}\left(\frac{1}{\theta n}\right)^L \left[\left(1 - \frac{1}{\theta n}\right)^{\theta n}\right]^{1/(\theta)} \frac{n^K}{K!}\left(\frac{1}{\theta n}\right)^K \left[\left(1 - \frac{1}{\theta n}\right)^{\theta n}\right]^{1/(\theta)} \\
&\approx \frac{1}{L!}\left(\frac{1}{\theta}\right)^L e^{-1/\theta}\, \frac{1}{K!}\left(\frac{1}{\theta}\right)^K e^{-1/\theta}. \qquad (3.6)
\end{aligned}$$

For example, for $L = 1$, $K \geq 2$, and $\theta = \frac{1}{3}$, we have that the fraction of the cells containing one sender and at least two receivers equals $\frac{1}{\theta} e^{-1/\theta}(1 - e^{-1/\theta} - \frac{1}{\theta} e^{-1/\theta}) \approx 0.12$. Therefore, for $K \geq 2$, approximately 12% of the cells can forward packets using the multi-copy scheme in *Phase 1*.

In addition, for $\theta = \frac{1}{3}$, we have that the fraction of the cells have one sender and one receiver equals $(\frac{1}{\theta} e^{-1/\theta})^2 \approx 0.02$. In this case, the scheduler does not select these cells

for packet transmission, because the delivery delay incurred can be significantly high, as we show subsequently.

The maximum number of nodes in any cell is $\Theta\left[\frac{\log(n)}{\log(\log(n^\theta))}\right]$ whp (see Lemma 1). Thus, whp, $K \leq \frac{c_6 \log(n)}{\log(\log(n^\theta))} << n$ for some positive constant c_6.

The feasibility that all of those K nodes successfully receive the same packet in the presence of interference is the subject of the next section.

3.4 Interference Analysis

In the previous section, we obtained the fraction of cells that has one sender surrounded by $K \geq 2$ receiving nodes within r_o, assuming a uniform distribution of nodes. Suppose that one of the K receiving nodes is at the maximum neighborhood distance r_o in any of these cells. We want to know how the SIR measured by this receiver behaves as the number of total nodes in the network (and therefore the number of total interferers) goes to infinity. We are interested in determining whether feasible communication between the sender and the farthest neighbor[2] (with distance r_o) is still possible, even if the number of interferers grows.

For a packet to be successfully received, Eq. (3.1) must be satisfied. Hence, consider a receiver at any location in the network during a given time t. Its distance from the center r' is shown in Fig. 3.2, where $0 \leq r' \leq \frac{1}{\sqrt{\pi}} - r_o$. Let us assume that the sender is at distance r_o from this receiver and transmitting at constant power P, so that the power measured by the

[2]This represents the worst case scenario, because the other $K-1$ neighbors are located either closer or at the same distance r_o to the sender, so they measure either a stronger or the same SIR level.

receiver P_R is given by

$$P_R = \frac{P}{r_o^{\alpha}}. \tag{3.7}$$

To obtain the interference at the receiver caused by all transmitting nodes in the disk, let us consider a differential element area $rdrd\gamma$ that is distant r units from the receiver (see Fig. 3.2). Because the nodes are uniformly distributed in the disk, the transmitting nodes inside this differential element of area generate the following amount of interference[3] at the receiver

$$dI = \frac{P}{r^{\alpha}}\,\theta\,\rho\,r\,dr\,d\gamma = \frac{P}{r^{\alpha-1}}\,\theta\,n\,dr\,d\gamma. \tag{3.8}$$

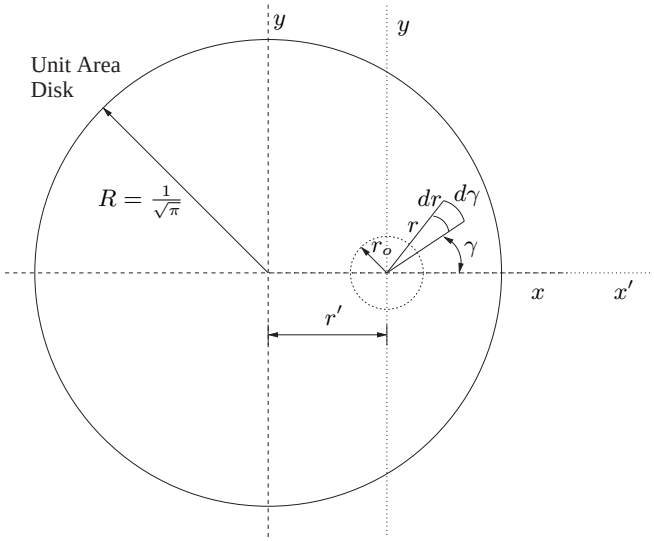

Figure 3.2: Snapshot of the unit area disk at a given time t. At this time, the receiver node being analyzed is located at r' from the center while the sender is at distance r_o from the receiver node.

[3]Because the nodes are considered to be uniformly distributed in the disk and n grows to infinity, we approximate the sum in the denominator of Eq. (2.3) by an integral.

3.4.1 The case $\alpha > 2$

For some propagation models [58, p. 139, Table 4.2], the path loss parameter is modeled to be always greater than two, i.e., $\alpha > 2$. The total interference at the receiver located at distance r' from the center with total of n nodes in the network is obtained by integrating Eq. (3.8) over all the disk area. Hence,

$$\begin{aligned} I_{r'}(n) &= \int_{disk} dI \\ &= \int_0^{2\pi}\int_{r_o}^{r_m(r',\gamma)} \frac{P}{r^{\alpha-1}}\theta n dr d\gamma \\ &= P\theta n \int_0^{2\pi} \frac{r^{2-\alpha}}{2-\alpha}\Big|_{r_o}^{r_m(r',\gamma)} d\gamma \\ &= \frac{P\theta n}{\alpha-2}\int_0^{2\pi}\left\{\frac{1}{r_o^{\alpha-2}} - \frac{1}{[r_m(r',\gamma)]^{\alpha-2}}\right\} d\gamma. \end{aligned} \tag{3.9}$$

r_m is the maximum radius that r can have and is a function of the location r' and the angle γ. To find this function, we can use the boundary disk curve (or circumference) equation expressed as a function of the x-axis and y-axis shown in Fig. 3.2, i.e.,

$$x^2 + y^2 = \left(\tfrac{1}{\sqrt{\pi}}\right)^2. \tag{3.10}$$

Define $x = x' + r'$, $x' = r_m\cos\gamma$, and $y = r_m \sin\gamma$, then Eq. (3.10) becomes

$$\begin{aligned} (r_m\cos\gamma + r')^2 + (r_m\sin\gamma)^2 &= \left(\tfrac{1}{\sqrt{\pi}}\right)^2 \\ \Longrightarrow r_m(r',\gamma) &= \sqrt{\tfrac{1}{\pi} - (r'\sin\gamma)^2} - r'\cos\gamma. \end{aligned} \tag{3.11}$$

Substituting this result in Eq. (3.9) we obtain

$$I_{r'}(n) = \frac{2\,P\,\theta\,n}{\alpha-2}\left[\frac{\pi}{r_o^{\alpha-2}} - f_\alpha(r')\right], \tag{3.12}$$

where

$$f_\alpha(r') = \int_0^\pi \frac{d\gamma}{\left[\sqrt{\frac{1}{\pi} - (r'\sin\gamma)^2} - r'\cos\gamma\right]^{\alpha-2}} \tag{3.13}$$

is a constant for a given position r'. For the case in which $\alpha = 4$, Eq. (3.13) reduces to

$$f_4(r') = \frac{\pi^2}{1 - 2\pi r'^2 + \pi^2 r'^4}\,. \tag{3.14}$$

We can obtain the SIR using Eqs. (3.1), (3.3), (3.7), and (3.12) to arrive at

$$SIR_{r'}(n) = \frac{P_R}{I} = \frac{\alpha-2}{2} \cdot \frac{1}{\left[1 - \frac{1}{\pi^{\frac{\alpha}{2}}(\theta\, n)^{\frac{\alpha-2}{2}}} f_\alpha(r')\right]} = \frac{\alpha-2}{2} \cdot q_{r',\alpha,\theta}(n)\,, \tag{3.15}$$

where $q_{r',\alpha,\theta}(n) = \left[1 - \frac{1}{\pi^{\frac{\alpha}{2}}(\theta\, n)^{\frac{\alpha-2}{2}}} f_\alpha(r')\right]^{-1}$. Taking the limit as $n \longrightarrow \infty$, we obtain

$$SIR = \lim_{n\to\infty} \frac{\alpha-2}{2} \cdot q_{r',\alpha,\theta}(n) = \begin{cases} \frac{\alpha-2}{2} \cdot 1 & \text{if } 0 \le r' < \frac{1}{\sqrt{\pi}} - r_o \\ \frac{\alpha-2}{2} \cdot q_{r',\alpha,\theta}(n \to \infty) & \text{if } r' = \frac{1}{\sqrt{\pi}} - r_o\text{, i.e., the network boundary.} \end{cases} \tag{3.16}$$

From Eq. (3.15), $q_{r',\alpha,\theta}(n \to \infty) = q_{r',\alpha}(n \to \infty)$ because θ is a scale factor on n and does not change the limit. Thus,

$$q_{r',\alpha,\theta}(n \to \infty) = \begin{cases} 1 & \text{if } 0 \le r' < \frac{1}{\sqrt{\pi}} - r_o \text{ and } \alpha > 2 \\ 1.467 & \text{if } r' = \frac{1}{\sqrt{\pi}} - r_o \text{ and } \alpha = 3 \\ 1.333 & \text{if } r' = \frac{1}{\sqrt{\pi}} - r_o \text{ and } \alpha = 4 \\ 1.270 & \text{if } r' = \frac{1}{\sqrt{\pi}} - r_o \text{ and } \alpha = 5 \\ 1.232 & \text{if } r' = \frac{1}{\sqrt{\pi}} - r_o \text{ and } \alpha = 6\,. \end{cases} \tag{3.17}$$

Fig. 3.3 shows the SIR as a function of n for $\alpha = 4$, $\theta = \frac{1}{3}$, and for different values of r'.

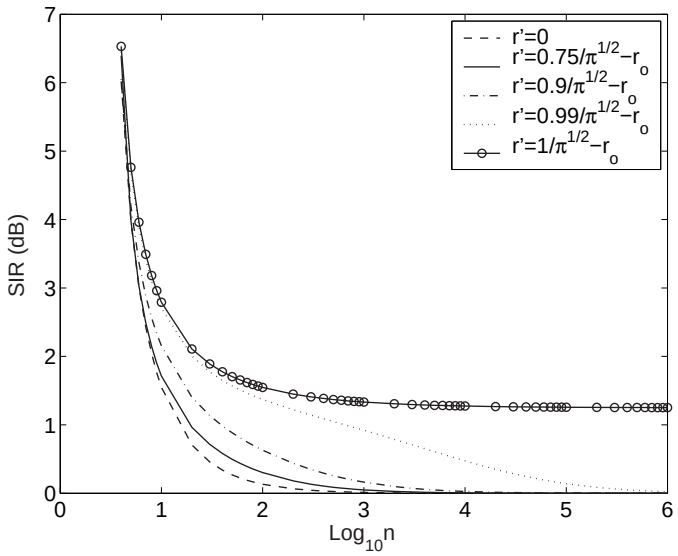

Figure 3.3: Signal-to-Interference Ratio curves as a function of n for $\alpha = 4$ and $\theta = \frac{1}{3}$, for the receiver node located at different positions in the network.

In addition, Figs. 3.3, 3.4, and Eqs. (3.16) and (3.17) show that *the SIR remains constant when n grows to infinity and this constant does not depend on r' if $0 \leq r' < \frac{1}{\sqrt{\pi}} - r_o$, i.e., it is the same value for any position of the receiver node inside the disk, whether the position is at the center, close to the boundary, or in the middle region of the radius disk.* Nevertheless, if the receiver node is at the boundary ($r' = \frac{1}{\sqrt{\pi}} - r_o$) then the SIR is still a constant when n scales to infinity but it has a greater value (see Figs. 3.3, and 3.4). For comparison purposes, Fig. 3.4 illustrates the SIR for $3 \leq \alpha \leq 6$ and $\theta = \frac{1}{3}$ for the receiver node located at the center and at the boundary of the network.

Hence, by having the SIR approaching a constant value as n grows to infinity, the network designer can properly devise the receiver (i.e., design modulation, encoding, etc.) such that Eq. (2.3) can be satisfied for a given β, allowing reliable (feasible) communication among close neighbors during *Phase 1*, and also during *Phase 2* for those cells that can

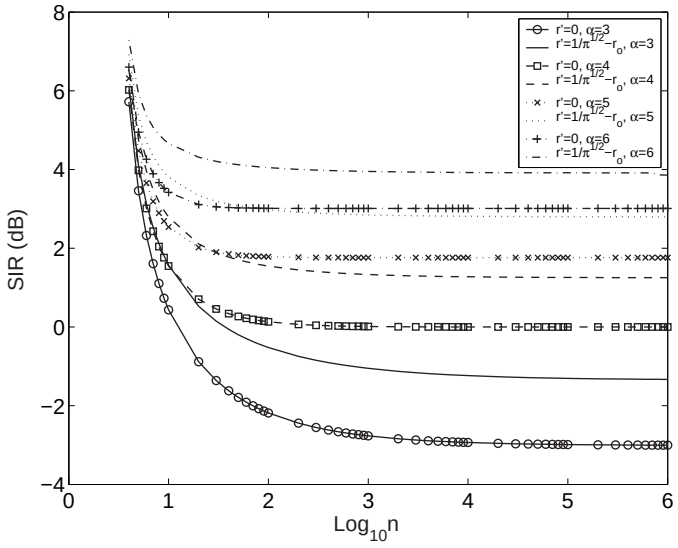

Figure 3.4: Signal-to-Interference Ratio curves as a function of n, for $3 \leq \alpha \leq 6$ and $\theta = \frac{1}{3}$, and the receiver node considered located at the center and at the boundary of the network.

successfully forward packets.

Also, Fig. 3.5 confirms that the limiting SIR does not depend on θ as predicted by (3.17).

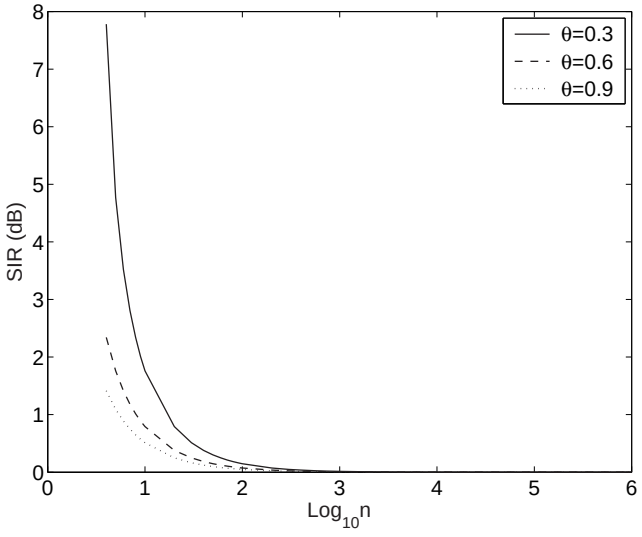

Figure 3.5: Signal-to-Interference Ratio curves as a function of n, for $\alpha = 4$, $r' = 0$ (i.e. receiver node at center of cell), and for different values of θ. In all cases the limiting SIR tends to the same value, i.e., it does not depend on θ.

3.4.2 The case $\alpha = 2$

For the free space propagation model [58, p. 107], the path loss parameter is modeled to be equal to two, i.e., $\alpha = 2$. Thus, the total interference at the receiver located at distance r' from the center with total n users in the network is obtained by integrating Eq. (3.8) over all disk area.

$$\begin{aligned} I_{r'}(n) &= \int_{disk} dI = \int_0^{2\pi} \int_{r_o}^{r_m(r',\gamma)} \frac{P}{r}\,\theta\, n\, dr\, d\gamma \\ &= 2P\theta n \int_0^{\pi} \log\left[\frac{r_m(r',\gamma)}{r_o}\right] d\gamma \\ &= 2P\theta n \int_0^{\pi} \log\left[\frac{\sqrt{\frac{1}{\pi} - (r'\sin\gamma)^2} - r'\cos\gamma}{r_o}\right] d\gamma\,. \end{aligned} \tag{3.18}$$

For this case, the SIR can readily be obtained by using Eqs. (3.1), (3.3), (3.7) and (3.18), so that

$$\begin{aligned} SIR_{r'}(n) &= \frac{P_R}{I} = \frac{\frac{1}{r_o^2}}{2\theta n \int_0^{\pi} \log\left[\frac{\sqrt{\frac{1}{\pi} - (r'\sin\gamma)^2} - r'\cos\gamma}{r_o}\right] d\gamma} \\ &= \frac{1}{2\theta n r_o^2}\left\{\int_0^{\pi} \log\left[\frac{\sqrt{\frac{1}{\pi} - (r'\sin\gamma)^2} - r'\cos\gamma}{r_o}\right] d\gamma\right\}^{-1} \\ &= \left\{\frac{2}{\pi}\int_0^{\pi} \log\left[\left(\sqrt{\pi\theta n}\right)\left(\sqrt{\frac{1}{\pi} - (r'\sin\gamma)^2} - r'\cos\gamma\right)\right] d\gamma\right\}^{-1}. \end{aligned} \tag{3.19}$$

Fig. 3.6 shows curves for SIR when $\alpha = 2$ and $\theta = \frac{1}{3}$. Although the limiting SIR tends to zero as n scales to infinity, the decay is not fast. This result is consistent with [61].

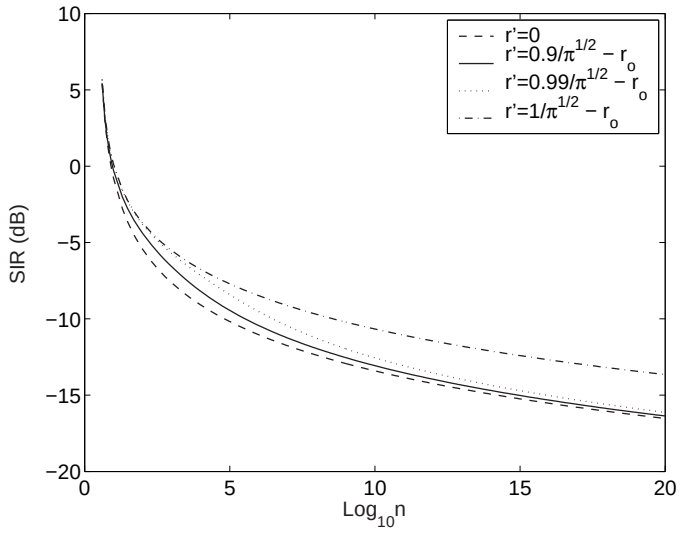

Figure 3.6: Signal-to-Interference Ratio curves as a function of n for $\alpha = 2$ and $\theta = \frac{1}{3}$, for the receiver node located at different positions in the network cell.

3.5 Per Source-Destination Throughput

We now show that the throughput per source-destination pair with our multi-copy relaying approach remains the same order of magnitude as the original single-copy relaying scheme, which is $\Theta(1)$ [26]. In the case of multi-copy forwarding, only one copy is delivered to the destination and the other copies are dropped from the additional relaying nodes either because the TTL timeout elapses, or the handshake between relay and destination informs the relay that the packet has been delivered. Therefore, only one node out of K nodes actually functions as a relay (as in Fig. 3.1(b)). Accordingly, only one copy passes successfully through the two-phase process, as in Fig. 2.1. Because node trajectories are iid and the system is in steady-state, the long-term throughput between any two nodes equals the probability that these two nodes are selected by the scheduler as a feasible sender-receiver pair, which has been shown to be $\Theta(\frac{1}{n})$ [26]. Also, there is one direct route and $n-2$ two-hop routes passing

through one relay node for a randomly chosen source-destination pair. Thus, the service rate is $\lambda_j = \Theta(\frac{1}{n})$ through each relay node, as well as the direct route. Accordingly, from Eq. (2.5), the total throughput per source-destination pair λ_T is $\Theta(1)$.

From the description given above and from Eqs. (3.5) and (3.6), the exact total throughput per source-destination pair is given by the fraction of cells that successfully forward packets (i.e, the cells that are selected by the scheduler containing feasible sender-receiver pairs). Then, for one sender and at least K receivers per cell, we have

$$\lambda_T = \mathbb{P}\{\text{senders } (L) = 1,\ \text{receivers are at least } K\} \approx \tfrac{1}{\theta}\, e^{-1/\theta} \left(1 - \sum_{k=0}^{K-1} \tfrac{1}{k!} \left(\tfrac{1}{\theta}\right)^k e^{-1/\theta}\right). \quad (3.20)$$

Hence, for at least two receivers per cell and $\theta = \frac{1}{3}$, $\lambda_T = \frac{1}{\theta} e^{-1/\theta}(1 - e^{-1/\theta} - \frac{1}{\theta} e^{-1/\theta}) \approx 0.12 = \Theta(1)$. Therefore, the multi-copy forwarding strategy attains the same throughput order as in [26].

Also, for at least one receiver per cell and $\theta = \frac{1}{3}$, $\lambda_T = \frac{1}{\theta} e^{-1/\theta}(1 - e^{-1/\theta}) \approx 0.14$. Hence, for the case in which $K \geq 1$, Eqs. (3.6) and (3.20) give the same throughput value obtained by Tse and Grossglauser [26], as well as Neely and Modiano [50]. The single-copy forwarding strategy [26] selects only the nearest neighbor amongst the K potential receiver nodes.

A practical observation worth making here is that the capacity for the case of the single-copy relaying scheme [26] can decrease when the relaying node goes out of service. Our relaying technique is more robust, because other relaying nodes can still be in service carrying other copies and find the destination and deliver it, functioning like backup copies.

3.6 Delay Equations

In Sections 3.3, 3.4 and 3.5, we showed that it is possible to have K feasible receivers that successfully obtain a copy of the same packet around a sender during *Phase 1*. Now we find the relationship between the delay value d obtained for the case of only one copy relaying [26], and the new delay d_K for $K \geq 2$ copies transmitted during *Phase 1* in steady-state behavior. Obviously, we have $d_K \leq d$. A naive guess would be to take $d_K = \frac{d}{K}$. However, the correct answer is obtained considering the random movement of the nodes. K is a small integer, much smaller than n whp, as explained in Section 3.3.

3.6.1 Single-Copy Forwarding Case

Because we have node trajectories independent and identically distributed, we focus on a given relay node labeled as *node 1*, and without loss of generality assume that *node 1* received a packet from the source during time $t_0 = 0$. Let $\mathbb{P}\{|X_1(s) - X_{dest}(s)| \leq r_o \mid s\}$ denote the probability that relay *node* 1 at position $X_1(s)$ is close enough to the destination node $dest$, given that the time interval length is s, where r_o is the radius distance given by Eq. (3.3), so that successful delivery is possible. The time interval length s is the delivery-delay random variable. Perevalov and Blum [56] obtained an approximation for the ensemble average with respect to all possible uniformly-distributed starting points, $(X_1(0), X_{dest}(0))$, where they considered the nodes moving on a sphere. We can extend their result to nodes moving in a circle by projecting the sphere surface movement in the sphere equator and thus have trajectories described in a circle and have [56]

$$
\begin{aligned}
&E_U\left[\mathbb{P}\{|X_1(s) - X_{dest}(s)| \leq r_o \mid s\}\right] \\
&\quad = \quad 1 - e^{-\lambda s}\left(1 - \lambda e^{-\lambda \int_0^s h_{X'}(t)dt} \int_0^s e^{\lambda \int_0^t h_{X'}(u)du} h_{X'}(t)dt\right) \\
&\quad = \quad \mathbb{P}\{S \leq s\} \\
&\quad = \quad F_S(s), \qquad (3.21)
\end{aligned}
$$

where $E_U[\cdot]$ means the ensemble average over all possible starting points that are uniformly distributed on the disk. $F_S(s)$ can be interpreted as the cumulative density function of the delay random variable S. The function $h_X(t)$ is the difference from the uniform distribution, such that $h_X(0) = 0$ and $|h_X(t)| < 1$ for all t, and X' is a point at distance r_o from the destination. The parameter λ is related to the mobility of the nodes in the disk and can be expressed by [56]

$$\lambda = \frac{2\, r_o\, v}{\pi R^2} = \frac{2\, r_o\, v}{1} = 2\, r_o\, v\,, \qquad (3.22)$$

which results from evaluating the flux of nodes entering a circle of radius r_o during a differential time interval, considering the nodes uniformly distributed over the entire disk of unit area and traveling at speed v. From Eq. (3.3), we see that the radius r_o decreases with $\frac{1}{\sqrt{n}}$. To model a real network in which a node would occupy a constant area, if the network grows, the entire area must grow accordingly. Therefore, because in our analysis we maintain the total area fixed, we must scale down the speed of the nodes [23]. Accordingly, the velocity of the nodes also must decrease with $\frac{1}{\sqrt{n}}$. Then

$$\lambda = \frac{1}{\Theta(n)}\,. \qquad (3.23)$$

Now, $h_X(t)$ has to be taken according to the random motion of the nodes [56]. If we consider the *uniform mobility model* [5], then a steady-state uniform distribution results as the random motion of the nodes in the disk. In such a case, $h_X(t) = 0 \; \forall \; t \geq 0$. Applying this result in Eq. (3.21) we have

$$\begin{aligned} E_U\left[\mathbb{P}\{|X_1(s) - X_{dest}(s)| \leq r_o \mid s\}\right] &= 1 - e^{-\lambda s} \\ &= \mathbb{P}\{S \leq s\} = F_S(s), \end{aligned} \tag{3.24}$$

which has the following probability density function:

$$f_S(s) = \frac{\mathsf{d}F_S}{\mathsf{d}s} = \begin{cases} \lambda e^{-\lambda s} & \text{for } \; 0 \leq s < \infty \\ 0 & \text{otherwise.} \end{cases} \tag{3.25}$$

Thus, the delay behaves exponentially with mean $\frac{1}{\lambda}$ and variance $\frac{1}{\lambda^2}$ for the *uniform mobility model*. We conclude from Eqs. (3.23), (3.24), and (3.25) that the average packet delivery delay is $\Theta(n)$ and its variance is $\Theta(n^2)$, i.e.,

$$E[S] = \frac{1}{\lambda} = \Theta(n) \text{ , and } Var[S] = \frac{1}{\lambda^2} = \Theta(n^2). \tag{3.26}$$

From now on, we replace s by d to indicate the delay for single-copy forwarding at *Phase 1* [26]. Accordingly,

$$E_U\left[\mathbb{P}\{|X_1(s) - X_{dest}(s)| \leq r_o \mid s = d\}\right] = 1 - e^{-\lambda d}, \tag{3.27}$$

for a uniform steady-state distribution resulting from the random motion of the nodes.

Also, from Eqs. (3.24) and (3.25), we have that the delay values are not bounded as a consequence of the tail of the exponential distribution, even if the number of total nodes in the network n is finite! Thus, the packet delivery time can grow to infinity for some packets, even though its average value is limited by Eq. (3.26) and n is finite.

3.6.2 Multi-Copy Forwarding Case

Now consider that K copies of the same packet were successfully received by adjacent relaying nodes during *Phase 1* (where $1 < K << n$). Let $\mathbb{P}_D(s)$ be the probability of having the first (and only) delivery of the packet at time interval length s. Hence, given that only one-copy delivery is enforced (see Section 3.2.2), and all K relays are looking for the destination, we have that

$$\mathbb{P}_D(s) = \mathbb{P}\left\{\bigcup_{i=1}^{K}[|X_i(s) - X_{dest}(s)| \leq r_o \mid s]\right\}. \tag{3.28}$$

Using union bound and considering that $\mathbb{P}_D(s)$ can be at most equal to 1, we arrive at

$$\mathbb{P}_D(s) \leq \min\left[\sum_{i=1}^{K}\mathbb{P}\{|X_i(s) - X_{dest}(s)| \leq r_o \mid s\}, 1\right], \tag{3.29}$$

in which Eq. (3.24) holds for each individual relay i because all the K nodes have independent and identically distributed movements and one can use the results in [56] for a single relay. However, when we attempt to compute the probabilities of multiple relays, since all these nodes start moving from the same area to search for destination (within a circle of radius r_o), their probability distributions are not mutually exclusive. If the time necessary for all these nodes to uniformly spread in the disk is equal to t_{spread}, since each node has a speed $v = \Theta(\frac{1}{\sqrt{n}})$, then in general, $t_{spread} = \Theta(\sqrt{n})$. However, as we will show later, the maximum delay $d_K^{max} = \Theta(n)$ given that $K << n$ whp. Therefore, $t_{spread} << d_K^{max}$ for large values of n, and consequently we can approximate all K probabilities using Eq. (3.24). This approximation for Eq. (3.29) results in

$$\mathbb{P}_D(s) \leq \min\left[K \cdot \mathbb{P}\{|X_1(s) - X_{dest}(s)| \leq r_o \mid s\}, 1\right]. \tag{3.30}$$

Furthermore, Eq. (3.30) describes two cases. The first case is when $\mathbb{P}_D(s)$ is less than 1 while the second case is when the union bound is greater than 1. Obviously, we can derive a meaningful relationship between d_K and d only for the first case and that is the basis of our remaining analysis. From Eqs. (3.24) and (3.30), and replacing s by d_K [4] to indicate the delay for K-copies forwarded during *Phase 1*, we have for the *uniform mobility model*,

$$\begin{aligned} E_U[\mathbb{P}_D(s)] &= E_U\left[\mathbb{P}\left\{\bigcup_{i=1}^{K}[|X_i(s)-X_{dest}(s)| \le r_o|\, s = d_K]\right\}\right] \\ &= \mathbb{P}\{D_K \le d_K\} \\ &= F_{D_K}(d_K) \\ &\approx K\left(1-e^{-\lambda d_K}\right), \end{aligned} \tag{3.31}$$

for a uniform steady-state distribution resulting from the random motion of the nodes. Exact computation of probability of d_K is a tedious task. Instead, we assume that the upper bound probability can be achieved, while this is simply an approximation. We make this assumption to find an approximate relationship between d_K and d and then by using computer simulation for MANETs given in Section 3.6.5, we show that this approximation can model the asymptotic behavior of d_K reasonably well. $F_{D_K}(d_K)$ can be interpreted as the cumulative density function of the delay random variable D_K for K copies transmission at *Phase 1*.

From Eq. (3.31) we see that the maximum value attained by D_K is given when

$$F_{D_K}(d_K^{max}) = 1 \approx K\left(1-e^{-\lambda d_K^{max}}\right) \Longrightarrow d_K^{max} \approx \frac{1}{\lambda}\log\left(\frac{K}{K-1}\right). \tag{3.32}$$

Eq. (3.32) suggests that, *for a finite* n, the new delay obtained by multi-copy forwarding is bounded by d_K^{max} after ensemble averaging over all possible starting points that are uniformly

[4] To be more accurate, we should use $\tilde{d}_K$ instead of d_K for the rest of the chapter because of the approximation. In order to make the paper easy to read, we will continue to use the same notation for simplicity.

distributed on the disk. On the other hand, our analysis to compute the relationship between d_K and d is based on the fact that $d_K < d_K^{max}$, otherwise, the cumulative density function is equal to one.

From Eqs. (3.23) and (3.32), and because $K << n$ whp, d_K^{max} grows to infinity and no bounded delay is guaranteed if n scales to infinity.

The probability density function for D_K is

$$f_{D_K}(d_K) = \frac{\mathsf{d}F_{D_K}}{\mathsf{d}d_K} \approx \begin{cases} K\lambda e^{-\lambda d_K} \text{ for } 0 \leq d_K \leq d_K^{max} \\ 0 \qquad\qquad \text{otherwise.} \end{cases} \tag{3.33}$$

Hence, in the multi-copy forwarding scheme the tail of the exponential delay distribution is cut off, and the average delay for K-copies forwarding is then given by

$$\begin{aligned} E[D_K] &= \int_0^{\infty} d_K f_{D_K}(d_K) \mathsf{d}d_K \\ &\approx \int_0^{d_K^{max}} d_K K\lambda e^{-\lambda d_K} \mathsf{d}d_K \\ &\approx \frac{1}{\lambda}\left[1 - \log\left(\frac{K}{K-1}\right)^{K-1}\right], \end{aligned} \tag{3.34}$$

and the delay variance is

$$\begin{aligned} Var[D_K] &= E[D_K^2] - (E[D_K])^2 \\ &\approx \frac{1}{\lambda^2}\left\{1 - K(K-1)\left[\log\left(\frac{K}{K-1}\right)\right]^2\right\}. \end{aligned} \tag{3.35}$$

Because $K << n$ whp, we conclude that the average delay and variance for any K are fractions of $\frac{1}{\lambda}$ and $\frac{1}{\lambda^2}$, respectively, and they also scale like $\Theta(n)$ and $\Theta(n^2)$. Note that d_K and λ scale to infinity and zero like n and $\frac{1}{n}$ respectively. Thus, λd_K which appears in Eqs. (3.32) and (3.33) is not a function of n. Nevertheless, the number of nodes does not scale

Table 3.1: Average Delay and Variance for single-copy [26] and multi-copy ($1 < K << n$) transmission obtained from Eqs. (3.26), (3.34), (3.35), and respective asymptotic delay values d_K^{max} from Eq. (3.32) (or (3.40)), for finite n.

Copies	**Mean**	**Variance**	d_K^{max}
Single-copy	$\frac{1}{\lambda}$	$\frac{1}{\lambda^2}$	∞
$K = 2$	0.307 $\frac{1}{\lambda}$	0.039 $\frac{1}{\lambda^2}$	$\frac{\log(2)}{\lambda}$
$K = 3$	0.189 $\frac{1}{\lambda}$	0.014 $\frac{1}{\lambda^2}$	$\frac{\log(3/2)}{\lambda}$
$K = 4$	0.137 $\frac{1}{\lambda}$	0.007 $\frac{1}{\lambda^2}$	$\frac{\log(4/3)}{\lambda}$

to infinity in real MANETs, and for a fixed n we can obtain significant average and variance delay reductions for small values of K compared to the single-copy relay scheme, as it is shown in Table 3.1. For example, if $K = 2$ a reduction of more than 69% over the average delay is obtained (i.e., for single-copy Mean$= \frac{1}{\lambda}$, for multi-copy ($K = 2$) Mean$= \frac{0.307}{\lambda}$). Observe also that the mean and variance values decrease when K increases, i.e., the dispersion from the mean delay is significantly diminished.

3.6.3 Relationship between Delays

We showed that the throughput of our multi-copy scheme is of the same order as the one-copy scheme [26]. Indeed, we showed that $\lambda_T \approx 0.14$ for single-copy and $\lambda_T \approx 0.12$ for multi-copy ($K > 1$), for $\theta = \frac{1}{3}$. This capacity is proportional to the probability of a packet reaching the destination. Hence, because only one copy of the packet is actually delivered to the destination for single-copy or multi-copy, their total probabilities can be approximated at their respective delivery time, i.e.,

$$\mathbb{P}\left\{\bigcup_{i=1}^{K}[|X_i(s) - X_{dest}(s)| \leq r_o \mid s = d_K]\right\} \approx \mathbb{P}\{|X_1(s) - X_{dest}(s)| \leq r_o \mid s = d\}, \tag{3.36}$$

and so their ensemble averages are

$$E_U\left[\mathbb{P}\left\{\bigcup_{i=1}^{K}[|X_i(s)-X_{dest}(s)|\leq r_o \mid s=d_K]\right\}\right] \approx E_U\left[\mathbb{P}\{|X_1(s)-X_{dest}(s)|\leq r_o \mid s=d\}\right], \quad (3.37)$$

whose solution must be obtained by substituting Eq. (3.21) (for $s = d_K$ and $s = d$ respectively) on both sides of Eq. (3.37) and solving for d_K for the particular model of random motion of nodes. For a steady-state uniform distribution for the motion of the nodes, a simplified solution is obtained by substituting Eqs. (3.27) and (3.31) in Eq. (3.37), i.e.,

$$K\left(1-e^{-\lambda d_K}\right) \approx 1-e^{-\lambda d}. \quad (3.38)$$

Solving for d_K we have

$$d_K \approx \frac{1}{\lambda}\log\left(\frac{K}{K-1+e^{-\lambda d}}\right). \quad (3.39)$$

This last equation reveals some properties for the strategy of transmitting multiple copies of a packet during *Phase 1*. If $K = 1$, then obviously $d_K = d$. If we let $d \to \infty$, with n finite, and because $K << n$, then we have

$$d_K^{max} \approx \lim_{d\to\infty}\frac{1}{\lambda}\log\left(\frac{K}{K-1+e^{-\lambda d}}\right) = \frac{1}{\lambda}\log\left(\frac{K}{K-1}\right) \overset{\text{if } K>1}{=} c_7. \quad (3.40)$$

This is the same asymptotic value already predicted by Eq. (3.32). The last column of Table I shows values of this asymptotic delay for the single-copy and multi-copy ($2 \leq K \leq 4$) cases, expressed as a function of the mobility parameter λ, obtained from Eq. (3.40) (or (3.32)) for a finite number of nodes n. Note that the time-to-live threshold must be set greater than the worst asymptotic delay ($K = 2$) to allow the packet to be delivered, i.e., $d_2^{max} = \frac{\log(2)}{\lambda} < TTL$.

Fig. 3.7 shows curves for Eq. (3.39), where λ was taken to be equal to one hundredth. The case of single-copy ($K = 1$) is also plotted. Except for the case of single-copy, the delay d_K tends to a constant value as d increases. *Hence, for a finite n, the multi-copy relay scheme can reduce a delay of hours of the single-copy relay scheme to a few minutes or even a few seconds, depending on the network parameter values.* Fig. 3.7 also shows that, a packet having two random routes to reach its destination produces an exponential reduction in delay compared to having only one random route, whereas having three (or more) random routes leads only to incremental improvements from having two random routes. This result is analogous to the power of two random choices studied by Azar et al [4] and Mitzenmacher [38].

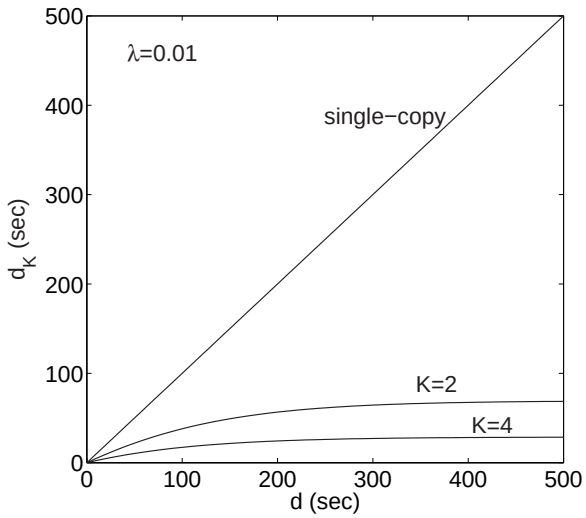

Figure 3.7: Relationship between delays d_K and d for single-copy, $K = 2$, and $K = 4$, for a uniform distribution resulting from the random motion of the nodes for the network in steady-state.

3.6.4 Memory Requirements

In most practical applications, there is a limit on the maximum buffer queue size for each node. Comparing the memory requirement for [26] and our proposal, we observe that

our memory requirement increases as K increases. On the other hand, the delay requirement in our technique is less than that of [26] by a factor larger than K (see (3.40) and Table 3.1). Therefore, on average, each packet is kept in memory for a shorter period of time. This observation suggests that our approach decreases the delay considerably while at the same time reduces the memory requirements without changing the order of the capacity of the system.

3.6.5 Simulation Results

Equation (3.30) and all the following results simply approximate the behavior of the delay d_K. In order to demonstrate if this approximation and the following results are justified, we have simulated a MANET system with 1000 nodes. Our simulations compare the behavior of multi-copy packet forwarding strategy with single relay strategy. We used the *BonnMotion* simulator [67], which creates mobility scenarios that can be used to study mobile ad hoc network characteristics.

In our simulations we implemented the simplified version of the *random waypoint mobility model* (as it resembles the *uniform mobility model* [5]), where no pause was used and $v_{min} = v_{max} = v$. Fig. 3.8 shows the results for 1000 seconds of simulations for $n = 1000$ nodes, $v = 0.13\ m/s$, $r_o = 0.02\ m$, and a unit area disk as the simulation area, which results $\lambda = 0.0052$. To obtain a solution close to the steady-state behavior, we run 40 random topologies and averaged them as follows. In each run we choose randomly a node with $K = 2$ and $K = 4$ neighbors, within r_o, respectively, and measured the time that each of these K nodes reach each of the other $n - K$ nodes in the disk (i.e., except the sender and its

other $K-1$ neighbors) considering each of them as a destination. The delay of the sender's nearest node reaching each destination is by definition d, and d_K is the minimum time among all the K nodes that reach the destination.

Figs. 3.8(a) and (b) show all pairs of points (d, d_K) obtained in this way for $K = 2$ and $K = 4$, respectively. In each graph we plot a 7^{th} degree polynomial fit for all the points as well as an average obtained by taking the mean of consecutive 90 points. We also plot the theoretical curve (from Eq. (3.39)) for the steady-state uniform distribution for the same parameters. We see that the averaged 90-points curve follows the polynomial fit and that they both accompany the steady-state uniform distribution predicted by theory as they are related mobility models. Our analysis did not develop exact delay analysis for this new scheme due to the complicated behavior of probabilities related to multi-copy forwarding; however, as it can be seen from the simulations, the approximation for delay analysis is consistent with simulation results. We only observe the asymptotic behavior for the experimental curves up to 800 seconds, after which the polynomial fit begins to fall and does not represent the actual asymptotic behavior anymore due to the natural lack of samples for this part of the graph. Furthermore, the simulation results present a better performance for the first two hundreds seconds of simulations compared to the theoretical curve. This indicate that one can take advantage of clustering among nodes, because in the random waypoint mobility model the nodes tends to be more concentrated at the center of the network area which helps to reduce delivery delay. Having more nodes close to each other reduces the time a node needs to find another node if compared to a steady-state uniform distribution of the nodes.

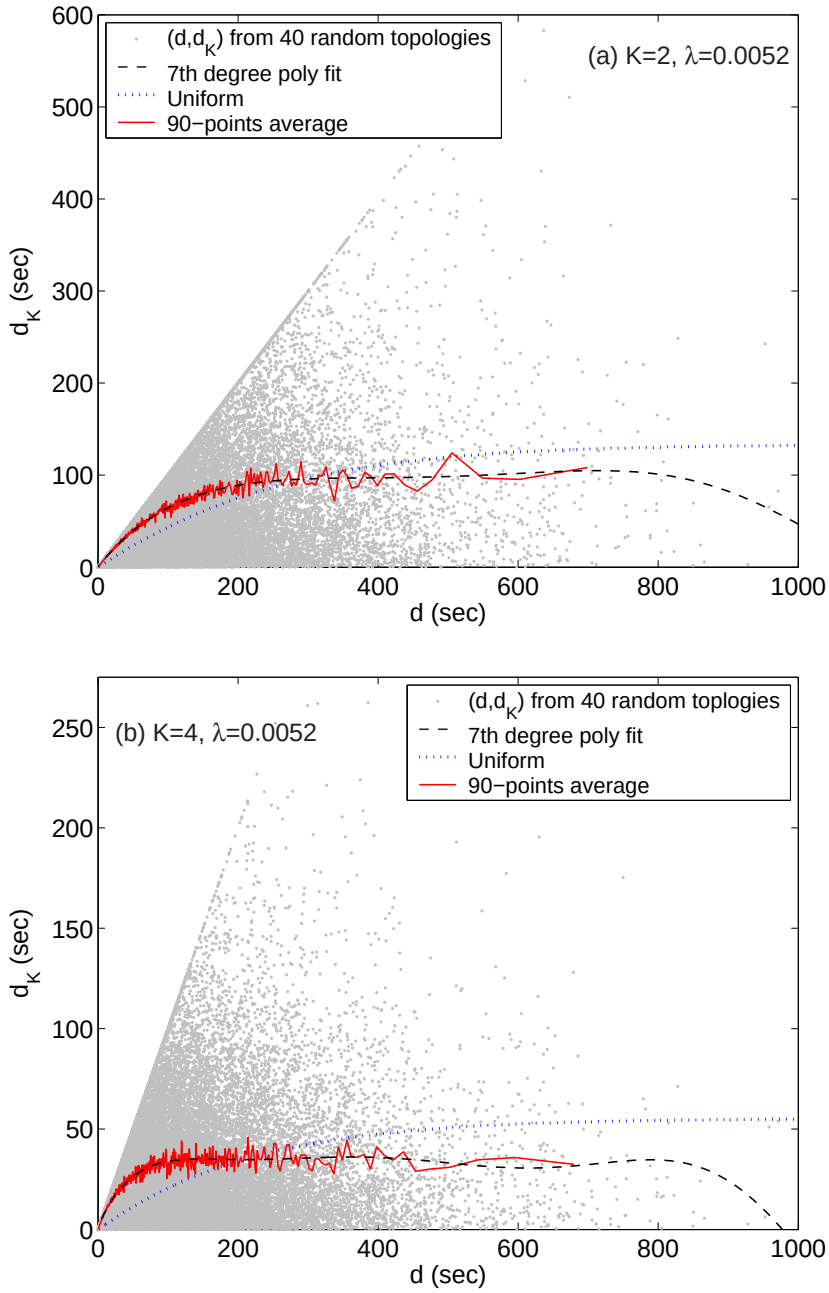

Figure 3.8: Simulation results for the *random waypoint mobility model*. Each gray point is a pair (d, d_K) delay measured for 40 random topologies all plotted together. A 7^{th} degree polynomial fit for all the points and a 90 consecutive points average are plotted for (a) $K = 2$ and (b) $K = 4$. The theoretical curve for the steady-state uniform distribution is also plotted.

3.7 Conclusions

We have analyzed delay issues for two packet forwarding strategies, namely, the single-copy two-phase scheme advocated by Grossglauser and Tse [26], and a multi-copy two-phase forwarding technique. We found that in both schemes the average delay and variance scale like $\Theta(n)$ and $\Theta(n^2)$ for n total nodes in a mobile wireless ad hoc network. In the case of multi-copy relaying, *multiuser diversity* is preserved by allowing one-time relaying of packets and by delivering only the copy of the packet carried by the node that first reaches the destination close enough so that it successfully delivers the packet. The handshake phase with the destination lasts a negligible amount of time and prevents the delivery of multiple copies of the same packet to the destination. A time-to-live threshold allows the additional nodes carrying the packet copy already delivered to drop it from their queues as soon as the lifetime expires. We also show that our technique does not change the order of the magnitude of the throughput in the MANET compared to the original multiuser diversity scheme by Grossglauser and Tse [26].

We showed that our multi-copy strategy can reduce the average delay value by more than 69% of that attained in the single-copy strategy for a finite number n of total nodes in the network. The multi-copy technique also has an advantage of presenting bounded delay for a finite n, after ensemble averaging with regard to all possible starting uniform distribution of the nodes in the disk. Theoretical and simulations results were presented. Our theoretical result does not describe the exact behavior of the delay but rather is an approximation that is confirmed by simulation results.

Lastly, we have analyzed the interference effects for a large number of nodes n in the

network. We showed that the signal-to-interference ratio for a receiver node communicating with a close neighbor tends to a constant as n scales to infinity, when the path loss parameter α is greater than two, regardless of the position of the receiver node in the network. Therefore, communication is feasible for close neighbors when the number of interferers scale to infinity. For the receiver nodes at the boundary of the network, we showed that, as expected, they experience less interference than those inside.

Chapter 4

Mobility-Capacity-Delay Trade-off in Wireless Ad Hoc Networks

In this chapter, we present new network models to show that mobility can also be varied as a resource together with capacity and delay [40], [42], [44]. The idea is to allow the nodes to execute *restricted* movements, i.e., each node moves only inside some given area in the network. By allowing transmissions to closest neighbor nodes only, we overcome interference from other transmitting nodes. Given that nodes have restrained mobility, the delivery from source to destination is done across multiple hops obtained by relaying packets along the path linking the source to the destination. Diggavi et al [16] considered one-dimensional mobility model in which nodes were allowed to execute movements on circles on a sphere. They showed that a constant throughput is still feasible; however, they did not present the corresponding trade-offs associated with mobility, capacity and delay.

Note that restrained mobility patterns have potential practical applications in cases

in which nodes are not allowed to leave a given region like a room, a hallway, or a predefined region covered by a sensor network, and has to rely on multiple hops (i.e., relays) to send a packet to farther destinations. Restrained mobility also provides insights on the performance of a network covering geo areas that are too vast for a single node to cover. Therefore, restricted mobility models are important to the study of ad hoc networks.

Section 4.2 presents a restricted mobility model, which we call *Scheme 1*, in which the size of the cell is function of the total number of nodes n in the network, and throughput and delay are computed and compared with previous work of Gupta and Kumar [28]. Section 4.3 presents another restricted mobility model, which we call *Scheme 2*. In this scheme, the size of the cell is not function of n but it is function of a constant. We compute again throughput and delay and compare with the results of Grossglauser and Tse [26]. Section 4.4 presents a modification of *Scheme 2* to allow multiple-copy relaying [39] so that the order of magnitude of the throughput is preserved, but lower delivery delay is attained. Section 4.5 investigates the effect of directional antennas in which packet relaying is done through the closest neighbor and it verifies that this approach attains better throughput than static networks employing omnidirectional antennas, without changing the delay behavior.

4.1 Basic Assumptions

The model considered here is that of a wireless ad hoc network with nodes assumed either fixed or mobile. The network consists of a normalized unit area torus containing n nodes [28], [27], [23].

For the case of *fixed nodes*, the position of node i is given by X_i. A node i is capable

of transmitting at a given transmission rate of $W\ bits/sec$ to j if the protocol model condition for successful transmission is satisfied as given in Eq. (2.1).

For the case of *mobile nodes*, the network model follows the assumptions given in Section 2.2. A successful transmission is governed again by the protocol model, where the positions of the nodes are time dependent.

4.2 Scheme 1

We present a restricted mobility scheme that attains a capacity gain of $\Theta(\log(n))$ compared to the static network model [28]. The throughput still decreases as the number of nodes n in the network grows to infinity. However, it models cases in which nodes can move around only a fraction of the geo region covered by the network, and serves as a building block for the scheme presented in the next section, which attains non-zero asymptotic throughput capacity in a dense network.

The model we propose is illustrated in Fig. 4.1. The network is a unit torus divided into square cells, each of area $a(n)$ as in [23], in which they showed that, if $a(n) \geq \frac{2\log(n)}{n}$, then each cell has at least one node whp. This condition guarantees connectivity whp [28], [23].

We now consider the additional assumption that each node has its movement confined to only one cell. This means that a node cannot cross the cell edge and percolate to a neighbor cell. By doing so, each cell is composed by at least one node whp, and such a node moves with speed $v(n)$, and no preferential direction of movement within the cell. Nodes move independently of each other, and once they hit the cell boundaries they are bounced

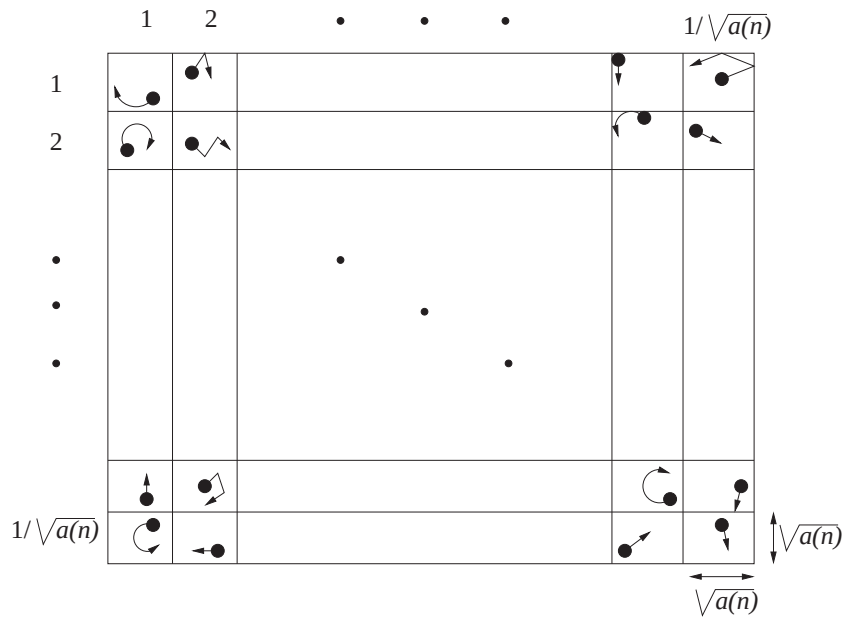

Figure 4.1: Unit area torus network divided into $1/a(n)$ cells, each with size of $a(n)$.

back (with relation to the edge normal).

We assume that each node only communicates with another node from an adjacent cell, and this happens only when the nodes are close enough to each other (i.e., both are near to the common edge that separates the cells) so that the effect of interference can be minimized. Thus, a source node relies on relays across several cells to have a packet delivered to a destination. Each packet travels via multiple relays from source to destination following the path close to the straight line linking source and destination. Each source-destination pair is chosen uniformly and independently from different cells. Fig. 4.2 illustrates a packet whose source and destination nodes are in cells i and d respectively, separated by an average distance $\overline{L}$. Possible cell paths for this packet are $\{i \to j \to f \to g \to c \to d\}$, $\{i \to j \to f \to g \to h \to d\}$, $\{i \to e \to f \to g \to c \to d\}$, $\{i \to e \to f \to g \to h \to d\}$, for example.

Grossglauser and Tse [27] showed that transmission to the nearest node is possible,

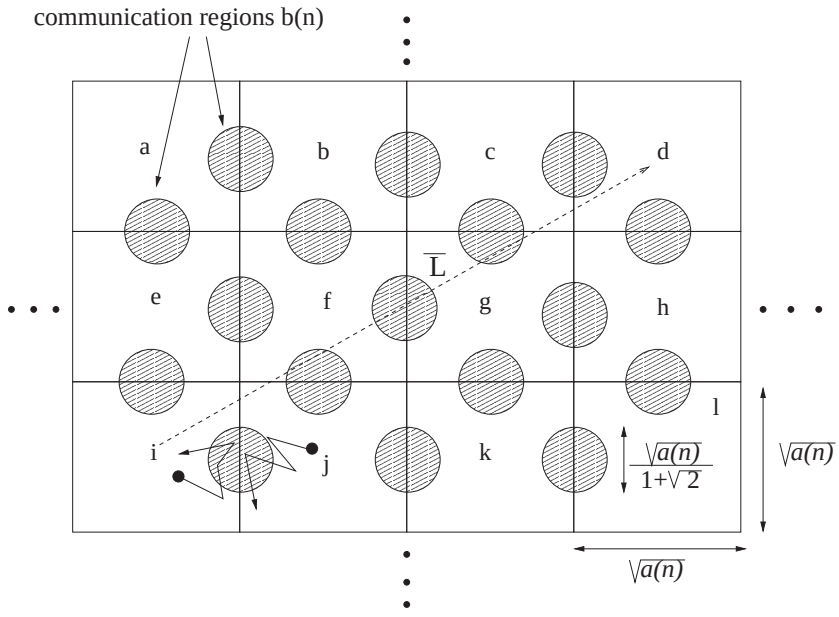

Figure 4.2: Region $b(n)$ where communication between nodes from adjacent cells is possible.

even when the number of interferers in the network scale to infinity. This allows a node to schedule transmission to a neighbor node from an adjacent cell when Eq. (2.1) is satisfied. In addition, we assume that both nodes are so close that communication is successful during the entire time slot (or session). The transmission is half-duplex so that each node uses half of the communication time slot to transmit at a rate of $W\ bits/sec$, and the other half to receive at the same rate. Thus, the average available bit rate is $\frac{W}{2}\ bits/sec$. Each time two nodes communicate with each other, they exchange packets, and these exchanges can be source-relay, relay-relay, or relay-destination transmissions.

The area in which successful communication can occur is shown in Fig. 4.2. Basically, it is a semi-circumference $b(n)$ of radius $\frac{\sqrt{a(n)}}{2+2\sqrt{2}}$ where two nodes from adjacent cells can come close to each other so that Eq. (2.1) is satisfied, i.e., no other node from the other cells will be closer to them than themselves. For the case in which more than one node in the same

cell are simultaneously traveling inside $b(n)$, only one of these nodes is allowed to communicate with a node from the adjacent cell. Accordingly, from Fig. 4.2, the two adjacent nodes in cells i and j are able to communicate during the time they simultaneously travel inside their respective regions $b(n)$'s in their cells as shown. We have that

$$b(n) = \frac{1}{2}\,\pi\left(\frac{\sqrt{a(n)}}{2+2\sqrt{2}}\right)^2 = \frac{\pi\,a(n)}{24+16\sqrt{2}}\,. \tag{4.1}$$

The probability of finding a node traveling inside $b(n)$ is $\frac{b(n)}{a(n)}$, because the node has no preferential direction of movement in the cell and tends to move uniformly inside the cell. In addition, because the nodes have iid movements, the probability that both nodes come to the communication region simultaneously, denoted by $\mathbb{P}_{comm}$, equals

$$\mathbb{P}_{comm} = \left[\frac{b(n)}{a(n)}\right]^2 = \left(\frac{\pi}{24+16\sqrt{2}}\right)^2 = c_8. \tag{4.2}$$

Hence, $\mathbb{P}_{comm}$ does not depend on n.

Because $\overline{L}$ is the mean distance between two uniformly and independently chosen source-destination nodes in the network, the average path distance across cells traversed by a packet from source to destination is $\Theta(\overline{L})$. Accordingly, each cell hop has an average size of $\sqrt{a(n)}$. Thus, the mean number of hops traversed by a packet is $\frac{\Theta(\overline{L})}{\sqrt{a(n)}}$.

According to the definition of throughput, each source generates $\Lambda(n)$ bits per second [1] and there are n sources in the network. Also, each bit needs to be relayed by $\frac{\Theta(\overline{L})}{\sqrt{a(n)}}$ nodes on the average. Thus, the total average number of bits per second served by the entire

[1] Here we use the notation $\Lambda(n)$ (instead of $\lambda(n)$ given in Section 1.1) to indicate that this throughput is related to restrained mobility models, or nodes using directional antennas.

network equals $\frac{\Theta(\overline{L})n\Lambda(n)}{\sqrt{a(n)}}$. To ensure that all required traffic is carried, we need that

$$c_9\, n\, \frac{W}{2}\mathbb{P}_{comm} \leq \frac{\Theta(\overline{L})n\Lambda(n)}{\sqrt{a(n)}} \leq c_{10}\, n\, \frac{W}{2}\mathbb{P}_{comm}$$

$$\Longrightarrow c_{11}\sqrt{a(n)} \leq \Lambda(n) \leq c_{12}\sqrt{a(n)}. \tag{4.3}$$

We have just proved the following Theorem.

Theorem 1 *For Scheme 1 with $a(n) = \frac{k\,\log(n)}{n}$ and $k \geq 2$, to guarantee connectivity, we have*

$$\Lambda_1(n) = \Theta\left(\sqrt{\frac{\log(n)}{n}}\right).$$

Compared to the capacity result obtained by Gupta and Kumar [28] which is $\Theta(1/\sqrt{n\,\log(n)})$, the result of Theorem 1 represents a gain of $\Theta(\log(n))$. *Thus, we obtain a throughput gain over the static network model by allowing the nodes to execute a restricted mobility pattern.*

Although we have used mobility and multiuser diversity [35] to overcome interference (note that Gupta and Kumar [28] could not use multiuser diversity because they consider only fixed nodes), the network still does not scale well with the number of nodes, i.e., $\Lambda_1(n) \longrightarrow 0$ when n goes to infinity. This happens because the number of hops necessary to reach a destination increases with n, so that the same packet is retransmitted infinite times as n grows to infinity, thus wasting the available bandwidth. The model we present in the next section does not have this problem, and it is indeed a generalization of the results obtained by Grossglauser and Tse [27].

The average delay incurred by a packet to reach the destination in *Scheme 1* is the sum of the average time a packet spends in each hopping cell in the path to its destination. A

node travels around the cell boundary on average every $t(n)$ time-slots that is proportional to

$$t(n) \propto \frac{\Delta S \cdot \mathbb{P}_{comm}}{v(n)} \implies t(n) = \Theta\left(\frac{\sqrt{a(n)}}{v(n)}\right), \tag{4.4}$$

where $\Delta S = \Theta(\sqrt{a(n)})$ is the average distance in one-round trip inside a cell. Note also that the total number of hops is $\Theta(\overline{L}/\sqrt{a(n)})$, and that the speed of each node $v(n)$ must decrease with $1/\sqrt{n}$. Combining all this information, the average delay (D_1) in *Scheme 1* is

$$D_1(n) = (\text{\# of hops}) \cdot t(n) = \Theta\left(\frac{1}{v(n)}\right) = \Theta(\sqrt{n}). \tag{4.5}$$

This delay is larger than that obtained by Gupta and Kumar [28], which was shown to be $\Theta(1/\sqrt{a(n)}) = \Theta(\sqrt{n/\log(n)})$ [23]. This is a direct consequence of the throughput-delay trade-off property [23]. *The capacity improvement is obtained at the cost of increase in delay.*

4.3 Scheme 2

In the previous section we saw that, by having an infinite number of relays (or hops), the capacity of the network decreases as the number of nodes increases. Here, we show that, by having a finite number of relays and using local transmission to overcome interference, we can attain constant throughput as n increases, but we can also trade-off the number of hops with capacity and delay, i.e., we can exchange mobility with capacity and delay, which is a generalization of the results by Grossglauser and Tse [27].

Fig. 4.3 shows the network and its cells. Now the network area is divided into l square cells and l is a network design parameter that does not depend on n. Hence, each cell has area of size $\frac{1}{l}$. Again, we assume that the n nodes are uniformly distributed over the entire network, but each node is restricted to move only inside of its cell (one of the l cells).

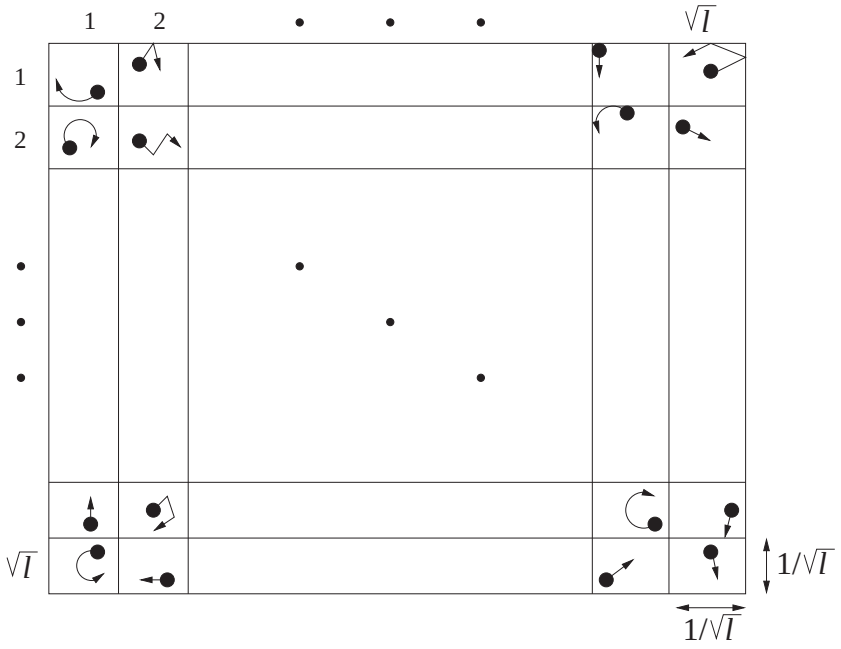

Figure 4.3: Unit area torus network divided into l cells, each with size area of $\frac{1}{l}$.

Among the total number of nodes n, a fraction of them, n_S, are randomly chosen as senders, while the remaining nodes, n_R, function like possible receiving nodes [27]. A sender density parameter θ is defined as $n_S = \theta n$, where $\theta \in$ (0,1), and $n_R = (1-\theta)n$. Each node can be a source for one session and a destination for another session. Nodes travel with velocity $v(n)$, have no preferential direction of movements, move independently of each other, and once they hit cell boundaries they bounce back with relation to the edge normal. Here, we consider that each node can communicate with its closest neighbor within the transmission range r_o, whether this neighbor is inside its own cell or from an adjacent cell (when it is traveling around the cell boundary). For a uniform distribution of the nodes, $r_o = 1/\sqrt{\theta \pi n}$ (for example, see Section 3.3). Thus, communication takes place every time nodes come close enough so that transmission is successful. Moreover, communication between two nodes from the same cell can only be a source-destination, or a relay-destination packet exchange. A relay-relay

communication only happens between nodes from different neighboring cells.

A source-destination pair is uniformly chosen among the n nodes, so that the destination does not have to be necessarily in the same cell as its source. Thus, again, a packet may traverse relays to reach its destination. We assume that, once a packet is relayed to a cell, it is not relayed again for another node in the same cell. Instead, the node keeps the packet in its queue until it reaches the neighborhood of an adjacent cell in the path toward the destination, so that it forwards the packet to the closest receiver node in the neighboring cell. In this model there is no fixed communication region as in the previous model. Once the node moves close enough around the cell boundary and there is a neighbor receiver node from the adjacent cell moving within the transmission range r_o, then it relays the packet to this neighbor if there is a packet to forward in that direction. Thus, it can be either a source-relay, or relay-relay, or relay-destination transmission. The communication is simplex, so that each sender node uses the entire communication time slot to transmit at rate W bits/sec.

Furthermore, because the nodes move independently of each other, once the network is in steady-state, each node in a cell will come closer to another node in that cell at some point in time so that they can exchange packets. This same idea applies to neighbor nodes: because nodes move independently of one another, two nodes from adjacent cells will come close to each other, around the boundary which separates their cells, at some point in time, such that they can exchange packets. Therefore, in steady-state, the traffic of each node will be uniformly distributed among neighbors in the same cell, as well as among neighbors from each adjacent cell. Accordingly, for the network in steady-state, we have

- Each node has a packet for another node in the same cell.

- Each node has a packet for another node in each of its neighbor cells whose communication is possible.

In addition, for a finite l and a sufficiently large n, connectivity is guaranteed if $\frac{1}{l} > \frac{2\log(n)}{n}$ (i.e., the cell size is greater than $2\log(n)/n$), and because of the uniform distribution of the nodes, each cell contains $\Theta(\frac{n}{l})$ nodes. Because $n \to \infty$, l can be chosen to be any positive integer to satisfy the connectivity criterion.

As before, $\overline{L}$ is the mean distance between a source and destination, uniformly and independently chosen in the network. Thus, the average path length across cells followed by a packet is $\Theta(\overline{L})$. Given that each cell hop has an average size of $1/\sqrt{l}$, the average number of hops traversed by a packet until it reaches its destination is $\frac{\Theta(\overline{L})}{1/\sqrt{l}}$.

According to the definition of throughput, each source generates $\Lambda(n)$ bits per second, with n_S being sources in the network. Because each bit needs to be relayed on the average by $\frac{\Theta(\overline{L})}{1/\sqrt{l}}$ nodes, the total average number of bits per second served by the entire network equals $\frac{\Theta(\overline{L})n_S\Lambda(n)}{1/\sqrt{l}}$. Hence, to ensure that all required traffic is carried, we need that

$$c_{13}n_S\,W \leq \frac{\Theta(\overline{L})n_S\Lambda(n)}{1/\sqrt{l}} \leq c_{14}n_S\,W \Longrightarrow \frac{c_{15}}{\sqrt{l}} \leq \Lambda(n) \leq \frac{c_{16}}{\sqrt{l}}. \tag{4.6}$$

This proves the following Theorem.

Theorem 2 *For Scheme 2, for finite l and sufficiently large n, we have*

$$\Lambda_2(n) = \frac{1}{\sqrt{l}}\,\Theta(1).$$

Theorem 2 is a generalization of the results by Grossglauser and Tse [27], given that we have divided the network into l equal cells. If we set $l = 1$, Theorem III.5 in [27] follows.

Because no node is allowed to move through the entire network, a packet stored in the relay queue of a node has to follow a path of cells in the direction of the destination. Therefore, we should expect a smaller delay than that obtained in the scheme by Grossglauser and Tse [27]. The average delay (D_2) in *Scheme 2* is given by the time the packet spends hopping until it reaches the destination cell, plus the amount of time the last relay in the destination cell needs to reach the destination node. The later is $\Theta\left(\frac{n}{l}\right)$, because we have $\Theta\left(\frac{n}{l}\right)$ nodes in each cell [23], [50]. The former is given by the number of hops traversed multiplied by the average time spent per hop (i.e., (# of hops) $\cdot\, t(n)$), which is $\Theta\left[\frac{\overline{L}}{1/\sqrt{l}}\left(\frac{1}{v(n)}\,\frac{1}{\sqrt{l}}\right)\right] = \Theta(\sqrt{n})$. Thus,

$$\begin{aligned} D_2(n) &= \text{delay during hopping} + \text{delay in destination cell} \\ &= \Theta\left(\sqrt{n} + \frac{n}{l}\right) \\ &\approx \Theta\left(\frac{n}{l}\right) \quad (\text{for } n \text{ large}), \end{aligned} \tag{4.7}$$

because the term $\frac{n}{l}$ dominates $\sqrt{n}$, for a sufficiently large value of n (and $l << \sqrt{n}$). Comparing $D_2(n)$ to the delay attained in the scheme by Grossglauser and Tse [27], whose delay was shown to be $\Theta(n)$ [50], [23], we conclude that, as we expected, the delay in *Scheme 2* is smaller by a factor of l.

From Theorem 2, Eq. (4.7), and comparing with [27], we conclude that we can trade-off mobility as a resource with capacity and delay. By restraining the nodes to move inside cells of size area $\frac{1}{l}$, the $\Theta(1)$ throughput obtained in [27] is reduced by a factor of $\sqrt{l}$, while the delivery delay is decreased by a factor of l. Thus, *Scheme 2* is a generalization of the network model by Grossglauser and Tse [27].

The next section presents a modified version of *Scheme 2* that allows more than one copy of a packet to be forwarded at the destination cell, such that lower delivery delay is possible.

4.4 Scheme 2 with Multi-Copy Relaying at Destination Cell

We now use the improved packet forwarding strategy described in Chapter 3 for mobile ad hoc networks that attains the $\Theta(1)$ capacity of the basic scheme by Grossglauser and Tse [27], but provides lower delay.

We maintain all assumptions from *Scheme 2*, but change the last relaying phase in which a node (a sender or relay) from an adjacent cell has to forward a packet to the destination cell. Hence, once a relay node reaches the boundary of the destination cell, it at once forwards copies of the packet to multiple one-time relay nodes located at the destination cell that are within its transmission range r_o. By doing so, the time within which a copy of the packet reaches its destination can be decreased in that cell. The first one-time relay node that reaches the destination close enough delivers the packet.

In *Scheme 2*, a relay approaching the destination cell transmits to its nearest receiver neighbor in the destination cell, so that the interference caused by other nodes is low, allowing reliable communication. However, it may be the case that the relay can have more than one receiver neighbor node from the destination cell in the transmission range, and we can take advantage of that. We allow those additional receiving neighbor nodes to also have a copy of the packet. Hence, instead of only one copy, K copies will follow different random routes in the destination cell and can find the destination node earlier compared to *Scheme 2*. In

addition, as in Chapter 3, packets are assumed to have header information for scheduling and identification purposes, and a time-to-live (TTL) threshold field as well. We assume that, before any packet is transmitted between nodes, a handshake takes place at the beginning of the time slot, such that no relay transmits a packet that a destination has already received. In this way we enforce only one-copy delivery. Also, after the TTL expires, the packet is dropped from the additional relaying nodes queues which did not deliver the copy of the packet.

Therefore, assuming that K copies of the same packet were successfully received by adjacent nodes in the destination cell, the maximum delay in the destination cell is approximated by $d_K^{max} \approx \frac{1}{\lambda} \log \frac{K}{K-1}$ (see also Eq. (3.32)), where λ is computed considering the area of the destination cell.

As in *Scheme 2*, the total delivery delay for a packet, measured from the source to the destination, is divided in two parts: the time the packet spends to reach the destination cell, plus the time the relay in the destination cell expends to reach the destination node. The former was shown to be $\Theta(\sqrt{n})$, and for a fixed n this delay is finite. However, as discussed above, the latter can last indefinitely if only one copy is looking for the destination. Hence, by forwarding K-copies in the destination cell, the total delivery delay is approximated by

$$D_{2_K} \approx \Theta(\sqrt{n}) + d_K^{max}. \tag{4.8}$$

Thus, a delay of hours in single-copy forwarding to the destination cell can be reduced to a few minutes or even a few seconds for multi-copy relaying, depending on the network parameters.

We have shown in Chapter 3 that the throughput per source-destination pair for the multi-copy relaying approach remains at $\Theta(1)$ [27]. Thus, by multi-copy forwarding at the destination cell in the modified version of *Scheme 2*, we do not change the order of the

capacity. Hence, Theorem 2 still holds here.

4.5 Fixed Nodes with Directional Antennas

In this section, we present a model where nodes are static, but endowed with directional antennas. Previous work [70], [55] has considered capacity analysis for static networks using directional antennas, where they showed that no scheme using directed beams can circumvent the constriction on capacity in dense networks. In our study, we present a slightly different modeling approach compared to these previous directional antenna analysis. We constrain communication to occur only between closest neighbors by using very narrow beams. The network model is shown in Fig. 4.4. A source-destination pair of nodes is randomly chosen so that we want to send a packet from cell a to cell t, for example, relying on multiple relays (or hops) using directional antenna transmission along close neighbors in the path to the destination. The nodes are deployed uniformly in the network area torus. As in *Scheme 1*, the network is divided in $1/a(n)$ cells, each with an area $a(n)$. We assume $a(n) \geq 2\ \log(n)/n$, so that each cell has at least one node whp [23]. In each cell a node is chosen to relay the traffic of the cell. Fig. 4.4 shows a source node in cell a that has destination at a node in cell t separated by a distance $\overline{L}$. Accordingly, the cell path along the closest neighbors is $\{a \rightarrow f \rightarrow g \rightarrow h \rightarrow m \rightarrow n \rightarrow o \rightarrow t\}$.

We want to obtain the average throughput for a source-destination pair uniformly chosen among all n nodes, as well as the delay behavior. The relay transmissions are scheduled at regular time intervals so that each node is assigned a time slot to transmit successfully to its closest neighbor in the path to the chosen destination. This is a time schedule constraint

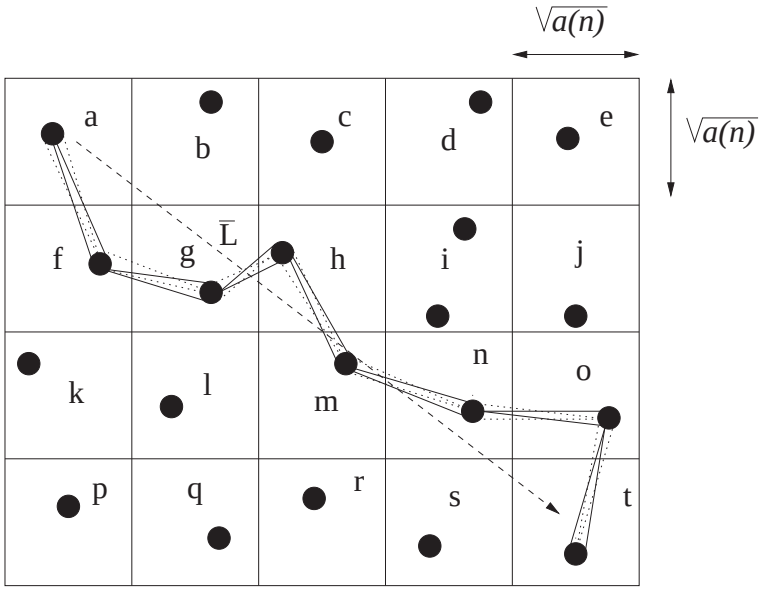

Figure 4.4: Unit area torus network divided into $1/a(n)$ cells each with size area of $a(n)$. Transmissions are employed using bi-directional antennas, with very narrow beams, between closest neighbors from adjacent cells along the path to destination.

because a node can only point its antenna to a close neighbor at consecutive time intervals. For the example shown in Fig. 4.4, each node has eight neighbors, given that we assume a torus net, so that it can communicate to each of them at regular eight slot time interval respectively, i.e., a time division multiple access (TDMA) with bi-directional beam transmission. Each time two nodes point their antennas toward each other, they exchange packets, so that each of these exchanges can involve either source-relay, relay-relay, or relay-destination transmissions. Interference is overcome by the use of directional beams to the nearest neighbor, so that Eq. (2.1) is satisfied. Again we assume that the transmissions are half duplex, i.e., the communication time slot is divided in two equal parts. Each node transmit at $W\ bits/sec$. Hence, the average available bit rate is $W/2\ bits/sec$.

Given that $\overline{L}$ is the mean distance between a uniformly and independently chosen

source-destination pair in the network, the average path distance across cells traversed by a packet is $\Theta(\overline{L})$. Accordingly, each cell hop has average size of $\sqrt{a(n)}$. Thus, the mean number of hops traversed by a packet until it reaches its destination is $\frac{\Theta(\overline{L})}{\sqrt{a(n)}}$.

According to the definition of throughput, each source generates $\Lambda(n)$ bits per second. Given that each bit needs to be relayed on the average by $\frac{\Theta(\overline{L})}{\sqrt{a(n)}}$ nodes, the total average number of bits per second served by the entire network equals $\frac{\Theta(\overline{L})n\Lambda(n)}{\sqrt{a(n)}}$. To ensure that all required traffic is carried, we need that

$$c_{17}\, n\, \frac{W}{2}\Delta t \leq \frac{\Theta(\overline{L})n\Lambda(n)}{\sqrt{a(n)}} \leq c_{18}\, n\, \frac{W}{2}\Delta t, \tag{4.9}$$

where $\Delta t = \frac{1}{8}$, which comes from the TDMA transmission schedule approach[2]. Thus,

$$c_{19}\sqrt{a(n)} \leq \Lambda(n) \leq c_{20}\sqrt{a(n)}. \tag{4.10}$$

This proves the following Theorem.

Theorem 3 *For a given node using directional antenna transmission to closest neighbor along the path to destination, with $a(n) = \frac{k\log(n)}{n}$, for $k \geq 2$, to guarantee connectivity, we have*

$$\Lambda_D(n) = \Theta\left(\sqrt{\frac{\log(n)}{n}}\right).$$

This result represents a better bound on throughput capacity than what Gupta and Kumar [28] obtained which was $\Theta(1/\sqrt{n\,\log(n)})$, and the results by Yi et al [70]. Indeed, it is a gain of $\Theta(\log(n))$ and is similar to Peraki and Servetto's results [55] obtained for a single directed

[2]Other diversity scheme could be assumed as well.

beam, where they use a different approach applying networking flow analysis to calculate the network transport capacity (i.e., maximum stable throughput). This is the same capacity scalability obtained for *Scheme 1*. We see that capacity is still constrained in dense networks. This is due to the wasting of the available bandwidth to forward the same packet over multiple hops by an amount of time that scales with n.

The average delay incurred by a packet to reach the destination is the sum of the average time a packet spends hopping along the path to its destination. The total number of hops to reach destination is $\Theta(\overline{L}/\sqrt{a(n)})$. Accordingly, the delay using directional antenna transmission to nearest neighbor is given by

$$D_D(n) = (\text{\# of hops})\Delta t = \Theta\left(\frac{1}{\sqrt{a(n)}}\right) = \Theta\left(\sqrt{\frac{n}{\log(n)}}\right). \tag{4.11}$$

Compared to Eq. (4.5) this represents a delay reduction of $\Theta(1/\sqrt{\log(n)})$. Thus, the use of directional antenna with fixed nodes offers a smaller delay on average than the restricted mobility case, while attaining the same throughput scalability as *Scheme 1*.

Therefore, employing directional antenna transmissions between closest nodes along the path to a destination is equivalent, in terms of throughput performance, to nodes executing restricted mobility as in *Scheme 1*, while providing a smaller packet delivery delay.

4.6 Performance Comparisons

To obtain a benchmark of throughput and delay for wireless ad hoc networks, we compare in Table 4.1 the schemes studied with the previous works by Gupta and Kumar [28], and Grossglauser and Tse [27]. The results suggest that using mobility or enhanced physical

Table 4.1: Throughput gain and delay increase obtained from comparing previous works [28], [27] with restricted mobility schemes and directional antenna transmission.

Schemes comparisons	Throughput gain	Delay increase
Scheme 1 / Gupta & Kumar	$\log(n)$	$\sqrt{\log(n)}$
Grossglauser & Tse / Scheme 2	$\sqrt{l}$	l
Directional antenna / Gupta & Kumar	$\log(n)$	none
Scheme 1 / Directional antenna	none	$\sqrt{\log(n)}$

layer properties (directional antennas in this case) can improve throughput or delay. This finding leaded us to modify the physical layer properties of wireless ad hoc networks, as described in the next chapter, in order to improve further the performance of such networks.

4.7 Conclusions

We have analyzed four schemes for ad hoc wireless networks. The first three schemes considered nodes with restricted mobility. The nodes have restrained mobility area that can be either a function of n, or independent of n. We show that on all these cases we can trade-off the mobility resource with capacity and delay. In the first scheme the capacity does not scale well, while in the second scheme the throughput has non-zero asymptotic behavior in dense networks, and it is shown to be a generalization of the Grossglauser and Tse [27] results. The third scheme is a modified version of the second, in which we allow multiple packet copies to be forwarded to the destination cell so that we attain a better delay performance. The fourth scheme studied was that of a static ad hoc network using directional antennas with transmission restricted to closest neighbors in the path along destination. We showed that the

capacity still decreases with n having the same scalability law as that obtained in the first scheme of restricted mobility, however presenting a smaller delay. Therefore, the directional antenna scheme provides better throughput performance than static networks employing omnidirectional antennas, and presents smaller delay than in restricted mobility. Furthermore, by changing the physical layer properties for the nodes (restricted mobility or directional antennas, for example) we can improve the performance of wireless ad hoc networks.

Chapter 5

Principles of Opportunistic Cooperation: A New Approach for Scalable Mobile Ad Hoc Networks

The protocol stacks of wireless ad hoc networks implemented or proposed to date have been designed to try to *avoid* interference and to support the communication among senders and receivers that are *competing* with one another for the use of the shared bandwidth. This "competition-driven" view of bandwidth sharing has had profound implications on network architectures and methods used to access the channel and disseminate information. For example, because all transmissions compete with one another, medium access control (MAC) protocols attempt to avoid or react to "collisions" of packets, given that a receiver can decode a single transmission at a time, and a single copy of a data packet is forwarded at each relay from source to destination, because additional copies would increase the destructive-

interference effect. Gupta and Kumar [28] showed that, in a wireless connected network with static nodes, the throughput and delay for each node degrade as the number of nodes increases under the competition-driven view of networking (see Section 2.1).

Grossglauser and Tse approach [26] and many subsequent studies focus on how to make MANETs scale by taking advantage of mobility [26], [23], [66], [5], and consider each transmission as competing with all the other concurrent transmissions in the network. However, these results do indicate that, because a relay cooperates with a source by storing the source's packet until it is close enough to the intended destination, the throughput of MANETs can be increased (see Section 2.2).

More recently, Toumpis and Goldsmith [65] have shown that the capacity regions for ad hoc networks are significantly increased when multiple access schemes are combined with spatial reuse (i.e., multiple simultaneous transmissions), multihop routing (i.e., packet relaying), and successive interference cancellation (SIC), [1] even without performing power control. Furthermore, SIC circuits with simple implementation and low complexity have been introduced [54], and code division multiple access (CDMA) [31] and global positioning system (GPS) [53] technologies have been already integrated into a single IC chip [1]. Xie and Kumar [68], proved that, for nodes on a line and under low attenuation channel condition, the network transport capacity can scale super-linearly like $\Theta(n^{\eta})$ for $\eta < 2$ when nodes cooperate in coherent multistage relaying with interference subtraction mode (CRIS).

From the above results, and motivated by the findings of the previous chapter where we observed that by changing the physical layer properties of the nodes we can improve

[1] SIC is a demodulation technique that decodes the information of interest. SIC first utilizes channel estimates to cancel received interference from the received signal in a successive order. In other words, the front end is a conventional receiver, and signal processing is used at the back end to clean up the signal iteratively [54], [3].

the performance of wireless networks, it appears that a cooperative approach to bandwidth sharing is not only desirable for attaining more scalable MANETs, but feasible in practice. In this chapter, we present the first integrated approach to cooperative bandwidth sharing in MANETs and propose what we call *opportunistic cooperation*. The term "opportunistic" is used here to indicate the fact that the number of nodes cooperating with one another in a cell at each communication session is a random variable.

Our earlier work (Chapter 3) describes a setting for one-to-many communication. In this scenario, a node relays its packet to multiple relay nodes that are close, allowing them to cooperate to search for the destination. In this scheme, however, all the transmitting nodes in each communication session compete with each other to transmit their packets (see Fig. 5.1). Ghez et al [24] and Tong et al [64] explain a framework for many-to-one communication. In this context, multiple nodes cooperate to transmit their packets simultaneously to a single node using CDMA and the receiver node utilizes multiuser detection to decode multiple packets. Under this condition, two groups of multiple transmitting nodes that are close to each other have to compete with one another to transmit their packets to their respective receivers. Similar to the previous scheme, the adjacent transmitting nodes compete with each other to access the channel. Opportunistic cooperation is a vision for multiple concurrent communication settings (i.e., a many-to-many framework). With opportunistic cooperation, nodes access the available channel(s) and forward information across a MANET in such a way that concurrent transmissions become useful at destinations or relays. Our cell size limits the number of nodes in each cell, on average, even as $n \to \infty$, making it feasible to decode the dominant interference using multiuser detection. Hence, sender-receiver pairs collaborate, rather than

compete, and the adjacent transmitting nodes with strong interference to each other are no longer an impediment to scaling laws but rather acceptable communication sources by all receiving nodes for detection and relaying purposes. Clearly, a consequence of such a strategy is an increase in the receiver complexity of all the nodes in the network.

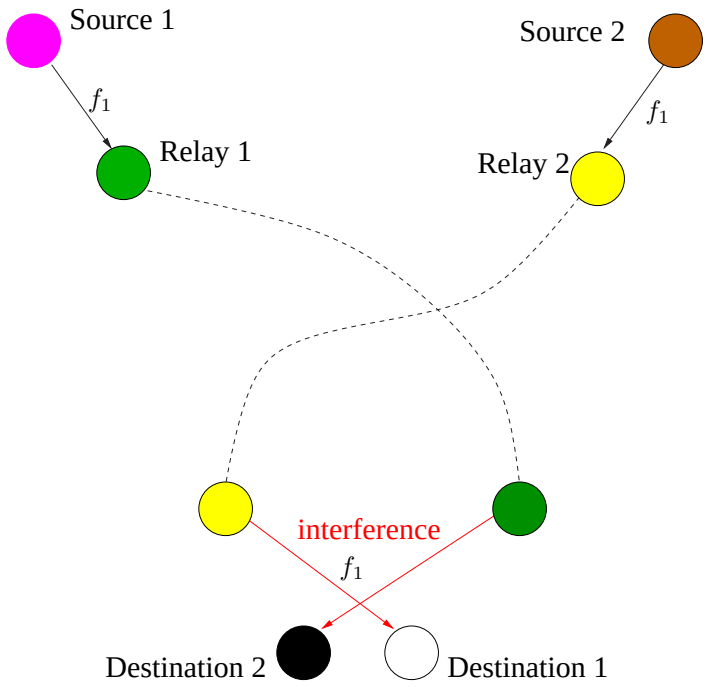

Figure 5.1: Interference due to transmission at same frequency f_1 causes collision and prevents packet delivery.

The two main questions that we address in this and the following two chapters are as follows.

- What cross-layer protocol mechanisms are suitable to attain opportunistic cooperation in MANETs?
- What are the fundamental performance limits of a MANET with opportunistic cooperation?

5.1 Network Model

The *decodable receiver range* (or simply receiver range) [2] of a node is defined as the radius, measured from the node, which contains all other nodes of the same cell. The *cluster* associated with a given node is the set of cells reached by the receiver range of that node.

Our assumptions are consistent with prior work (see Chapter 2). The modeling problem we address is that of a MANET in which n mobile nodes move in a square area. The size of the area will be considered in two distinct cases in the following two chapters. We will first assume a unit (fixed) area and a size area that grow with the total number of nodes n. We consider that communication occurs only among those nodes that are close enough (i.e., in the same cell), so that interference caused by nodes farther away is low, allowing reliable communication. In other words, the receiver chooses the closest nodes because they present the best channel due to the assumption of the simple path propagation model (i.e., the receiver takes advantage of multiuser diversity [35]). Our model resembles the one introduced by Grossglauser and Tse [26], who consider a packet to be delivered from source to destination via one-time relaying.

Each node simultaneously transmits and receives data during a communication time period, through different frequency bands, since each data link is assumed half-duplex. This period of communication is called a *communication session*. Furthermore, each session is divided into two parts. A neighbor discovery protocol is used by nodes during the first part to obtain their neighbors information (e.g., node identifier (ID)), and the transmission of data

[2] We adopt *receiver range* for a node because it is used here to distinguish constructive interference from destructive one (as described later), in contrast to the common use of *transmission range* as in [28].

is performed during the second part. Each node has a unique ID that does not change with time, and each node can simultaneously be a source (or relay) while transmitting and a destination (or relay) while receiving, during a session. Each source node picks a single arbitrary destination to whom it sends packets and this association does not change with time.

5.2 Opportunistic Cooperation

In a competition-driven paradigm for MANETs, when two nodes become close enough to each other, they can transmit information to one another without any delay. With opportunistic cooperation, many nodes transmit concurrently to many other nodes that are close enough, and all such transmissions are decoded. Hence, a node may concurrently send to and receive from multiple nodes. Because full-duplex data communication in the same frequency band is not practical, we propose in the next two chapters two different approaches of how opportunistic cooperation can be implemented. FDMA is used in both cases to allow simultaneous transmissions among close nodes as shown in Fig. 5.2. In the example illustrated, the nodes transmit packets concurrently to each other using different frequency bands. The nodes travel and eventually find the destination for a relayed packet (for example, nodes 4 and 5). The delivery is done similarly, where we assume in Fig. 5.2 that relays 4 and 5 approach simultaneously the destination nodes and deliver the relayed packets using FDMA. Beyond FDMA, the nodes are assumed to employ multiuser detection to decode the simultaneous transmissions. For example, Chapters 6 and 7 describes the multiuser detection implementation with CDMA-SIC and multiple-input multiple-output (MIMO) systems respectively.

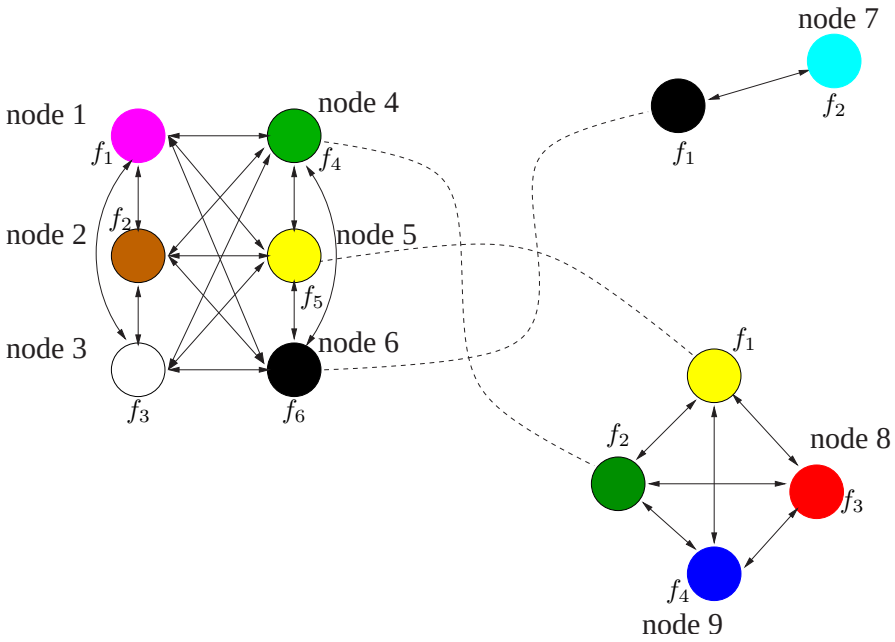

Figure 5.2: Opportunistic Cooperation: nodes transmit simultaneously to different neighbors using distinct frequencies. The nodes use multi-user detection to separate the signals from different senders.

5.2.1 Control and Data Channels

In our specific implementation of opportunistic cooperation, we use two types of channels. *Control channels* are used by nodes to obtain such information as the IDs of strong interference sources and the state of data channels (by virtue of training sequences). Nodes employ conventional digital transceivers [58] for the control channels. *Data channels* are used to transmit data taking advantage of multiuser detection at the receivers. Thus, there are two separate transmitter (receiver) circuits in each node. One circuit is intended to transmit (receive) control packets, and the other is used to transmit (receive) data packets. Both circuits operate at different times and frequencies with respect to each other.

5.2.2 Channel Access

Access to the channel is controlled by the signaling that takes place over the control channels assigned to cells. Such signaling occurs simultaneously in all cells, without suffering high interference from each other, because of the different frequency assignment and safe guard-zone separation, as explained in Section 6.2.

The signaling among the nodes in the same cell must be one-to-many and cannot assume knowledge of who the nodes in a cell are, because nodes are mobile. Each node needs to inform the other nodes in its present cell about its presence, plus other control information. We use a very simple approach that allow nodes to convey such control information with a high probability of success, even when the number of nodes in the network is large.

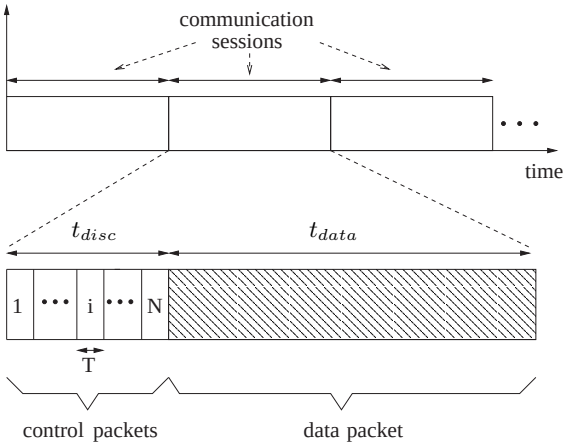

Figure 5.3: Time series representation of control and data packets. t_{disc} is the neighbor discovery period. t_{data} is the time period for transmission of data. t_{disc} plus t_{data} form a communication session.

As illustrated in Fig. 5.3, access to the channel is divided in time into a discovery phase and a data-transmission phase. The time period of "neighbor discovery" (t_{disc}) and the time period for transmission of data (t_{data}) are constant and independent of the number of

nodes (n) in the network. Together, they compose a "communication session." The common time reference for communication sessions is assumed to be obtained through GPS for simplicity. The values of t_{disc} and t_{data} are system-design parameters. t_{disc} is subdivided into multiple slots, each of length T. Hence, $T = \frac{t_{disc}}{N}$, where N is a positive integer number to calculate according to some given criterion as explained later. For practical considerations, the overhead incurred by t_{disc} must be small compared to t_{data}. Each control packet conveys, as a minimum, the node ID, a short training sequence and the expected packet sequence numbers (SNs), while a data packet bears long sequences of bits. Therefore, we assume that $t_{disc} << t_{data}$. The control frequency band $\Delta\omega$ (see Section 6.2.1) must be a function of n in order to have t_{disc} not depending on n. Consequently, when n increases, $\Delta\omega$ also increases (see Section 6.4.3), such that t_{disc} remains constant.

Because each node senses the channel to detect collision while transmitting in the control channel, the nodes involved in a collision do not participate in that session anymore, i.e., they remain silent until the next session. In addition, due to practical limitations of CDMA or MIMO systems (e.g., hardware complexity, maximum number of receive antennas, power consumption constraint, costs, etc.), only a small number of nodes can communicate per cell. Let $\mathcal{A}$ be the maximum number of nodes allowed to communicate per cell. Hence, only the first $\mathcal{A}$ nodes that successfully announced their control packets during the neighbor discovery phase transmit (or receive) data during t_{data} right after t_{disc} for that session. Given that this access is random and independent from the node ID, no privilege is given to a node with high ID value. As described in the following chapters, the IDs are used only to order the code and frequency assignments in each cell.

Each time the discovery period is about to begin, each node randomly chooses one of the N mini-slots and transmits its control packet. If there is no collision, i.e., if the other nodes in the same cell choose different mini-slots to transmit, then all the other nodes in the cell will receive this packet. A collision happens every time two or more nodes in the same cell choose to transmit in the same mini-slot. Let Z_i be the number of nodes in the same cell choosing mini-slot i to transmit their control packets. Let Z_{max} be the maximum number of nodes in any cell. The probability of collision $\mathbb{P}_c$ is given by

$$\begin{aligned}\mathbb{P}_c = \mathbb{P}\{Z_i \geq 2\} &= 1 - \left[\sum_{i=0}^{1} \binom{Z_{max}}{i} \left(\tfrac{1}{N}\right)^i \left(1-\tfrac{1}{N}\right)^{Z_{max}-i}\right] \\ &= 1 - \left(1-\tfrac{1}{N}\right)^{Z_{max}} - \tfrac{Z_{max}}{N}\left(1-\tfrac{1}{N}\right)^{Z_{max}-1}. \end{aligned} \tag{5.1}$$

The criterion used to choose N is as follows. We calculate N such that there is no collision with probability approaching 1 as $n \to \infty$, for example, with probability $\geq 1 - \frac{\log(\log(n))}{\log(n)}$. From Eq. (5.1), $\mathbb{P}_c \leq 1 - \left(1-\frac{1}{N}\right)^{Z_{max}}$. Accordingly, we choose

$$\begin{aligned} &\mathbb{P}_c \leq 1 - \left(1-\tfrac{1}{N}\right)^{Z_{max}} \leq \tfrac{\log(\log(n))}{\log(n)} \\ \Longrightarrow N \geq &\left\lceil \frac{1}{1-\left(1-\frac{\log(\log(n))}{\log(n)}\right)^{\frac{1}{Z_{max}}}} \right\rceil = N_{min}, \end{aligned} \tag{5.2}$$

in which $\lceil x \rceil$ stands for the ceil function (i.e., the smallest integer greater than or equal to x), and N_{min} is the actual value to be implemented for N. Thus, we have

$$T = \tfrac{t_{disc}}{N_{min}}. \tag{5.3}$$

Note that Z_{max} is function of the network model. In the next two chapters we compute it for two different models.

Although Z_{max} is the maximum number of nodes in any cell whp, as explained before, at most $\mathcal{A}$ nodes in any cell are allowed to communicate during t_{data}. However, Z_{max} grows very slowly with n as we show later. Thus, for example, by choosing small values for $\mathcal{A}$ for practical values of network parameters, we show in the following chapters that the fraction of cells having more than $\mathcal{A}$ nodes can be bounded by a small constant for large values of n.

5.2.3 Packet Forwarding

Data packet forwarding is composed of two phases (see Figs. 2.1 and 3.1): The packet is transmitted from the source to possibly several relay nodes during *Phase 1* (i.e. multi-copies can be relayed), and it is delivered later to its destination by only one of the relay nodes during *Phase 2*. As discussed in Chapter 3, these multiple one-time relays for the same packet provide better delay performance since the copies of the same packet follow different random routes, looking for the destination, reducing delay.

For the multi-copy technique to work properly, the one-copy delivery of each data packet must be enforced (see Chapter 3). For example, each data packet is assigned a destination identifier (DEST) and a sequence number (SN) in the header field. In each session, during the neighbor discovery phase, each node announces in the control channel its own identifier (ID). Furthermore, given that a node may be engaged with multiple sources as a destination, each node also includes in the control packet a table with the SNs expected from the sources with which it is associated. Accordingly, each node delivers a packet it holds to a destination only if it has the packet intended for the destination and its SN is greater than or equal to the SN announced by the destination. Nodes can discard those packets having SNs smaller than

those announced by their destinations. If there is no destination around a node, it relays a new packet to all its neighbors. Each node compares the DEST of the received packet with the IDs of the other same cell nodes and drops the packet in case of match to avoid keeping a packet that has already been delivered to its destination. In addition, it is obvious that there is no need to use TTL here.

5.3 Conclusions

In this chapter we have introduced the principles of opportunistic cooperation. We proposed a new approach for scalable mobile ad hoc networks where communication among nodes is many-to-many as opposed to the traditional one-to-one. The basic idea is to allow multiple simultaneous nodes to communicate to each other using distinct frequency bandwidths where receiver nodes employ multiuser detection. The next two chapters specifically describe two possible approaches to implement opportunistic cooperation.

Chapter 6

Opportunistic Cooperation with CDMA-SIC

In this chapter, we present and analyze opportunistic cooperation based on a hybrid FDMA/CDMA-SIC scheme for mobile ad hoc networks [45], [46].

First, the model that we adopt to analyze the capacity of wireless networks and MANETs is summarized. This is the same basic network model that has been used recently by several other researchers [28], [23], [26], [66], [5], [39], [51]. The elements of opportunistic cooperation in the context of our model are described. These elements consists of: (a) allocating the available bandwidth to facilitate the task of SIC receivers by reducing non-cooperative (destructive) interference around receivers, (b) acquiring knowledge about the sources with which a given receiver and sender should cooperate, (c) scheduling transmissions based on the allocation of bandwidth and knowledge of the "neighborhood," and (d) forwarding multiple copies of each packet to improve reliability and to reduce delay by exploiting SIC receivers.

Section 6.3 introduces the interference analysis for opportunistic cooperation, and presents the data transceiver structure for each node.

Section 6.4 presents the calculation of the link's Shannon capacity, the per source-destination throughput, and the bandwidth scalability for opportunistic cooperation. We show that, by utilizing mobility [26], multiuser diversity [35], SIC, cognition,[1] and bandwidth expansion, the link's Shannon capacity and the per source-destination throughput attain an upper-bound of $O(n^{\frac{\alpha}{2}})$ and a lower-bound of $\Omega[f(n)]$, where $1 \leq f(n) < n^{\frac{\alpha}{2}}$, for n total nodes in the network, and a path loss parameter $\alpha > 2$. The capacity improvement obtained is consistent with the predictions made by Xie and Kumar [68] and Toumpis and Goldsmith [65].

Besides bandwidth expansion, one main reason why the above performance improvement can be attained with opportunistic cooperation is the ability of nodes to concurrently transmit their packets to one another cooperatively over non-overlapping frequency bands. Although CDMA and SIC have been studied in the past [59], [48], [32], prior approaches have assumed that each transmission competes with others. Similarly, prior schemes that combine different forms of channel division (e.g., frequency division multiple access (FDMA) and CDMA [18], or CDMA with space division [7]) do not consider the use of SIC and assume that transmissions compete with one another.

Section 6.5 addresses the delay performance associated with opportunistic cooperation. Section 6.6.1 corroborates our capacity analysis by applying the same CDMA-SIC feature we propose for MANETs to static networks. The per source-destination throughput is shown to have a lower-bound similar to the result obtained by Negi and Rajeswaran [51].

[1] i.e., allowing a node to know where it is and who the nodes in the same cell are.

However, our scheme produces a reduced bandwidth expansion, which is expected given that we use SIC at the receivers in our scheme. Section 6.6.2 describes a comparison with mobile networks [26], [39] in terms of the fraction of cells that forward the packets. We show that opportunistic cooperation improves the throughput by a constant factor compared to the results in [26] and [39] under similar bandwidth expansion. Section 6.7 concludes the chapter summarizing its main ideas.

6.1 Network Model

The network model is the same as presented in Section 2.2, except that the unit area is assumed to have a square shape.

6.2 Attaining Opportunistic Cooperation Using CDMA

We present a simple example of how opportunistic cooperation can be implemented with a hybrid scheme based on FDMA and CDMA [2] that supports many-to-many communication. Therefore, to take advantage of SIC circuits at receivers, we use direct sequence CDMA (DS-CDMA) [31] with non-overlapping frequency bands (i.e., FDMA/CDMA), in which distinct pseudo-noise (PN) sequences (or codes) are assigned to different nodes in the same region of the network.

The FDMA/CDMA-SIC scheme works by implementing *control* and *data* channels. To simplify our analysis, we assume that cells have square shapes, which leads to the network

[2] Note that a hybrid FDMA/CDMA is one example to implement opportunistic cooperation. Other multiple access schemes based on MIMO systems can be also utilized which will be discussed in the next chapter.

structure illustrated in Fig. 6.1. Every cell has an area equal to $a(n) = \frac{1}{\phi n}$, in which $\phi \in (0, 1)$ is the cell area parameter of the network.

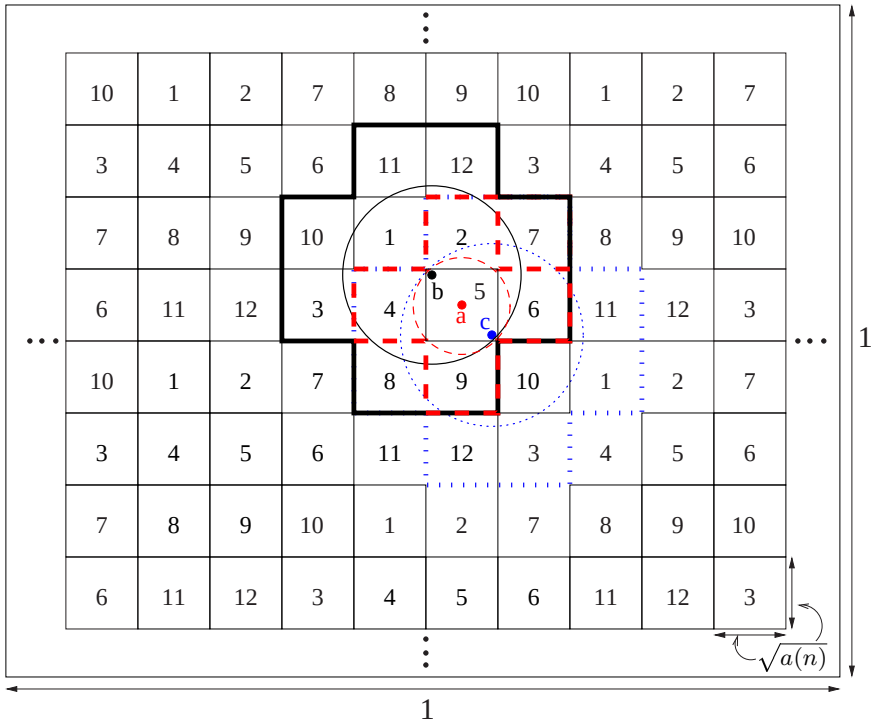

Figure 6.1: Cells numbering in the unit square network. $a(n) = \frac{1}{\phi n}$ is the cell area. Each cell is associated to a control frequency bandwidth (ω_1 to ω_{12}) and to a PN sequence set (ξ_1 to ξ_{12}).

6.2.1 Control Channels

Each cell is allocated a control frequency band from twelve non-overlapping control frequency bands required (and available), ω_1 to ω_{12}, to enable frequency reuse while avoiding interference in the control channels from nearby cells (see Fig. 6.1). Each control frequency band ω_i has a size of $|\omega_i| = \Delta\omega$ for $i = 1, ..., 12$ (see Fig. 6.2). Hence, the total bandwidth required for the control channels is $\Delta\omega_C = 12\Delta\omega$.

The maximum number of cells in a cluster associated to a given node is twelve. The

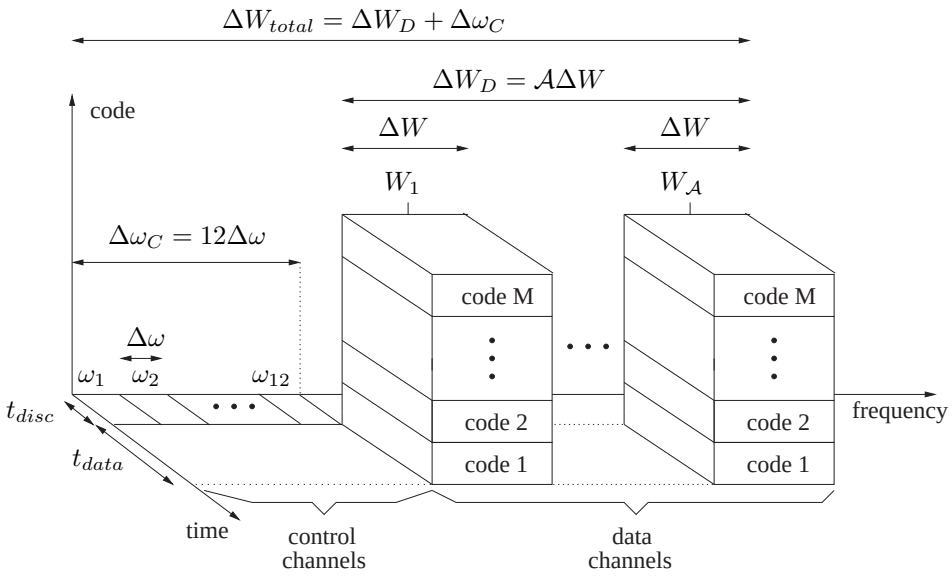

Figure 6.2: Data and control channels spectra for the network.

number of cells and the cluster shape are chosen such that if the receiver range has maximum value, (i.e., almost $\sqrt{2a(n)}$), then the receiver range reaches all these cells. Accordingly, two cells employing the same control frequency band are kept at least $\sqrt{5a(n)}$ units away from each other (a safe guard-zone separation), thus guaranteeing an asymptotic constant non-zero signal-to-noise and interference ratio (SNIR) as $n \to \infty$ [39] in the control channel, and making local communication feasible and allowing control frequency reuse.

To simplify the control signaling required among nodes to determine which control channel a given node should use, each node is assumed to:

- Know its own position (but not the position of any other node) by utilizing a GPS circuit [53] or some other technique.

- Store a geographical map of the cells in the network with the associated control frequencies and data codes (as illustrated in Fig. 6.1).

The GPS receiver is assumed to be used to provide an accurate common time reference to keep all nodes synchronized.

Each node has twelve receiver circuits (called control channel receivers) to listen to the control channel of the cell as well as to the other eleven control channels. Therefore, one control receiver circuit is used to transmit or receive in the control channel where the node is currently located, while the other eleven control circuits are used to receive (listen) the control channels of the neighbor cells. This permits the nodes to obtain the IDs of the other nodes in its cell and the node IDs from the cluster it perceives, while not transmitting during the neighbor discovery phase.

We assume that, while transmitting in the control channel of the cell, any node simultaneously uses its control channel receiver circuit to sense the cell control channel (e.g., using echo cancelling techniques [8], [69]) in order to detect collisions during its transmission in the neighbor discovery phase.

6.2.2 Data Channels

Due to practical limitations of CDMA systems, the number of PN sequences (or codes) available for communication is finite. To allow code reuse in the data channels of the network while reducing the negative effects of interference, each cell is allocated a set of PN sequences from the twelve different code sets available, ξ_1 to ξ_{12}, for communication in each data channel. Because a PN sequence can be associated with a sequence of bits [31], they can be ordered and grouped as follows. $\xi_1 = \{C_1, ..., C_{\mathcal{A}}\}$, $\xi_2 = \{C_{\mathcal{A}+1}, ..., C_{2\mathcal{A}}\}$, ..., $\xi_{12} = \{C_{11\mathcal{A}+1}, ..., C_{12\mathcal{A}}\}$, in which C_i stands for the i^{th} PN sequence. Therefore, $12\mathcal{A}$ is the

maximum number of codes used. In this way, any set of twelve cells, numbered from 1 to 12 according to Fig. 6.1, has a different set of codes.

A simple way to reduce the effects of interference at the receivers is to partition the available data bandwidth into orthogonal channels. Accordingly, each non-overlapping data channel is a half-duplex link of bandwidth ΔW (see Fig. 6.2). Since $\mathcal{A}$ is the maximum number of nodes allowed to communicate in any cell, then $\Delta W_D = \mathcal{A}\Delta W$ is the data bandwidth required for the entire network, and $M = 12\mathcal{A}$ distinct PN sequences are needed for local data communication. M is also called the spreading factor (or processing gain). ΔW is related to M by $\Delta W = BM$, where B is the original data bandwidth before spreading [31].

As we discuss in Section 6.2.3, the signaling in the control channel provides each node in a cell i knowledge of who the other nodes in this same cell are, and the node uses this information to choose a data channel to receive data, as well as to select a code for transmission from the available PN sequences in ξ_i based on its own and neighbor IDs, in the following order[3]:

- The node with the highest ID in cell i is associated (for reception) with the data channel ΔW centered at W_1, and it is assigned the first PN sequence in ξ_i.

- The node with the second highest ID in cell i is associated (for reception) with the data channel ΔW centered at W_2, and it is assigned the second PN sequence in ξ_i, and this continues for all nodes in cell i.

- The data channels not utilized become idle in cell i. This happens in those cells where

[3]To simplify our notation, we will also denote W_j as the data frequency channel (or sub-spectrum) associated to node j.

the number of nodes is smaller than $\mathcal{A}$.

Each node also executes this same procedure for the association between node-IDs and codes for all cells within its receiver range. In this way, each node has the IDs and training sequences from the nodes in the same cell in which it is located, as well as from the other nodes in the cluster it perceives within its receiver range.

Note that, in a communication session, each node only needs to know the nodes in its cell (obtained during the neighbor discovery phase) and the signal strengths received from them (by virtue of CDMA-SIC), in order to set its receiver range.

With the deployment illustrated in Fig. 6.1, two or more nodes, while moving in the same cell, can perceive clusters composed of different cells with at most twelve distinct numbers. For example, in the middle of Fig. 6.1, node a, located exactly at the center of the cell 5, can apply SIC to decode the data signal from node b and node c in that same cell. Each node is almost at a distance of $\sqrt{a(n)/2}$ from node a as shown, and hence, the receiver range for a is approximately $\sqrt{a(n)/2}$ and it is indicated by the dashed circle. Node a perceives the cluster composed of the five cells $\{2,4,5,6,9\}$ indicated in a dashed line (i.e., those cells reached by a's receiver range), and the other remaining closest four different cells $\{1,7,8,10\}$ are not necessary for decoding purposes. However, node b has to decode signals from nodes a and c, which is almost $\sqrt{2a(n)}$ away; thus, the receiver range for b is approximately $\sqrt{2a(n)}$ and it is indicated by the solid circle. Hence, node b perceives the cluster with all the twelve cells $\{11,12,10,1,2,7,3,4,5,6,8,9\}$ shown in solid line, i.e., those cells reached by its receiver range. Analogously, node c perceives $\{2,7,4,5,6,11,8,9,10,1,12,3\}$ illustrated in dotted line. Therefore, by construction, the cluster perceived by any node is composed of cells having

distinct numbers, and consequently, different codes.

At time t, a cell has Z nodes such that the data communication is Z-to-Z, i.e., many-to-many communications (see Fig. 6.3) where Z is a random variable given that nodes are mobile and can move among cells. Each node employs a multi-user transmitter DS-CDMA [31] (i.e., it transmits up to $Z-1$ simultaneous data packets per session in which each packet is sent through a different data channel due to FDMA, as illustrated in Fig. 6.3 (downlink)) and spreads the data using the PN sequence associated to its ID. The node can transmit a different data packet in each sub-spectrum or choose to send the same data packet in all (non-idle) bands, or a combination of both, depending on whether the node has a data packet for any destination in the same cell where it is located. Thus, multi-copies of the same packet can be simultaneously relayed to different nodes, which helps to reduce delivery delay, as explained in Section 5.2.3.

Given that each node is endowed with a multi-user detector (the SIC circuit) for its associated receiving data channel, it is able to decode the $Z-1$ simultaneous transmissions from all nodes in its cell (see Fig. 6.3(uplink)).

Summarizing, as illustrated in Fig. 6.3, each node transmits (spreading the data with its associated code) different (or the same) data packets to the other $Z-1$ nodes in the same cell, using $Z-1$ distinct data channels (downlink), while it simultaneously receives up to $Z-1$ different data packets from the other $Z-1$ nodes through its assigned data channel (uplink), in which each distinct packet was spread with a different PN sequence. Hence, every node can concurrently transmit (receive) to (from) all other nodes in the same cell.

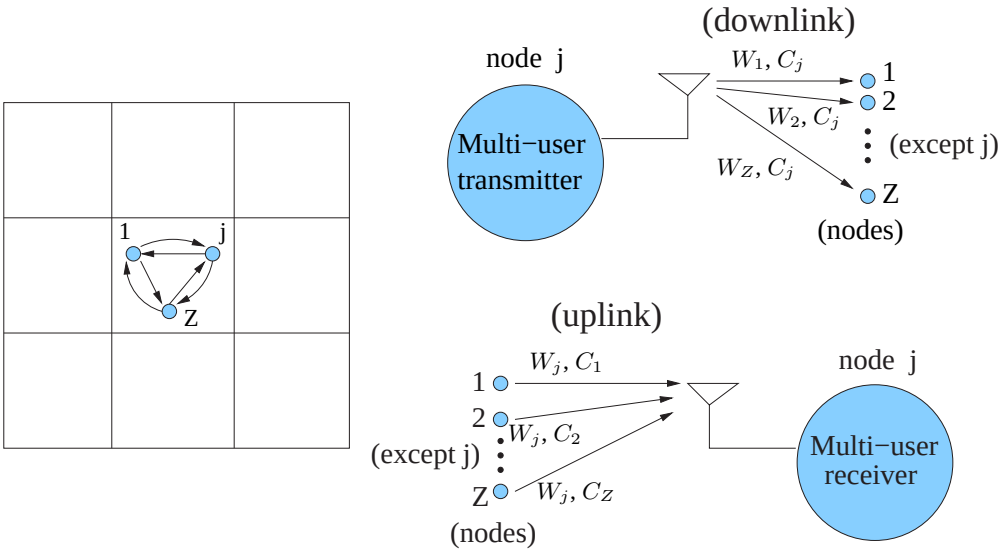

Figure 6.3: Uplink and downlink description for data channels in a cell. Communication is Z-to-Z (i.e., many-to-many).

6.2.3 Channel Access

As discussed in Section 5.2.2, access to the channel is controlled by the signaling that takes place over the control channels assigned to cells. Such signaling occurs simultaneously in all cells, without suffering high interference from each other because of the different frequency assignment and safe guard-zone separation, as explained in Section 6.2.

The following lemma provides the relationship between Z_{max} and n.

Lemma 1 *For the uniform mobility model, with high probability (whp), i.e., with probability* $\geq 1 - \frac{c_5}{n}$*, for some positive constant* c_5*, the maximum number of nodes in any cell is given by*

$$Z_{max} = \left\lceil \frac{3\log(n)}{\log(\log(n^{\phi}))} \right\rceil . \tag{6.1}$$

Proof: Let $\mathcal{E}_{j,z}$ denote the event that cell j contains at least z nodes. Let $z = Z_{max} =$

$\left\lceil \frac{3\log(n)}{\log(\log(n^\phi))} \right\rceil$. The total number of cells in the network is $(\#\text{ of cells}) = 1/a(n) = \phi n$. For any cell j, due to the uniform mobility model, the distribution of the nodes is Binomial [47]. Therefore, we have

$$\begin{aligned}
\mathbb{P}\{\mathcal{E}_{j,z}\} &= \sum_{i=z}^{n} \binom{n}{i} \left(\frac{1}{\#\text{ of cells}}\right)^i \left(1 - \frac{1}{\#\text{ of cells}}\right)^{n-i} \\
&= \sum_{i=z}^{n} \binom{n}{i} \left(\frac{1}{\phi n}\right)^i \left(1 - \frac{1}{\phi n}\right)^{n-i} \\
&\leq \sum_{i=z}^{n} \binom{n}{i} \left(\frac{1}{\phi n}\right)^i \\
&\leq \sum_{i=z}^{n} \left(\frac{ne}{i}\right)^i \left(\frac{1}{\phi n}\right)^i \qquad (6.2) \\
&\leq \sum_{i=z}^{\infty} \left(\frac{e}{\phi i}\right)^i \\
&= \left(\frac{e}{\phi z}\right)^z \left(\frac{1}{1 - \frac{e}{\phi z}}\right) \\
&\leq 2\left(\frac{e}{\phi z}\right)^z \qquad (6.3) \\
&\leq 2\left(\frac{e/\phi}{\frac{3\log(n)}{\log(\log(n^\phi))}}\right)^z \\
&= 2\left(e^{1-\log(3)-\log(\log(n^\phi))+\log(\log(\log(n^\phi)))}\right)^z \\
&\leq 2\left(e^{-\log(\log(n^\phi))+\log(\log(\log(n^\phi)))}\right)^z \\
&\leq 2\, e^{-3\log(n)+\frac{\log(\log(\log(n^\phi)))}{\log(\log(n^\phi))}\,3\log(n)} \\
&\leq 2\, e^{-2\log(n)} \qquad (6.4) \\
&= \frac{2}{n^2}\,, \qquad (6.5)
\end{aligned}$$

Table 6.1: Performance values for the neighbor discovery phase for $\phi = 1/3$. $\mathbb{P}_c$ refers to Z_{max}.

n	Z_{max}	N_{min}	$\mathbb{P}_c$
1000	25	77	0.04
10^6	28	134	0.02
10^9	33	210	0.01

where we used $\binom{n}{i} \leq \frac{n^i}{i!} \leq (\frac{ne}{i})^i$ to obtain Eq. (6.2), and for large values of n, we utilized $\left(\frac{1}{1-\frac{e}{\phi z}}\right) \leq 2$ for Eq. (6.3), as well as $\frac{\log(\log(\log(n^\phi)))}{\log(\log(n^\phi))} < \frac{1}{3}$ for Eq. (6.4).

Now, since there are ϕn cells, the probability that any cell receives at least z nodes is bounded by

$$\mathbb{P}\left\{\bigcup_{j=1}^{\text{\# of cells}} \mathcal{E}_{j,z}\right\} = \mathbb{P}\left\{\bigcup_{j=1}^{\phi n} \mathcal{E}_{j,z}\right\} \leq \sum_{j=1}^{\phi n} \mathbb{P}\{\mathcal{E}_{j,z}\}. \tag{6.6}$$

Let $\overline{\mathcal{E}}_z$ be the event that no cell has more than z nodes. Hence,

$$\begin{aligned} \mathbb{P}\{\overline{\mathcal{E}}_z\} &= 1 - \mathbb{P}\left\{\bigcup_{j=1}^{\phi n} \mathcal{E}_{j,z}\right\} \\ &\geq 1 - \sum_{j=1}^{\phi n} \mathbb{P}\left\{\mathcal{E}_{j,z}\right\} \\ &\geq 1 - \phi n \frac{2}{n^2} \\ &= 1 - \frac{2\phi}{n}. \end{aligned} \tag{6.7}$$

Thus, no cell has more than $\left\lceil \frac{3\ \log(n)}{\log(\log(n^\phi))} \right\rceil$ nodes whp. ■

Table 6.1 shows the values attained by Z_{max}, N_{min}, and $\mathbb{P}_c$, for different values of n. As the table shows, the probability of collision $\mathbb{P}_c$ remains very low for a wide range of values of n. Note that collisions are even rarer within cells having fewer nodes than Z_{max}. Moreover, we defined the criterion for collision such that $\mathbb{P}_c \to 0$ as $n \to \infty$.

Although Z_{max} is the maximum number of nodes in any cell whp, the number of codes to be used is limited in practice. Therefore, as explained before, at most $\mathcal{A}$ nodes in any cell are allowed to get a code and communicate during t_{data}. However, Z_{max} grows very slowly with n as shown in Table 6.1. Thus, for example, by choosing small values for $\mathcal{A}$ for practical values of ϕ, we show next that the fraction of cells having more than $\mathcal{A}$ nodes can be bounded by a small constant for large values of n. Accordingly, the total number of cells in the network is (# of cells) $= 1/a(n) = \phi n$. By applying random occupancy theory [47], considering the uniform mobility model, the fraction of cells containing $Z = j$ nodes is

$$\begin{aligned} \mathbb{P}\{Z = j\} &= \begin{pmatrix} n \\ j \end{pmatrix} \left(\frac{1}{\text{\# of cells}}\right)^j \left(1 - \frac{1}{\text{\# of cells}}\right)^{n-j} \\ &= \begin{pmatrix} n \\ j \end{pmatrix} \left(\frac{1}{\phi n}\right)^j \left(1 - \frac{1}{\phi n}\right)^{n-j}. \end{aligned} \tag{6.8}$$

Given that $\begin{pmatrix} n \\ j \end{pmatrix} \approx \frac{n^j}{j!}$ for $n >> j$, and using the limit $\left(1 - \frac{1}{x}\right)^x \longrightarrow e^{-1}$ as $x \to \infty$, we have the following result

$$\lim_{n\to\infty} \mathbb{P}\{Z = j\} = \frac{1}{j!}\left(\frac{1}{\phi}\right)^j e^{-1/\phi}. \tag{6.9}$$

The fraction of cells having more than $\mathcal{A}$ nodes for given ϕ is obtained by

$$\begin{aligned} \lim_{n\to\infty} \mathbb{P}\{Z > \mathcal{A}\} &= \sum_{j=A+1}^{\infty} \frac{1}{j!}\left(\frac{1}{\phi}\right)^j e^{-1/\phi} \\ &= 1 - \frac{\Gamma(\mathcal{A}+1, 1/\phi)}{\Gamma(\mathcal{A}+1)}, \end{aligned} \tag{6.10}$$

where $\Gamma(m+1) = m!$, and $\Gamma(m,x) = \int_x^\infty y^{m-1}e^{-y}dy$ is the incomplete Gamma function.

For example, $\lim_{n\to\infty} \mathbb{P}\{Z > 8\} = 0.0038$ for $\phi = 1/3$. Therefore, the fraction of cells having more than $\mathcal{A}$ nodes is very small as $n \to \infty$ and $\mathcal{A} \geq 8$.

Now, the average number of communication sessions (H) per node per cell is a function of the time the node moves in the cell. A node travels inside a cell on average every t_{trip}, which is proportional to

$$t_{trip} \propto \frac{\Delta S}{v(n)} \Longrightarrow t_{trip} = \Theta\left(\frac{\sqrt{a(n)}}{v(n)}\right), \tag{6.11}$$

where $\Delta S = \Theta(\sqrt{a(n)})$ is the average distance traveled inside the cell. For a fixed area network, $v(n) = \Theta(1/\sqrt{n})$ and $\sqrt{a(n)} = 1/\sqrt{\phi n}$. It follows from (6.11) that t_{trip} is indeed a constant. Hence, the average number of sessions H per node per cell is given by

$$H = \frac{t_{trip}}{t_{disc} + t_{data}} = c_{21}, \tag{6.12}$$

i.e., H is a constant and does not depend on n. Therefore, t_{disc} and t_{data} must be chosen such that $H \geq 1$.

The data packet forwarding consists of two phases (see Figs. 2.1 and 3.1) and was explained in Section 5.2.3.

6.3 Interference Analysis and Transceiver Scheme

6.3.1 Interference in a Data Channel

Although we have assumed that transmitters and receivers are synchronized, packets are received at a given node asynchronously due to the different distances from each transmitting node. Besides, fading effects can amplify the asynchronous nature of packet reception.

Consequently, even if the PN sequences of data channels are orthogonal, they exhibit partial cross-correlation at the receiver, which results in multiple access interference (MAI) [31].

According to the definitions given in Section 1.1, the interference can be decomposed in the following two types according to the receiver range of node j.

Destructive Interference (DEI) for node j comes from nodes outside the receiver range of j and transmitting in W_j. DEI constitutes the part of the interference that cannot be decoded.

Constructive Interference (COI) comes from nodes within the receiver range of j and transmitting in W_j. By construction, as shown in Section 6.2, the nodes within the receiver range of j and transmitting in W_j use different codes (since they are in the same cluster perceived by j) exhibiting partial cross-correlation, as explained before, due to the asynchronous nature of the uplink channel [31]. COI constitutes the decodable part of the interference.

If node i transmits data to node j at time t over the sub-spectrum W_j, the signal-to-noise and interference ratio (SNIR) at the receiver j, without SIC, is given by [26]

$$SNIR = \frac{P_{ij}(t)g_{ij}(t)}{BN_0 + \underbrace{\frac{1}{M}\sum_{\substack{k \in range \\ k \neq i}} P_{kj}(t)g_{kj}(t)}_{COI} + \underbrace{\frac{1}{M}\sum_{\substack{k \notin range \\ C_k \neq C_i}} P_{kj}(t)g_{kj}(t) + \sum_{\substack{k \notin range \\ C_k = C_i}} P_{kj}(t)g_{kj}(t)}_{DEI}}. \tag{6.13}$$

where $range$ [4] is the set of nodes transmitting in W_j and reached by the receiver range of node j, C_i is the PN sequence used by sender node i, $P_{ij}(t) = P \; \forall (i,j)$ is the transmit power

[4] Note that the notation $k \notin range$ in (6.13) indicates that node k is outside the receiver range of node j transmitting in W_j.

chosen by node i to transmit to node j (i.e., $P_{ij}(t)$ is constant for all pairs (i,j)); $g_{ij}(t)$ is the channel path gain from node i to j and it is given by Eq. (2.4), B is the original bandwidth of the data signal (before spreading). BN_0 is the noise power (where N_0 is the noise power spectral density), $M = 12\mathcal{A}$ is the spreading factor, COI and DEI are the total interference in W_j at node j. Note that the summation terms in the denominator containing the factor $1/M$ constitute the multiple access interference (MAI) [31], and the last summation term (without the factor $1/M$) results from code reuse in the network and we call it *same-code interference* (SCI). Thus,

$$MAI = \frac{1}{M} \sum_{\substack{k \in range \\ k \neq i}} P_{kj}(t) g_{kj}(t) + \frac{1}{M} \sum_{\substack{k \notin range \\ C_k \neq C_i}} P_{kj}(t) g_{kj}(t) \tag{6.14}$$

$$SCI = \sum_{\substack{k \notin range \\ C_k = C_i}} P_{kj}(t) g_{kj}(t), \tag{6.15}$$

such that, $MAI + SCI = COI + DEI$. MAI and SCI are easier for calculating SNIR, as explained later.

6.3.2 FDMA/CDMA Transmitter Scheme

The FDMA/CDMA transmitter scheme for a node j is shown in Fig. 6.4(a). All packets previously relayed to node j are stored in the *buffer for relayed packets*. In each session, after the discovery phase, node j knows who its neighbors are in the cell where it is located, and loads the *buffer for destination packets* if it has packet for each destination in the cell. Each packet signal p_x coming from the *banks of buffers* passes through a switch S_x, for integer $x \in [1, \mathcal{A}]$. After S_x, the signal is spread by the code C_j assigned to node j. The outcome is modulated by the frequency carrier associated with the node the packet is intended

for. Finally, all modulated signals are summed up and transmitted through the antenna (see also Fig. 6.3(downlink)).

The *banks of buffers* not only store the packets relayed by node j but also packets generated locally by node j. The position of each switch S_x is chosen according to the existence of the destination node (assigned to W_x) for the packet p_x, in the same cell j is moving. Accordingly, the switch S_x gives priority to the packet in the *buffer for destinations*. If the node assigned to the data channel W_x is not a destination for a relayed packet, then the switch selects the new packet (p_j) generated locally by node j. Furthermore, if no node is assigned to the data sub-spectrum W_x in the cell that j is located, then S_x is set to 0 (ground) and no information is transmitted, contributing no increase in the interference through this data channel. Therefore, the objective of the switches is to give absolute priority to the *delivery* of packets (i.e., *Phase 2*) as described in Section 5.2.3, and prevent any unnecessary transmission of data through an idle data channel in the cell.

Note that the packet generated locally in node j is transmitted to those nodes that are not destinations. In this way, multi-copies of the same packet generated locally at j can be relayed to other nodes in the same cell [39].

6.3.3 CDMA-SIC Receiver Scheme

The basic decoding scheme of the CDMA-SIC receiver circuit is illustrated in Fig. 6.4(b) [54] (see also Fig. 6.3(uplink)). The signal coming from the antenna passes through a band pass filter (BPF) centered at W_j which selects only the data sub-spectrum ΔW associated with j. The filtered signal is demodulated to the baseband spectrum. The received

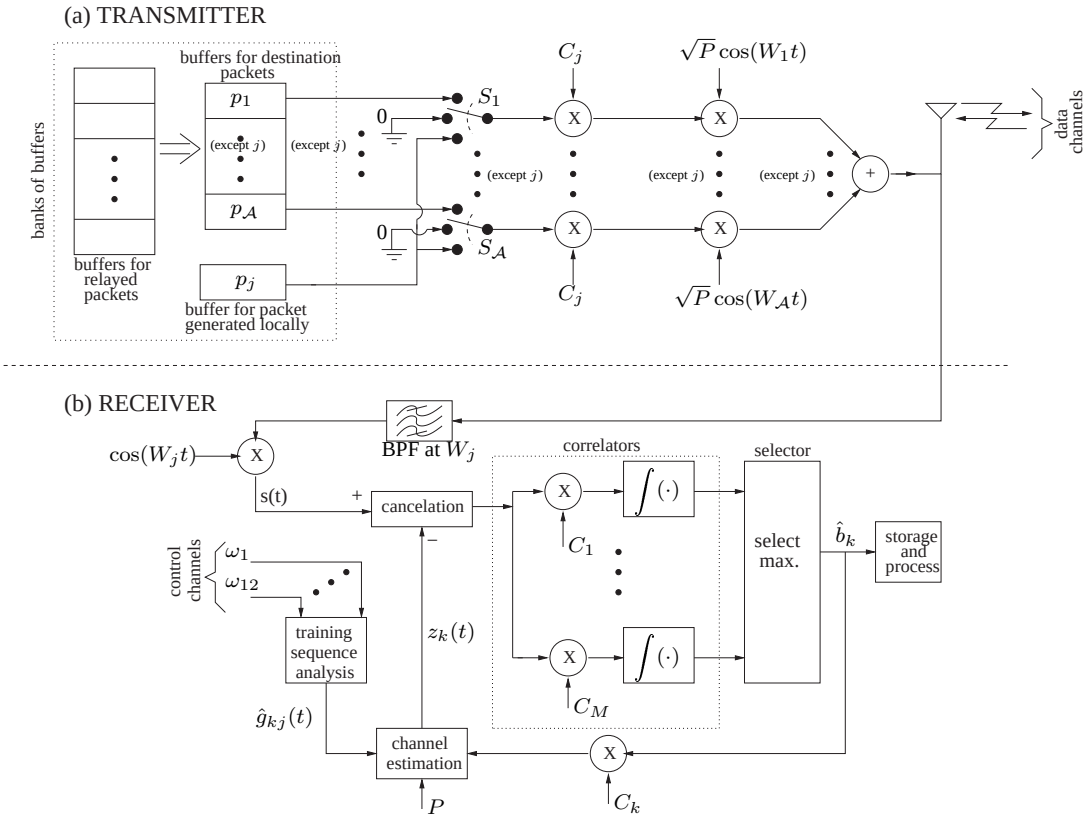

Figure 6.4: Hybrid FDMA/CDMA data transceiver scheme for node j. (a) FDMA/CDMA transmitter. (b) CDMA successive interference cancellation receiver.

baseband data signal $s(t)$ is subtracted (in the *cancellation* block) from an estimation locally generated $z_k(t)$, and fed into a bank of *correlators*. Each correlation is performed by using a distinct PN sequence. A *selector* decides which output from the correlators is the highest. This operation is also known as maximum a posteriori (MAP). The decoding is performed successively from the strongest signal to the weakest. Thus, with the simple path propagation model assumed in Eq. (2.4), the strongest signal decoded first comes from the closest neighbor to node j (not necessarily in the same cell of j but in the cluster it perceives), while the weakest (decoded last) is the farthest node to node j in the cell node j is located. After a decision in *selector*, the estimated decoded data bits $\hat{b}_k$ associated with node k are stored for further processing and are also locally re-encoded using the associated PN sequence C_k. Therefore, it results in the locally re-generated baseband signal $z_k(t)$ using an estimation $\hat{g}_{kj}(t)$ of the channel related to node k. The *channel estimation* can be obtained in different ways. One way is by the receiving node listening in the control channels (ω_1 to ω_{12}), during the neighbor discovery phase, in which each node transmits a training sequence (or even a pilot signal) in the control packet such that each receiver can estimate the attenuation incurred in the data channel from each node, assuming that the control and data channels incur similar propagation effects. This entire SIC process is repeated until all signals from the nodes in the same cell are successfully obtained. We assume that the processing time required to perform the SIC operation is negligible compared to each data bit duration. Accordingly, let MAI' be the remaining multiple access interference at node j after applying SIC up to node i, i.e.,

$$MAI' = \frac{1}{M} \sum_{\substack{k \in range \\ g_{kj} < g_{ij}}} P_{kj}(t) g_{kj}(t) + \frac{1}{M} \sum_{\substack{k \notin range \\ C_k \neq C_i}} P_{kj}(t) g_{kj}(t)$$

$$= \frac{1}{M} \sum_{\substack{\forall k\,:\, g_{kj} < g_{ij} \\ C_k \neq C_i}} P_{kj}(t) g_{kj}(t). \tag{6.16}$$

Therefore, the resulting SNIR (called $SNIR'$) from node i to node j after applying SIC is given by

$$SNIR' = \frac{P_{ij}(t) g_{ij}(t)}{BN_0 + \underbrace{\frac{1}{M} \sum_{\substack{\forall k : g_{kj} < g_{ij} \\ C_k \neq C_i}} P_{kj}(t) g_{kj}(t)}_{MAI'} + \underbrace{\sum_{\substack{k \notin range \\ C_k = C_i}} P_{kj}(t) g_{kj}(t)}_{SCI}}. \tag{6.17}$$

Note that node j may have nodes transmitting from adjacent cells closer than a far node in the same cell depending on its position. Therefore, node j has to be able to decode the data signals from these adjacent cell nodes before decoding the signal from the far node of the same cell. This explains why each node also needs to obtain the training sequences from the other nodes located outside its cell but still within its receiver range. The *storage and process* block uses the information obtained during the neighbor discovery phase to retain the data packets from nodes in the same cell as j, dropping the outside cell packets since node j cannot keep track of all nodes in adjacent cells to see if this packet is for relaying or destination. This block also processes the DEST and SN information associated with each data packet.

From Eq. (6.13), we observe that SIC is fundamental to derive Eq. (6.17) and for a node to have all packets from the same cell successfully decoded.

In this way, the interference in the data channel caused by the close nodes in the same cluster relative to j are partially removed, resulting in an improved link's Shannon capacity, as shown in Section 6.4.1, making the data communication feasible among j and all other nodes in its same cell.

6.4 Capacity and Bandwidth Analysis

6.4.1 Link's Shannon Capacity

From Eq. (1.1), the link's Shannon capacity R_{ij} in the data channel W_j, in which node j receives from node i, after node j applies SIC up to node i, is given (in units of nats) by [15]

$$\begin{aligned} R_{ij} &= B\log\left(1+SNIR'\right) \\ &= B\log\left(1+\frac{P_{ij}(t)g_{ij}(t)}{BN_o+MAI'+SCI}\right). \end{aligned} \tag{6.18}$$

To calculate R_{ij}, MAI' and SCI must be obtained. MAI' can be computed using Fig. 6.5. Assume that the center of the unit square area is the origin O of the (x,y) coordinates, and that

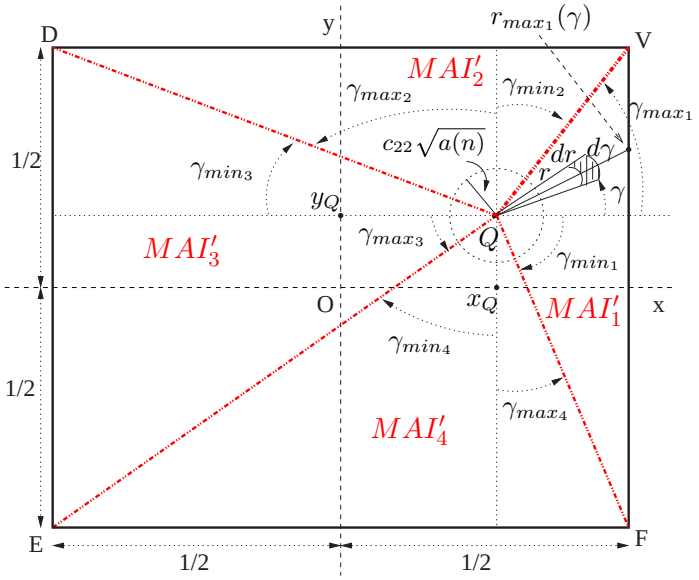

Figure 6.5: Interference regions for node i communicating with node j. The angle γ increases in the counterclockwise direction.

node j is located at point Q with coordinates (x_Q, y_Q) at time t, where $x_Q, y_Q \in (-\frac{1}{2}, \frac{1}{2})$. The calculation considers that the transmitting node i is located at a distance $c_{22}\sqrt{a(n)}$ from j,

while all the remaining interfering nodes are located at a distance greater than $c_{22}\sqrt{a(n)}$ from j due to SIC, where $c_{22} \in (0, \sqrt{2})$ depends on the distance between nodes j and i in the cell. For example, if node j is closer to a corner of the cell and node i is closer to the other corner (diagonally from j) then $c_{22} \approx \sqrt{2}$. We divide the square unit-area network in four triangles and compute the interference generated from each of these regions. The triangle formed by points QVF outlines the interference region MAI'_1, triangle QVD profiles MAI'_2, triangle QDE confines MAI'_3, and triangle QEF contours MAI'_4, such that $MAI' = \sum_{l=1}^{4} MAI'_l$. We consider a differential element area $rdrd\gamma$ that is r units away from the receiver node j. Because the nodes are considered to be uniformly distributed and n grows to infinity, the node density in the network is $\frac{n}{1}$, and the summation in Eq. (6.16) can be upper-bounded by an integral (see also Section 3.4). Hence, the multiple access interference from region MAI'_l at node j is upper-bounded by

$$MAI'_l(n) \leq \int d(MAI'_l) = \int\limits_{region\ MAI'_l} \int \frac{P}{Mr^{\alpha}}\, \phi\, \epsilon_j\, \frac{n}{1}\, r\, dr\, d\gamma, \tag{6.19}$$

in which $l \in \{1, 2, 3, 4\}$, and ϵ_j is the fraction of cells using the bandwidth W_j.

The fraction of cells using the sub-spectrum W_j equals the fraction of cells containing at least j nodes, in which $j \in [2, A]$. Accordingly,

$$\begin{aligned} \epsilon_1 = \epsilon_2 &= \mathbb{P}\{Z \geq 2\} = 1 - \mathbb{P}\{Z = 0\} - \mathbb{P}\{Z = 1\} \\ \epsilon_j &= \mathbb{P}\{Z \geq j\} = 1 - \sum_{k=0}^{j-1} \mathbb{P}\{Z = k\}. \end{aligned} \tag{6.20}$$

Thus, for $\alpha > 2$, given that $a(n) = \frac{1}{\phi n}$, from Eq. (6.19) we have

$$MAI'_l(n) \leq \int_{\gamma_{min_l}}^{\gamma_{max_l}} \int_{c_{22}\sqrt{a(n)}}^{r_{max_l}(\gamma)} \frac{P\, \phi\, \epsilon_j\, n}{Mr^{\alpha-1}}\, dr\, d\gamma$$

$$
\begin{aligned}
&= \frac{P\,\phi\,\epsilon_j\,n}{M} \int_{\gamma_{min_l}}^{\gamma_{max_l}} \frac{r^{2-\alpha}}{2-\alpha}\Big|_{c_{22}\sqrt{a(n)}}^{r_{max_l}(\gamma)} d\gamma \\
&= \frac{P\,\phi\,\epsilon_j\,n}{M(\alpha-2)} \left[\underbrace{\left(\frac{\gamma_{max_l}-\gamma_{min_l}}{c_{22}^{\alpha-2}\,\phi^{1-\frac{\alpha}{2}}}\right)}_{c_{1_l}} n^{\frac{\alpha}{2}-1} - \underbrace{\int_{\gamma_{min_l}}^{\gamma_{max_l}} (r_{max_l}(\gamma))^{2-\alpha} d\gamma}_{c_{2_l}} \right] \\
&= c_{3_l}\epsilon_j\, n^{\frac{\alpha}{2}} \left(1 - \frac{c_{4_l}}{n^{\frac{\alpha}{2}-1}}\right), \qquad (6.21)
\end{aligned}
$$

where c_{1_l}, c_{2_l}, c_{2_l} and c_{3_l} are positive constants given l, (x_Q, y_Q), c_{22}, ϕ, P, M, and α. From Fig. 6.5, the values for γ_{max_l} and γ_{min_l} can be easily obtained once the location (x_Q, y_Q) of node j is given and they are indicated in Table 6.2. Therefore,

$$
MAI' = \sum_{l=1}^{4} MAI'_l \leq \epsilon_j\, n^{\frac{\alpha}{2}} \sum_{l=1}^{4} c_{3_l}(1 - \frac{c_{4_l}}{n^{\frac{\alpha}{2}-1}}) \leq c_{23}\, n^{\frac{\alpha}{2}}, \qquad (6.22)
$$

because $\epsilon_j \in [0, 1]$ given that it is a probability, and $(1 - \frac{c_{4_l}}{n^{\frac{\alpha}{2}-1}}) \leq 1$ for n sufficiently large. Note that the results in Eqs. (6.21) and (6.22) hold for any location (x_Q, y_Q) of node j inside the square area network, and c_{23} is a positive constant function of this location.

On the other hand, the same-code interference (SCI) can be upper-bounded using the same procedure shown for MAI' by considering that these remaining destructive interfering nodes are uniformly distributed over the network area and $\epsilon_j \in [0, 1]$. This result is

$$
SCI = \sum_{\substack{k \notin range \\ C_k = C_i}} P_{kj}(t) g_{kj}(t) \;\leq\; c_{24}\,\epsilon_j\, n^{\frac{\alpha}{2}} \;\leq\; c_{24}\, n^{\frac{\alpha}{2}}, \qquad (6.23)
$$

where c_{24} is a positive constant.

Hence, from Eqs. (6.22) and (6.23), the total remaining interference after SIC at node j is upper-bounded by

$$
MAI' + SCI \;\leq\; c_{25}\, n^{\frac{\alpha}{2}}. \qquad (6.24)
$$

Table 6.2: Values for γ_{max_l} and γ_{min_l} for given the location (x_Q, y_Q) of node j in Fig. 6.5 for computation of Eq. (6.21).

Region (MAI'_l)	γ_{max_l}	γ_{min_l}
MAI'_1	$tan^{-1}\left(\frac{\frac{1}{2}-y_Q}{\frac{1}{2}-x_Q}\right)$	$-tan^{-1}\left(\frac{\frac{1}{2}+y_Q}{\frac{1}{2}-x_Q}\right)$
MAI'_2	$tan^{-1}\left(\frac{\frac{1}{2}+x_Q}{\frac{1}{2}-y_Q}\right)$	$-tan^{-1}\left(\frac{\frac{1}{2}-x_Q}{\frac{1}{2}-y_Q}\right)$
MAI'_3	$tan^{-1}\left(\frac{\frac{1}{2}+y_Q}{\frac{1}{2}+x_Q}\right)$	$-tan^{-1}\left(\frac{\frac{1}{2}-y_Q}{\frac{1}{2}+x_Q}\right)$
MAI'_4	$tan^{-1}\left(\frac{\frac{1}{2}-x_Q}{\frac{1}{2}+y_Q}\right)$	$-tan^{-1}\left(\frac{\frac{1}{2}+x_Q}{\frac{1}{2}+y_Q}\right)$

Now, if we consider the bandwidth expansion $B = f(n)$ such that $1 \leq f(n) < n^{\frac{\alpha}{2}}$, then a lower-bound for R_{ij} can be obtained by using the maximum interference. Accordingly, from Eqs. (6.18) and (6.24), the corresponding link's Shannon capacity lower-bound for node j receiving from node i as $n \to \infty$ is

$$\begin{aligned} R_{ij} &= f(n)\log\left(1+\frac{\frac{P}{\left(c_{22}\sqrt{a(n)}\right)^{\alpha}}}{f(n)N_o+MAI'+SCI}\right) \\ &\geq f(n)\underbrace{\log\left(1+\frac{c_{26}}{\frac{f(n)N_o}{n^{\frac{\alpha}{2}}}+c_{25}}\right)}_{\stackrel{n\to\infty}{\longrightarrow} c_{27}} \\ &= c_{27}f(n), \end{aligned} \tag{6.25}$$

in which c_{26} and c_{27} are positive constants for a given set of chosen values for α, ϕ, P, M, N_o, c_{22}, and position (x_Q, y_Q) of node j.

Eq. (6.25) is a lower-bound because we used the maximum value of interference (obtained from Eq. (6.24)), and this interference dominates noise for the bandwidth expansion $1 \leq B < n^{\frac{\alpha}{2}}$.

On the other hand, if we consider a scenario in which there is no limitation on

available bandwidth, then we can obtain an upper-bound for R_{ij}. From Eq. (6.18),

$$\begin{aligned} R_{ij} &= B\log\left(1+\frac{\frac{P}{\left(c_{22}\sqrt{a(n)}\right)^{\alpha}}}{BN_o+MAI'+SCI}\right) \\ &= B\log\left(1+\frac{c_{26}}{\frac{BN_o}{n^{\frac{\alpha}{2}}}+\frac{1}{n^{\frac{\alpha}{2}}}(MAI'+SCI)}\right). \end{aligned} \tag{6.26}$$

Now, from Eq. (6.24), we have for the term associated with the maximum interference

$$\frac{1}{n^{\frac{\alpha}{2}}}\left(MAI'+SCI\right) \leq c_{25}. \tag{6.27}$$

Therefore, from Eq. (6.26) and by taking $B \geq c_{28}\, n^{\frac{\alpha}{2}}$ for some positive constant c_{28} and n sufficiently large, we obtain

$$\frac{1}{n^{\frac{\alpha}{2}}}\left(MAI'+SCI\right) \leq c_{25} \leq \frac{BN_o}{n^{\frac{\alpha}{2}}}. \tag{6.28}$$

Thus, the term $\frac{BN_o}{n^{\frac{\alpha}{2}}}$ becomes dominant in the denominator of Eq. (6.26) when $B \geq c_{28}\, n^{\frac{\alpha}{2}}$ and $n \to \infty$. Accordingly, from Eqs. (6.26) and (6.28), for $B \geq c_{28}\, n^{\frac{\alpha}{2}}$, we have the following upper-bound for the link's Shannon capacity as $n \to \infty$

$$R_{ij} = n^{\frac{\alpha}{2}} \underbrace{\frac{B}{n^{\frac{\alpha}{2}}}\log\left(1+\frac{c_{26}}{\frac{BN_o}{n^{\frac{\alpha}{2}}}+\frac{1}{n^{\frac{\alpha}{2}}}(MAI'+SCI)}\right)}_{\stackrel{n\to\infty}{\longrightarrow} c_{29}} \leq c_{29}\, n^{\frac{\alpha}{2}}, \tag{6.29}$$

in which c_{29} is a positive constant. Eq. (6.29) is an upper-bound because the noise dominates the interference (as a consequence of large bandwidth expansion), such that, for $B \geq c_{28}\, n^{\frac{\alpha}{2}}$ and $n \to \infty$, we have

$$\frac{B}{n^{\frac{\alpha}{2}}}\log\left(1+\frac{c_{26}}{\frac{BN_o}{n^{\frac{\alpha}{2}}}+\frac{1}{n^{\frac{\alpha}{2}}}(MAI'+SCI)}\right) \leq c_{29}. \tag{6.30}$$

Eqs. (6.25) and (6.29) describe two limiting cases. The former is the minimum capacity attained if we use the bandwidth expansion $1 \leq B < n^{\frac{\alpha}{2}}$. The latter is the maximum capacity reachable if the available bandwidth is large, such that $B \geq c_{28}\, n^{\frac{\alpha}{2}}$. An increase in B beyond $c_{28}\, n^{\frac{\alpha}{2}}$ does not change the order of the upper-bound of the capacity of wireless ad hoc network using CDMA and SIC. Furthermore, Eqs. (6.25) and (6.29) represent capacity values that increase with n, compared to the asymptotic (constant) value result obtained by Negi and Rajeswaran [51] for CDMA static wireless ad hoc networks.

6.4.2 Per Source-Destination Throughput

From Sections 5.2.2 and 6.2.3, each node accesses the data channel at a constant rate $\delta = \frac{t_{data}}{t_{disc}+t_{data}}$ with probability approaching 1 as $n \to \infty$, such that each source sends one packet per session. Each node is guaranteed a communication rate of R_{ij} in each data channel that is lower- and upper-bounded according to Eqs. (6.25) and (6.29), respectively. This available communication rate has to be divided among all routes the node must serve per session per channel. However, due to the mobility and the forwarding scheme described in Section 5.2.3, each node serves only one route per session per data channel, i.e., the node either relays a new packet or it delivers a packet to a destination. Thus, the number of routes every node has to service per session per data channel is (# of served routes) $= 1$. Moreover, all cells containing at least two nodes are able to execute FDMA/CDMA and SIC successfully. From Eq. (6.9), $\mathbb{P}\{Z \geq 2\} = (1 - e^{-1/\phi} - \frac{1}{\phi} e^{-1/\phi})$, as $n \to \infty$. Accordingly, with probability approaching 1 as $n \to \infty$, the per source-destination throughput $\lambda(n)$ is [23], [66], [39],

$$\begin{aligned}\lambda(n) &= \frac{R_{ij}\,\delta\,\mathbb{P}\{Z \geq 2\}}{\#\text{ of served routes}} \\ &= R_{ij}\,\underbrace{\frac{\frac{t_{data}}{t_{disc}+t_{data}}\left(1 - e^{-1/\phi} - \frac{1}{\phi}e^{-1/\phi}\right)}{1}}_{c_{30}} \\ &= c_{30}\,R_{ij}, \end{aligned} \tag{6.31}$$

where c_{30} is a positive constant for given choices of values for t_{disc}, t_{data}, and ϕ. Thus, from Eqs. (6.25), (6.29), and (6.31), we have proven the following Theorem.

Theorem 4 *By employing mobility, CDMA, SIC, one-time relaying of packets, and bandwidth expansion using the opportunistic cooperation strategy, the wireless ad hoc network attains, with probability approaching 1 as $n \to \infty$, a per source-destination throughput given by*

$$\lambda(n) = O\left(n^{\frac{\alpha}{2}}\right) \quad \textit{(upper-bound)}, \tag{6.32}$$

and

$$\lambda(n) = \Omega\left[f(n)\right] \quad \textit{(lower-bound)}, \tag{6.33}$$

where $1 \leq f(n) < n^{\frac{\alpha}{2}}$.

Theorem 4 shows that, by using opportunistic cooperation, the per source-destination throughput *increases* with n. Furthermore, the throughput upper-bound is the highest reported in the literature for ad hoc networks. This increase is related to the fact that adjacent strong interferences are decoded which improves the SNIR, and the bandwidth expansion.

6.4.3 Bandwidth Scalability

As illustrated in Fig. 6.2, the total bandwidth requirement (ΔW_{total}) for the entire network has two components. The control channels ($\Delta\omega_C$) and the data channels (ΔW_D).

From Eqs. (5.2) and (5.3), Lemma 1, and noting that the bandwidth $\Delta\omega$ in each control channel equals $2/T$ due to the Nyquist rate [52], we obtain

$$\begin{aligned}\Delta\omega_C &= 12\Delta\omega = \tfrac{24}{T} = \tfrac{24N_{min}}{t_{disc}} \\ &= \Theta\left[1-\left(1-\tfrac{\log(\log(n))}{\log(n)}\right)^{\frac{1}{\left\lceil\frac{3\log(n)}{\log(\log(n^{\phi}))}\right\rceil}}\right]^{-1}. \end{aligned} \tag{6.34}$$

On the other hand, the bandwidth ΔW needed in each data channel is related to the total number of distinct codes (M) used and the original bandwidth B (before spreading) of the data signal. From Section 6.2, in order to obtain distinct PN sequences used in the same cluster, M must equal $12\mathcal{A}$. Therefore, the bandwidth expansion ΔW in each data channel is given by $\Delta W = BM = 12\mathcal{A}B$ [31]. Accordingly, the data bandwidth scalability in each data channel associated to the upper- and lower-bound capacity, is given respectively by

$$\Delta W = \Omega\left(n^{\frac{\alpha}{2}}\right), \text{ and } \Delta W = \Theta[f(n)], \tag{6.35}$$

where $1 \leq f(n) < n^{\frac{\alpha}{2}}$.

The total bandwidth for the entire network is

$$\Delta W_{total} = \Delta\omega_C + \Delta W_D = \Delta\omega_C + \mathcal{A}\Delta W, \tag{6.36}$$

where $\Delta\omega_C$ and ΔW are given by Eqs. (6.34) and (6.35), respectively.

6.5 Delay

The opportunistic cooperation strategy employs relaying of multiple copies of a packet. As described in Chapter 3, the chance of a packet finding its destination earlier is increased by using multiple copies, because K copies follow different random routes and can reach the destination node sooner.

For $K = 1$, it has been shown [57] that the delivery delay random variable d has an exponential distribution with parameter $\lambda = 2\,r'\,v$, which results from evaluating the flux of nodes entering a circle of radius r' during a differential time interval considering the nodes uniformly distributed over the entire network of unit area and traveling at speed $v(n)$. In our analysis, r' is the receiver range of a node. For a uniform distribution of the nodes, $r' = \Theta(1/\sqrt{n})$. Hence, the radius r' decreases with $1/\sqrt{n}$. Furthermore, the velocity of the nodes also decreases with $1/\sqrt{n}$ [23], [39]. Hence, $\lambda = \frac{1}{\Theta(n)}$. We extended this model to consider the case $K > 1$ (see Chapter 3), and we found that the delay d_K for K copies attains an exponential reduction compared to the single-copy delay d given by Eq. (3.39), that is

$$d_K \approx \frac{1}{\lambda}\,\log\left(\frac{K}{K-1+e^{-\lambda d}}\right). \tag{6.37}$$

Because we employ multi-copy relaying of packets, the delay performance of the ad hoc network with opportunistic cooperation is improved and follows the description in Chapter 3 and [39].

6.6 Comparison with Previous Schemes

6.6.1 The Static Network Case

Here, we consider the capacity and bandwidth expansion performance of the CDMA-SIC scheme assuming a static network, and compare it with the results by Negi and Rajeswaran [51], who employed bandwidth expansion in the model presented by Gupta and Kumar [28].

The model we consider is that of a network formed by n fixed nodes, independently and uniformly distributed on a unit sphere surface. This model is also known as a random network [28]. The set of assumptions assumed here are basically the same as those adopted in the previous sections, except that the n nodes are considered to be static on a unit sphere surface, and that the routing of packets is done through multiple hops along cells following the minimum distance path from source to destination. These assumptions are also consistent with the works by Negi and Rajeswaran [51] and Gupta and Kumar [28] (see also Section 2.1). Because the communication framework is one-to-one, we use only one data channel ΔW for the entire network. Therefore, no simultaneous data channels are needed given that only one copy of each packet is relayed along the route to its destination, and so we can apply the CDMA-SIC without FDMA.

In this model, the surface of the sphere is divided into cells. The number of nodes in any cell is a random variable Z. A node is randomly chosen to relay all traffic in each cell, and is called the head node of the cell. Thus, to guarantee relaying of traffic between cells, it is required that every cell has at least one node whp [28], i.e., $\mathbb{P}\{Z \geq 1\} \stackrel{n\to\infty}{\longrightarrow} 1$. Within

a cell, all sources send traffic to the head node, and destinations receive traffic from the head node.

A useful property of the Voronoi tessellation described in Section 2.1 is that every cell $V \in \mathcal{V}_n$ has no more than c_{31} interfering neighbors, and hence the maximum number of interfering nodes is bounded by some positive constant [28]. Consequently, similarly to what we did in the mobile case, we can assign distinct PN sequences to each node, such that every cell in $\mathcal{V}_n$ has interfering neighbors using different codes. Therefore, we need $M \geq c_{31}$ distinct PN sequences, and we reuse the codes in order to save bandwidth. Note that GPS (or some other technique) is no longer required since nodes are static. However, as explained before, MAI has to be considered even when transmission synchronization among nodes is employed [31]. Because nodes are static, we only need to assign the different codes during the initialization of the network.

We compute the link's Shannon capacity for an arbitrary pair of nodes from adjacent cells, noting that the analysis applied for the mobile network can be used for the static network as well. Thus, similar to the description in Section 6.3, each node communicating with another node applies SIC to eliminate MAI from close neighbors and the $SNIR'$ computation follows Eq. (6.17). The MAI calculation is done following an approach similar to that of Eq. (6.21), but considering the unit sphere surface. Furthermore, because the communication is either between two nodes in the same cell or between two head nodes from adjacent cells, any two communicating nodes are located at distance $c_{32}\varepsilon(n)$ apart from each other. Therefore, if node j is receiving data from node i, after node j applies SIC up to node i, all the remaining interfering nodes are placed at distance greater than $c_{32}\varepsilon(n)$. Hence, for $\alpha > 2$ and n suffi-

ciently large, we have the following bound for the remaining multiple access interference at a node j receiving data from node i, after SIC,

$$\begin{aligned} MAI'(n) &\leq \int_0^{2\pi} \int_{c_{32}\varepsilon(n)}^{\frac{\sqrt{\pi}}{2}} \frac{P\,\phi\,n}{Mr^{\alpha-1}}\,dr\,d\gamma \\ &= \frac{P\,\phi\,n}{M} \int_0^{2\pi} \frac{r^{2-\alpha}}{2-\alpha}\Big|_{c_{32}\varepsilon(n)}^{\frac{\sqrt{\pi}}{2}} d\gamma \\ &= \frac{P\,\phi\,n}{M(\alpha-2)} \left[\frac{1}{(c_{32}\varepsilon(n))^{\alpha-2}} - \frac{1}{\left(\frac{\sqrt{\pi}}{2}\right)^{\alpha-2}}\right] \int_0^{2\pi} d\gamma \\ &= \frac{2\pi P\phi n}{M(\alpha-2)} \left[\left(\frac{n}{c_{33}\,\log(n)}\right)^{\frac{\alpha}{2}-1} - \left(\frac{2}{\sqrt{\pi}}\right)^{\alpha-2}\right] \\ &= \frac{c_{34}\,n^{\frac{\alpha}{2}}}{(\log(n))^{\frac{\alpha}{2}-1}} \left[1 - c_{35}\left(\frac{\log(n)}{n}\right)^{\frac{\alpha}{2}-1}\right] \\ &\leq \frac{c_{34}\,n^{\frac{\alpha}{2}}}{(\log(n))^{\frac{\alpha}{2}-1}}, \end{aligned} \tag{6.38}$$

where c_{34} is a positive constant given that c_4, c_{32}, ϕ, P, M, and α are specified.

Analogously, the same-code interference (SCI) can be upper-bounded by

$$SCI = \sum_{\substack{k \notin range \\ C_k = C_i}} P_{kj}(t) g_{kj}(t) \;\leq\; \frac{c_{36}\,n^{\frac{\alpha}{2}}}{(\log(n))^{\frac{\alpha}{2}-1}}. \tag{6.39}$$

Hence, from Eqs. (6.38) and (6.39), the total remaining interference after SIC at node j is upper-bounded by

$$MAI' + SCI \;\leq\; \frac{c_{37}\,n^{\frac{\alpha}{2}}}{(\log(n))^{\frac{\alpha}{2}-1}}. \tag{6.40}$$

From Eq. (6.18), assuming that node i transmits to j, in which the original data bandwidth is B (before spreading), we obtain the following link's Shannon capacity

$$R_{ij} = B \log\left(1 + \frac{\frac{P}{(c_{32}\varepsilon(n))^{\alpha}}}{BN_o + MAI' + SCI}\right)$$

$$= B \log\left(1+ \frac{c_{38}}{\frac{BN_o\,(\log(n))^{\frac{\alpha}{2}}}{n^{\frac{\alpha}{2}}} + \frac{(\log(n))^{\frac{\alpha}{2}}}{n^{\frac{\alpha}{2}}}\,(MAI' + SCI)}\right). \tag{6.41}$$

For the term associated with the maximum interference over the unit sphere surface, we have from Eq. (6.40) that

$$\frac{(\log(n))^{\frac{\alpha}{2}}}{n^{\frac{\alpha}{2}}}\left(MAI' + SCI\right) \leq c_{37}\,\log(n). \tag{6.42}$$

Thus, from Eqs. (6.41) and (6.42), and by taking $B \geq \frac{c_{39}\,n^{\frac{\alpha}{2}}}{(\log(n))^{\frac{\alpha}{2}-1}}$, for some positive constant c_{39} and n sufficiently large, we obtain

$$\begin{aligned}\frac{(\log(n))^{\frac{\alpha}{2}}}{n^{\frac{\alpha}{2}}}\left(MAI' + SCI\right) &\leq c_{37}\,\log(n) \\ &\leq \frac{BN_o(\log(n))^{\frac{\alpha}{2}}}{n^{\frac{\alpha}{2}}}.\end{aligned} \tag{6.43}$$

The term $\frac{BN_o\,(\log(n))^{\frac{\alpha}{2}}}{n^{\frac{\alpha}{2}}}$ becomes dominant in the denominator of Eq. (6.41) when $B \geq \frac{c_{39}\,n^{\frac{\alpha}{2}}}{(\log(n))^{\frac{\alpha}{2}-1}}$ and $n \to \infty$. Consequently, for $B \geq \frac{c_{39}\,n^{\frac{\alpha}{2}}}{(\log(n))^{\frac{\alpha}{2}-1}}$, the link's Shannon capacity as $n \to \infty$ is given by

$$\begin{aligned}R_{ij} &= B \log\left(1+\frac{c_{38}}{\frac{BN_o(\log(n))^{\frac{\alpha}{2}}}{n^{\frac{\alpha}{2}}} + \frac{(\log(n))^{\frac{\alpha}{2}}}{n^{\frac{\alpha}{2}}}\,(MAI' + SCI)}\right) \\ &= \frac{n^{\frac{\alpha}{2}}}{(\log(n))^{\frac{\alpha}{2}}}\,\underbrace{\frac{B}{\frac{n^{\frac{\alpha}{2}}}{(\log(n))^{\frac{\alpha}{2}}}}\,\log\left(1+\frac{c_{38}}{\frac{BN_o\,(\log(n))^{\frac{\alpha}{2}}}{n^{\frac{\alpha}{2}}} + \frac{(\log(n))^{\frac{\alpha}{2}}}{n^{\frac{\alpha}{2}}}\,(MAI' + SCI)}\right)}_{\stackrel{n\to\infty}{\longrightarrow} c_{40}} \\ &= c_{40}\,\frac{n^{\frac{\alpha}{2}}}{(\log(n))^{\frac{\alpha}{2}}},\end{aligned} \tag{6.44}$$

in which c_{40} is a positive constant.

Eq. (6.44) is the link's Shannon capacity obtained from the noise dominance over interference due to large bandwidth expansion. Note that any increase in B beyond $\frac{c_{39}\,n^{\frac{\alpha}{2}}}{(\log(n))^{\frac{\alpha}{2}-1}}$ does not change the value of this capacity.

The bandwidth expansion associated to this capacity, in which $B \geq \frac{c_{39}\, n^{\frac{\alpha}{2}}}{(\log(n))^{\frac{\alpha}{2}-1}}$, is given by

$$\Delta W = BM = \Omega\left[\frac{n^{\frac{\alpha}{2}}}{(\log(n))^{\frac{\alpha}{2}-1}}\right]. \tag{6.45}$$

To obtain the throughput behavior, note that each cell has one node whp, and any node in this cell can be the head node to relay all the traffic the cell must handle, while the other nodes can simply serve as sources or destinations. Accordingly, analogous to Eq. (6.31), the per source-destination throughput is given whp by

$$\lambda(n) = \frac{R_{ij}\, \delta\, \mathbb{P}\{Z \geq 1\}}{\#\text{ of served routes}}, \tag{6.46}$$

where $\mathbb{P}\{Z \geq 1\} \stackrel{n\to\infty}{\longrightarrow} 1$, and δ is a constant that depends on c_{31} and can be computed based on the channel access scheme employed [28].

The number of routes served by any cell is a consequence of the routing strategy. As mentioned before, the routing of packets is done through multiple hops along cells following the minimum distance path from source to destination, i.e., every packet follows the straight line segment connecting the source to its destination. Therefore, the traffic to be carried by any cell is proportional to the number of straight line segments passing through the cell. Accordingly, the number of routes intersecting any cell is bounded by the following lemma, which was proved by Gupta and Kumar [28].

Lemma 2 *The total number of source-destination lines (i.e., routes) intersecting every cell in the random network can be bounded whp by*

$$\sup_{V\in\mathcal{V}_n} \textit{(Number of routes intersecting } V\textit{)} \leq c_{41}\sqrt{n\log(n)}. \tag{6.47}$$

Therefore, using the network model assumptions provided in this Section, from Eqs. (6.44) and (6.46), and from Lemma 2, we proved the following Theorem.

Theorem 5 *The static random wireless ad hoc network using CDMA and SIC attains whp the following per source-destination throughput lower-bound*

$$\lambda(n) = \Omega\left[\frac{n^{\frac{\alpha-1}{2}}}{(\log(n))^{\frac{\alpha+1}{2}}}\right]. \tag{6.48}$$

Theorem 5 provides the same throughput lower-bound order as that obtained by Negi and Rajeswaran [51], which corroborates the capacity analysis technique employed throughout this chapter. However, our bandwidth expansion associated with this lower-bound, given by Eq. (6.45), is much smaller than the $\Theta(n(n^2\log(n))^{\frac{\alpha}{2}})$ required by Negi and Rajeswaran [51] because we take advantage of SIC. SIC allows every node in the network to successfully receive the packets from its close neighbors, increasing the minimum distance of the destructive interferers. In our case, the closest destructive interferer is located whp at distance $\Omega(\varepsilon(n)) = \Omega(\sqrt{\log(n)/n})$ due to SIC, while in [51] this distance is $\Omega(1/n\sqrt{\log(n)})$ whp.

6.6.2 The Mobile Network Case

A direct comparison between opportunistic cooperation and the strategy proposed by Grossglauser and Tse [26] is not appropriate even after applying CDMA and bandwidth expansion, because their model does not require the use of cell we assume to enable frequency reuse. Accordingly, we extend Grossglauser and Tse's network model by introducing cells in

which nodes are endowed with FDMA/CDMA-SIC and GPS capabilities, such that every node behaves simultaneously like sender and receiver of data packets for each communication session. Therefore, another comparison, not necessarily based on the physical layer properties (like link's Shannon capacity or bandwidth expansion), is more suitable.

In Chapter 3, we presented a cell description [39] for Grossglauser and Tse's scheme [26] using assumptions that are similar to those used by El Gamal et al [23]. Because only one half-duplex data channel is used for the entire network in Grossglauser and Tse's model [26], a node cannot be sender and receiver simultaneously, but rather every node behaves like either a sender or a receiver for each communication session. Accordingly, $r_o = 1/\sqrt{\pi\theta n}$ determines a cell in such a model [26], [39] for a uniform distribution of the nodes, where the parameter $\theta \in (0,1)$ is defined as the fraction of sender nodes n_S in the network. Therefore, $n_S = \theta n$, and $n_R = (1-\theta)n$ is the fraction of receiver nodes. It has been shown [23], [39] that the per source-destination throughput is proportional to the fraction of cells in the network that can successfully forward packets. In the work by Grossglauser and Tse [26], and in our previous work (see Chapter 3), only the cells containing exactly one sender (i.e., $L = 1$) and at least one receiver (i.e., $K \geq 1$) are able to forward packets, because no SIC capability is assumed, and therefore, the cells containing more than one sender present transmission collisions, preventing successful relaying of packets. From Eq. (3.6), for Grossglauser and Tse's scheme [26], we have that as $n \to \infty$

$$\mathbb{P}\{L = 1, K \geq 1\} = \frac{1}{\theta}\, e^{-1/\theta} \left(1 - e^{-1/\theta}\right). \tag{6.49}$$

With opportunistic cooperation, in order to obtain the same cell size as in [26] and Chapter 3, i.e, $a(n) = \pi r_o^2 = \frac{1}{\theta n} = \frac{1}{\phi n}$, we must set $\theta = \phi$, and use a finite bandwidth expansion.

In addition, all cells containing at least two nodes are able to successfully forward packets in opportunistic cooperation. Thus, from Eq. (6.9), $\mathbb{P}\{Z \geq 2\} = (1 - e^{-1/\phi} - \frac{1}{\phi}e^{-1/\phi})$ as $n \to \infty$. Hence, our collaboration-driven strategy provides the following performance gain G over the Grossglauser and Tse's scheme [26] based on a comparison of the fraction of cells that successfully forward packets as $n \to \infty$,

$$G = \frac{\mathbb{P}\{Z \geq 2\}}{\mathbb{P}\{L = 1, K \geq 1\}} = \frac{1 - e^{-1/\phi} - \frac{1}{\phi}e^{-1/\phi}}{\frac{1}{\phi}e^{-1/\phi}\left(1 - e^{-1/\phi}\right)}. \tag{6.50}$$

Fig. 6.6 illustrates the behavior of the gain G given in Eq. (6.50) as a function of ϕ. Note that $G > 1 \ \forall \ \phi \in (0, 1)$. This gain shows that the throughput is improved by a constant factor compared to the results in [26] and Chapter 3 under similar bandwidth expansion. There is additional gain in the link Shannon capacity, as a constant gain factor, due to the use of SIC and the improvement in SNIR. However, an exact computation of this constant factor turns out to be a tedious task.

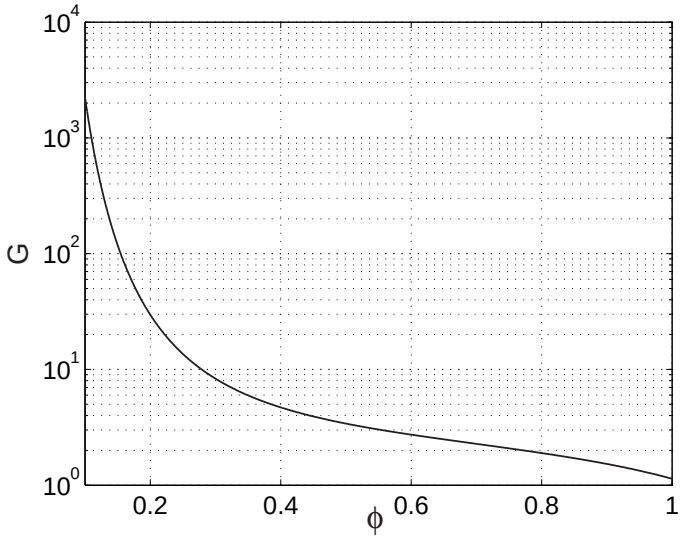

Figure 6.6: Gain performance for fraction of cells that successfully forward packets in *opportunistic cooperation* compared to Grossglauser and Tse's scheme [26].

6.7 Conclusions

It was shown that the Shannon capacity and per source-destination throughput can increase with the total number of nodes n in wireless ad hoc networks by employing mobility, FDMA/CDMA, SIC, and one-time relaying of packets taking advantage of opportunistic cooperation among nodes. Such performance is attained by using successive interference cancellation and distinct codes among close neighbors, which is enabled by running a simple neighbor-discovery protocol. Accordingly, interference from close neighbors is no longer harmful, but rather endowed with valuable data. This technique also allows for code reuse and reduces the bandwidth demands of the network. It was also shown that the delay performance is improved by employing multi-copy relaying of packets. Besides bandwidth expansion, the overall improvement in the network performance is obtained at a cost of increased processing complexity in the nodes. Furthermore, the principles of opportunistic cooperation are applied to static [28], [51] and mobile [26], [39] networks. It is shown that, by using this approach, similar capacity of [51] can be attained with much smaller bandwidth expansion. We have shown that opportunistic cooperation improves the throughput of mobile wireless networks by a constant factor compared to the results in [26] and [39] under similar bandwidth expansion. These results are consistent with the predictions reported by Xie and Kumar [68].

Chapter 7

Opportunistic Cooperation with MIMO Nodes

The multiple access scheme that is proposed in this chapter is based on multiple-input multiple-output (MIMO) systems employing frequency division multiple access (FDMA). In this chapter, we explore the capacity behavior of wireless ad hoc networks when every single node has M antennas. The neighbor discovery and scheduling techniques are required before transmission of packets in a cell. For simplicity of the analysis, we assume that all the nodes in the network have the same number of antennas. Nodes transmit and receive simultaneously using different portions of the available spectrum (bandwidth), which characterizes an FDMA/MIMO approach. During transmission, the node sends packets from only one of its antennas, while during reception, it uses all of its antennas to receive and decode packets from multiple nodes simultaneously. Therefore, each MIMO system in this scheme consists of multiple transmitting nodes acting as a single-array of multiple antennas, and a single receiver

node with multiple antennas in a cell. This approach does not require any coordination among receiving nodes for decoding the received packets. We also assume that these antennas create statistically independent channels.

We show that per node ergodic capacity does not depend on the total number of nodes n; however, it is a function of such other physical layer and network parameters as the number of receiving antennas, cell area, average node density, noise, and the path loss parameter. Surprisingly, we also demonstrate that each node capacity grows as the transmit power of each node in the network increases, up to a point where interference is dominant such that no increase in capacity is possible by increasing transmit power. This result proves that increasing interference does not reduce each node capacity if the interference is properly treated. It is also shown that the total bandwidth required is finite for the proposed FDMA/MIMO system.

The rest of this chapter is organized as follows. Section 3.1 presents the network and communication models. Section 7.2 is dedicated to the capacity analysis. Section 7.3 shows the numerical and simulation results. We conclude the chapter in section 7.4.

7.1 Model

7.1.1 Network Model

The network model we assume is the same as presented in Section 2.2, except that the total area of the network grows linearly with n.

Accordingly, the modeling problem we address is that of a MANET in which n mobile nodes move in the total network area $A_T(n)$. The network is divided in cells. To

simplify our analysis, the cells have square shapes, each with area equal to a_{cell} that does not depend on n.

Therefore, with the uniform mobility model, the average node density ρ and the total network area are related by the following definition

$$A_T(n) := \frac{n}{\rho}. \tag{7.1}$$

Consequently, the total number of cells in the network is given by

$$\text{\# of cells} = \frac{A_T(n)}{a_{cell}} = \frac{n}{\rho a_{cell}}. \tag{7.2}$$

Each node is assumed to know its own position (but not the position of any other node) by utilizing a GPS circuit [53] or some other technique, and to store a geographical map of the cells in the network with the associated frequencies as described later. The GPS receiver is also assumed to be used to provide an accurate common time reference to keep all nodes synchronized.

We use two types of channels. *Control channels* are used by nodes to obtain such information as the identities of strong interference sources, the data packets expected by destinations, and the state channel information (CSI) (by means of training sequences). The detailed description of the control channel is given in Chapters 5 and 6. *Data channels* are used to transmit data taking advantage of FDMA/MIMO. Each node simultaneously transmits and receives data during a communication session (see Section 5.2.2).

As illustrated in Fig. 7.1, there are nine different cell numbers. Note that twelve distinct control frequency bands were used in Chapter 6, instead of nine used here. Many cells use the same number, however they are placed regularly far apart from each other to

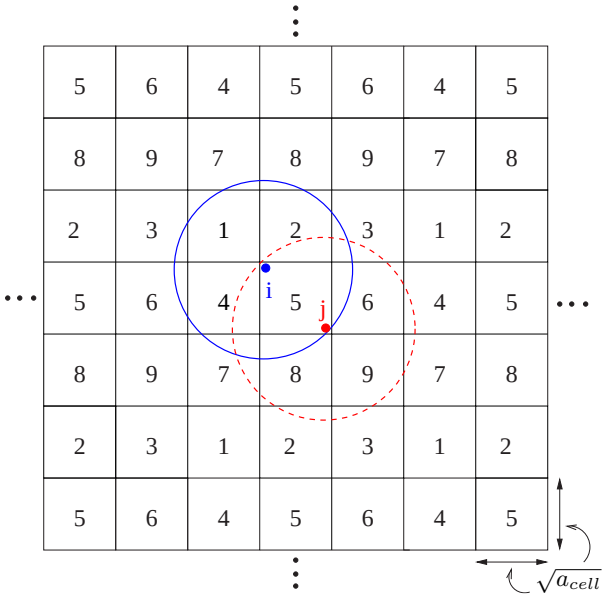

Figure 7.1: Cells numbering in the network with a_{cell} as the cell area.

reduce interference. Consequently, the frequency division assignment is such that each set of cells numbered from 1 to 9 employs different frequency channels (bandwidth), as explained in Section 7.1.2. Accordingly, for the cell configuration given, nodes i and j in cell 5 at the center of Fig. 7.1 use different frequency bandwidths to communicate with each other such that, for any other node k located in another cell numbered as 5 and using the same frequency channels, it is true that $|X_k(t) - X_j(t)| \geq (1 + \Delta)|X_i(t) - X_j(t)|$, so that X_k is at a distance greater than$|X_i(t) - X_j(t)|$ to node j. This is called the *protocol model* and fulfills the condition for successful communication [28] (see also Section 2.1).

As discussed in Chapters 5 and 6, the number of nodes per cell allowed to communicate is limited. Thus, consider that at most $\mathcal{A}$ nodes in any cell are allowed to have a non-overlapping frequency channel for communication. We now show that the fraction of cells having more than $\mathcal{A}$ nodes can be bounded by a small constant when n is large. From

Eq. (7.2), the total number of cells in the network is (# of cells) $= \frac{n}{\rho a_{cell}}$. Analogous to Eq. (6.8), the fraction of cells containing $S = s$ nodes is obtained by

$$\begin{aligned}\mathbb{P}\{S = s\} &= \begin{pmatrix} n \\ s \end{pmatrix} \left(\frac{1}{\text{\# of cells}}\right)^s \left(1 - \frac{1}{\text{\# of cells}}\right)^{n-s} \\ &= \begin{pmatrix} n \\ s \end{pmatrix} \left(\frac{\rho\, a_{cell}}{n}\right)^s \left(1 - \frac{\rho\, a_{cell}}{n}\right)^{n-s}. \end{aligned} \tag{7.3}$$

In this chapter, we use S to represent the random variable for the number of nodes in a cell, instead of Z used in Chapter 6. The distinction is to remind that, in this chapter, the network modeling is different from the previous chapter in which the total area of the network is constant.

Given that $\begin{pmatrix} n \\ s \end{pmatrix} \approx \frac{n^s}{s!}$ for $n >> s$, and using the limit $\left(1 - \frac{1}{x}\right)^x \longrightarrow e^{-1}$ as $x \to \infty$, we have

$$\lim_{n\to\infty} \mathbb{P}\{S = s\} = \frac{1}{s!}(\rho\, a_{cell})^s e^{-\rho\, a_{cell}}. \tag{7.4}$$

Following the analysis given in Lemma 1, it can be shown that the maximum number of nodes in a cell is given by $\left\lceil \frac{3\,\log(n)}{\log\left(\log\left(n^{1/(\rho\, a_{cell})}\right)\right)} \right\rceil$. The fraction of cells having more than $\mathcal{A}$ nodes, given ρ and a_{cell}, is obtained by

$$\begin{aligned}\lim_{n\to\infty} \mathbb{P}\{S > \mathcal{A}\} &= \lim_{n\to\infty} \sum_{s=A+1}^{n} \mathbb{P}\{S = s\} \\ &= \sum_{s=\mathcal{A}+1}^{\infty} \frac{1}{s!}(\rho\, a_{cell})^s e^{-\rho\, a_{cell}} \\ &= 1 - \frac{\Gamma(\mathcal{A}+1, \rho a_{cell})}{\Gamma(\mathcal{A}+1)}, \end{aligned} \tag{7.5}$$

where $\Gamma(m+1) = m!$, and $\Gamma(m,x) = \int_x^\infty y^{m-1}e^{-y}dy$ is the incomplete Gamma function. For example, $\lim_{n\to\infty} \mathbb{P}\{S > 8\} = 0.0038$ for $\rho a_{cell} = 3$. Therefore, the fraction of cells having more than $\mathcal{A}$ nodes can be designed to be very small. Obviously, if a cell contains more than $\mathcal{A}$ nodes, only $\mathcal{A}$ nodes are allowed to participate in each communication session.

7.1.2 Bandwidth Allocation

In a competition-driven paradigm for MANETs, when two nodes become close enough to each other, they can transmit information to one another without any delay. With opportunistic cooperation, many nodes transmit concurrently to many other nodes that are close enough, and all such transmissions are decoded. Hence, a node may concurrently send to and receive from multiple nodes. Because full-duplex data communication in the same frequency band is not practical, we present an example of how opportunistic cooperation can be implemented with a hybrid scheme based on FDMA and MIMO that supports many-to-many communications. This approach together with the cell arrangement given in Fig. 7.1 reduce the effect of interference at the receivers.

Let ξ_i denote the set of non-overlapping data frequency bands (channels) used in cell i. Accordingly, the data channels are ordered and grouped as follows. $\xi_1 = \{W_1^{(1)}, ..., W_{\mathcal{A}}^{(1)}\}$, $\xi_2 = \{W_{\mathcal{A}+1}^{(2)}, ..., W_{2\mathcal{A}}^{(2)}\}$, ..., $\xi_9 = \{W_{8\mathcal{A}+1}^{(9)}, ..., W_{9\mathcal{A}}^{(9)}\}$, in which $W_j^{(i)}$ stands for the j^{th} bandwidth in cell i. In this way, any set of nine cells, numbered from 1 to 9 according to Fig. 7.1, has a different (non-overlapping) set of frequency bands.

As mentioned earlier, the signaling in the control channel provides each node in cell i knowledge of who the other nodes in the same cell are, and the node uses this information to

choose a data channel (or data sub-spectrum) to receive data in the following order based on its own ID and the IDs of its neighbors

- The node with the highest ID in cell i is associated (for reception) with the data sub-spectrum (or channel) ΔW centered at $W^{(i)}_{(i-1)\mathcal{A}+1}$ in ξ_i.
- The node with the second highest ID in cell i is associated (for reception) with the data sub-spectrum (or channel) ΔW centered at $W^{(i)}_{(i-1)\mathcal{A}+2}$ in ξ_i, and this continues for all nodes in cell i.
- The data sub-spectra (or channels) not utilized become idle in cell i. This happens in those cells where the number of nodes is smaller than $\mathcal{A}$.

Accordingly, the total bandwidth required for the entire network is $\Delta W_{total} = 9\mathcal{A}\Delta W$. Because ΔW and $\mathcal{A}$ are finite, the total bandwidth necessary for the FDMA/MIMO ad hoc network is also finite.

7.1.3 Many-to-Many Communication

At time t, a cell has S nodes such that the data communication is S-to-S (see Fig. 7.2) where S is a random variable due to the mobility of the nodes. Each node transmits through a single antenna (employing FDMA) the same or different data packets to the other $S-1$ nodes in the same cell, using $S-1$ distinct data channels (downlink), while it simultaneously receives (through many antennas) up to $S-1$ different data packets from the other $S-1$ nodes through its assigned data channel (uplink). Hence, every node can concurrently transmits (receives) to (from) all other nodes in the same cell. Thus, multi-copies of the same packet

can be simultaneously relayed to reduce delay [39].

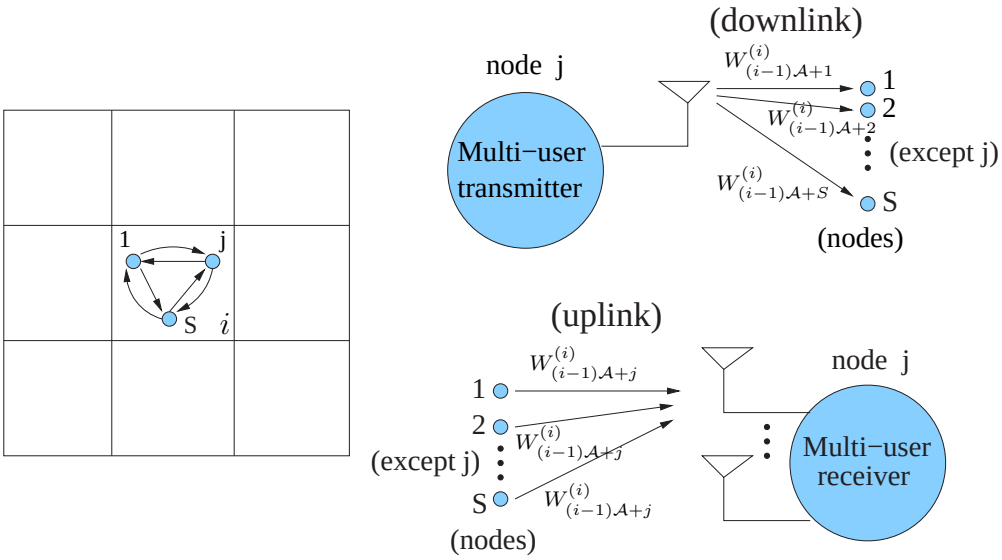

Figure 7.2: FDMA/MIMO downlink and uplink description for data channels in a cell i. Communication is S-to-S (i.e., many-to-many).

The data packet forwarding consists of two phases (see Figs. 2.1 and 3.1) and it was explained in Section 5.2.3.

7.1.4 FDMA/MIMO Transmitter and Receiver Scheme

The FDMA/MIMO transmitter scheme for a node j in cell i is shown in Fig. 7.3(a). All packets previously relayed to node j are stored in the *buffer for relayed packets*. In each session, after the discovery phase, node j knows who its neighbors are in the cell which it is located and loads the *buffer for destination packets* if it has packet for each destination in the cell. Each packet signal p_k coming from the *banks of buffers* passes through a switch Q_k, where $k \in [1, \mathcal{A}]$ is an integer. After Q_k, the signal is modulated by the frequency carrier associated with the node the packet is intended for (in this case $W^{(i)}_{(i-1)\mathcal{A}+k}$). Because each

node uses only one antenna for transmission and channel state information (CSI) is assumed to be known only at the receiver side, the node transmits with constant power P for another node, such that the total node transmit power is $P_T \leq \mathcal{A}P$. Finally, all modulated signals are summed up and transmitted through the antenna (see also Fig. 7.2(downlink)).

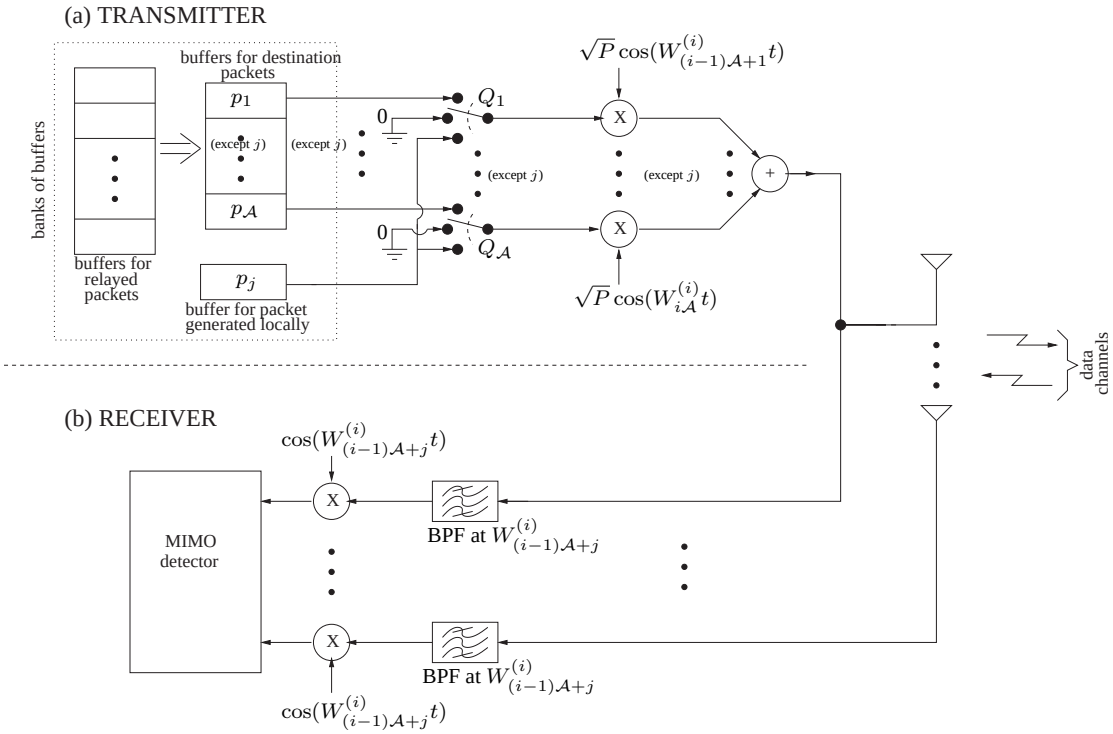

Figure 7.3: Hybrid FDMA/MIMO data transceiver scheme for node j in cell i. (a) FDMA/MIMO transmitter. (b) MIMO receiver.

The *banks of buffers* store the packets relayed by node j and the packets generated locally by node j. The position of each switch Q_k is chosen according to the existence of the destination node (assigned to $W^{(i)}_{(i-1)\mathcal{A}+k}$) for the packet p_k. Accordingly, the switch Q_k gives priority to the packet in the *buffer for destinations*. If the node assigned to the data channel $W^{(i)}_{(i-1)\mathcal{A}+k}$ is not a destination for a relayed packet, then the switch selects the new packet (p_j) generated locally by node j. Furthermore, if no node is assigned to the data sub-spectrum

$W^{(i)}_{(i-1)\mathcal{A}+k}$ in the cell that j is located, then Q_k is set to 0 (ground) and no information is transmitted, contributing no increase in the interference through this data channel. Therefore, the objective of the switches is to give absolute priority to the *delivery* of packets (i.e., *Phase 2*) as described in Section 7.1.3, and prevent any unnecessary transmission of data through an idle data channel in the cell.

Note that the packet generated locally in node j is transmitted to those nodes that are not destinations, and thus, multiple copies of the same packet generated locally at j can be relayed to other nodes in the same cell [39].

The basic decoding scheme of the MIMO receiver circuit is illustrated in Fig. 7.3(b) (see also Fig. 7.2(uplink)). The signal coming from each antenna passes through a band pass filter (BPF) centered at $W^{(i)}_{(i-1)\mathcal{A}+j}$, which selects only the data sub-spectrum ΔW associated to node j in cell i. Finally, the filtered signal is demodulated to the baseband spectrum and fed to the MIMO detector, for example a V-BLAST decoder [20], or other space-time decoding techniques [11].

7.1.5 Communication Model

Without loss of generality, let the cell where node j is currently located be denoted by cell 0. Also, assume that the other cells (employing the same set of frequencies as cell 0) are numbered from $i = 1$ to ∞. P is the transmit power chosen by node s to transmit to node j. The distance between a transmitting node s (located at cell i) and the receiver j is denoted

as $r_{s,j}(i)$. Assuming **no fading**, the received signal power at node j from node s is [1]

$$P_{s,j}(i) = \frac{P}{(1 + r_{s,j}(i))^{\alpha}}, \tag{7.6}$$

where α is the path loss parameter and assumed to be greater than or equal to 2.

In Eq. (7.6), $r_{s,j}(i)$ is not a function of receive antennas, i.e., m. The reason is because the distances between the transmitting node s and all M antennas of the receiver j are assumed to be equal for practical considerations.

In our analysis, we consider that channel state information (CSI) is only known at the receiver side. Furthermore, in every cell, each MIMO system consists of multiple transmitting nodes and a single receiver node (with M receiving antennas).

We use boldface capital letters to represent matrices and boldface lower case letters to denote vectors. In addition, the following standard notation will be used: $'$ for vector transpose, $\dagger$ for conjugate transpose of a matrix (or vector), $*$ for conjugate transpose of a scalar, $\mathrm{tr}(\cdot)$ for trace, $\mathrm{rank}(\cdot)$ for rank and $\det(\cdot)$ for determinant of a matrix. The received signal vector (from cell i) for one receiver node j is defined as $\mathbf{y}_j(i) = [y_{1,j}(i), y_{2,j}(i), ..., y_{M,j}(i)]'$. The transmission vector from cell i is $\mathbf{x}(i) = [x_1(i), x_2(i), ..., x_{S_i}(i)]'$, where S_i is the number of nodes in cell i (we assume that the nodes in cell i are transmitting in the same frequency band as node j is using to receive data). This assumption implies that transmit nodes in cell i only use one antenna while receiving nodes utilize all their M antennas for communication. The received signal (from a cell i) for each node is defined as $\mathbf{y}_j(i) = \mathbf{H}_j(i)\,\mathbf{x}(i) + \mathbf{z}_j$, where $\mathbf{z}_j = [z_{1,j}, z_{2,j}, ..., z_{M,j}]'$ is a zero-mean complex additive white Gaussian noise (AWGN) vector. We assume that $E[\mathbf{z}_j\,\mathbf{z}_j^{\dagger}] = \sigma_{\mathbf{z}}^2\mathbf{I}_M$, where $\mathbf{I}_M$ is the $M \times M$ identity matrix and $\sigma_{\mathbf{z}}^2$ is

[1] This path loss channel model ensures that the received power is never greater than the transmitted power [34], as opposed to the more common approach of $1/r_{s,j}^{\alpha}(i)$ [28], [26], [39], [51], [66].

the noise variance. $\mathbf{H}_j(i)$ is the $M \times S_i$ channel matrix from cell i to node j with its elements defined as [34]

$$h_{ms,j}(i) := (\mathbf{H}_j(i))_{ms} = \frac{\phi_{ms,j}(i)}{(1 + r_{s,j}(i))^{\alpha}}, \tag{7.7}$$

where $1 \leq m \leq M$, $1 \leq s \leq S_i$. The fading coefficient $\phi_{ms,j}(i)$ is zero-mean, Gaussian, with independent real and imaginary parts, each with variance 1/2. Equivalently, $\phi_{ms,j}(i)$ is a stationary and ergodic stochastic fading process that is independent for each sender and receiver antenna pair, where $E_{\phi}[\phi_{ms,j}(i)\, \phi^{*}_{ms,j}(i)] = E_{\phi}[|\phi_{ms,j}(i)|^2] = 1$. The fading coefficients can also be given in matrix notation, i.e., $\phi_{ms,j}(i) = (\mathbf{\Phi}_j(i))_{ms}$. Thus, $\mathbf{\Phi}_j(i)$ is a $M \times S_i$ matrix of complex variates whose columns are independently normally distributed with mean vector $\mathbf{0}$ and covariance matrix $\mathbf{\Psi}_j(i) = \mathbf{I}_M \, \forall (i, j)$, i.e., $N(\mathbf{0}, \mathbf{I}_M)$ [33]. Consequently, $\mathbf{\Phi}_j(i)\mathbf{\Phi}^{\dagger}_j(i)$ is a positive definite Hermitian matrix having the complex Wishart distribution characterized by the following probability density function [33]

$$f(\mathbf{\Phi}_j(i)\mathbf{\Phi}^{\dagger}_j(i)) = \frac{e^{-\operatorname{tr}[\mathbf{\Psi}_j^{-1}(i)\mathbf{\Phi}_j(i)\mathbf{\Phi}^{\dagger}_j(i)]}}{\pi^{\frac{1}{2}M(M-1)}\{\det[\mathbf{\Psi}_j(i)]\}^{S_i}\prod_{k=1}^{M}\Gamma(S_i - k + 1)}\left\{\det[\mathbf{\Phi}_j(i)\mathbf{\Phi}^{\dagger}_j(i)]\right\}^{S_i - M}. \tag{7.8}$$

This complex Wishart distribution for a matrix $\mathbf{\Phi}_j(i)\mathbf{\Phi}^{\dagger}_j(i)$ will be denoted by $\mathbf{\Phi}_j(i)\mathbf{\Phi}^{\dagger}_j(i) \sim \mathcal{W}_M(\mathbf{\Psi}_j(i), S_i)$.

7.2 Ergodic Capacity

Let $\mathbf{H}_j(0)$ represent the channel matrix for cell 0, i.e., $\mathbf{H}_j(0)$ describes the channel matrix to node j from the nodes in the same cell as j is located. The analysis is asymptotic in n, i.e., $n \to \infty$. Therefore, $A_T(n) \to \infty$, and without loss of generality, we consider that the cell 0 is located at the center of the network area. Given that each node transmits to another

node with power P using only one antenna, and CSI is only known at the receiver side, the ergodic capacity of a receiving node j is given (in units of bits/s/Hz) by [13], [10], [62], [21]

$$R_j = \frac{1}{9} E_{\mathbf{H}} \left\{ \log_2 \det \left[\mathbf{I}_M + P\mathbf{H}_j(0)\mathbf{H}_j^{\dagger}(0) \left(\sigma_{\mathbf{z}}^2 \mathbf{I}_M + \sum_{i \geq 1} P\mathbf{H}_j(i)\mathbf{H}_j^{\dagger}(i) \right)^{-1} \right] \right\}, \quad (7.9)$$

where the term $\frac{1}{9}$ accounts for the frequency division multiple access, $E_{\mathbf{H}}[\cdot]$ denotes the ergodic expectation over all instantaneous $\mathbf{H}_j(i)$, and the summation in i refers to the interference coming from all cells in the network using the same frequency band ΔW as j uses for reception. Noting that $\log_2 \det(\cdot)$ is concave and using Jensen's inequality, we arrive at [13]

$$R_j \leq \frac{1}{9} \log_2 \det \left\{ \mathbf{I}_M + E_{\mathbf{H}} \left[P[\mathbf{H}_j(0)\mathbf{H}_j^{\dagger}(0)] \left(\sigma_{\mathbf{z}}^2 \mathbf{I}_M + P \sum_{i \geq 1} \mathbf{H}_j(i)\mathbf{H}_j^{\dagger}(i) \right)^{-1} \right] \right\}. \quad (7.10)$$

Now, observe that, given j, $\mathbf{H}_j(i)$ is independent distributed for all i. Therefore, we obtain

$$R_j \leq \frac{1}{9} \log_2 \det \left\{ \mathbf{I}_M + PE_{\mathbf{H}}[\mathbf{H}_j(0)\mathbf{H}_j^{\dagger}(0)] E_{\mathbf{H}} \left[\left(\sigma_{\mathbf{z}}^2 \mathbf{I}_M + P \sum_{i \geq 1} \mathbf{H}_j(i)\mathbf{H}_j^{\dagger}(i) \right)^{-1} \right] \right\}. \quad (7.11)$$

The above upper-bound is computed in three cases according to the transmit power level P. Compared with noise, we consider the cases of strong interference, no interference, and the intermediate case. Note that these thresholds for P depends on the network parameters as will be described latter.

The intermediate case is analyzed first. Accordingly, we present the following lemma and corollary.

Lemma 3 *Let the same order square Hermitian matrices* $\mathbf{G}$ *and* $\mathbf{V}$ *be positive definite. Then*

$$(\mathbf{G} + \mathbf{V})^{-1} \leq \frac{1}{4}(\mathbf{G}^{-1} + \mathbf{V}^{-1}), \quad (7.12)$$

with equality if and only if $\mathbf{G} = \mathbf{V}$.

Proof: Let $\mathbf{G}$ and $\mathbf{V}$ be M-square positive definite Hermitian matrices. Therefore, $\mathbf{G}+\mathbf{V} > \mathbf{V} > \mathbf{0}$, i.e., $\mathbf{G}+\mathbf{V}$ is also a positive definite Hermitian matrix. Hence, there exists $\mathbf{B}$, a nonsingular $M \times M$ matrix such that [73]

$$\mathbf{B}^\dagger(\mathbf{G}+\mathbf{V})\mathbf{B} = \mathbf{I}_M. \tag{7.13}$$

Now, because $\mathbf{B}^\dagger\mathbf{V}\mathbf{B}$ is also positive definite Hermitian, then we can find $\mathbf{T}$, a unitary $M \times M$ matrix such that $\mathbf{D_V} = \mathbf{T}^\dagger\mathbf{B}^\dagger\mathbf{V}\mathbf{B}\mathbf{T}$ is a positive definite diagonal matrix [73]. Let $\mathbf{R} = \mathbf{B}\mathbf{T}$, and note that $\mathbf{R}$ is nonsingular. Then, from Eq. (7.13), $\mathbf{R}^\dagger(\mathbf{G}+\mathbf{V})\mathbf{R} = \mathbf{I}_M$. Thus, $\mathbf{D_V}$ and $\mathbf{D_G} = \mathbf{R}^\dagger\mathbf{G}\mathbf{R} = \mathbf{R}^\dagger(\mathbf{G}+\mathbf{V})\mathbf{R} - \mathbf{R}^\dagger\mathbf{V}\mathbf{R} = \mathbf{I}_M - \mathbf{D_V}$ are both real diagonal matrices. Consequently,

$$\begin{aligned}
(\mathbf{G}+\mathbf{V})^{-1} &= \left[(\mathbf{R}^\dagger)^{-1}\mathbf{D_G}\mathbf{R}^{-1} + (\mathbf{R}^\dagger)^{-1}\mathbf{D_V}\mathbf{R}^{-1}\right]^{-1} \\
&= \left[(\mathbf{R}^\dagger)^{-1}(\mathbf{D_G}+\mathbf{D_V})\mathbf{R}^{-1}\right]^{-1} \\
&= \mathbf{R}(\mathbf{D_G}+\mathbf{D_V})^{-1}\mathbf{R}^\dagger \\
&= \mathbf{R}\begin{bmatrix} \frac{1}{(\mathbf{D_G})_{11}+(\mathbf{D_V})_{11}} & & \\ & \ddots & \\ & & \frac{1}{(\mathbf{D_G})_{MM}+(\mathbf{D_V})_{MM}} \end{bmatrix}\mathbf{R}^\dagger,
\end{aligned} \tag{7.14}$$

where $(\mathbf{D_G})_{ii}$ and $(\mathbf{D_V})_{ii}$ are the i^{th} diagonal elements of $\mathbf{D_G}$ and $\mathbf{D_V}$ respectively.

Now, we know that $[(\mathbf{D_G})_{ii} - (\mathbf{D_V})_{ii}]^2 \geq 0$ for all $i \in [1, M]$, with equality if and only if $(\mathbf{D_G})_{ii} = (\mathbf{D_V})_{ii}\ \forall i$, i.e., $\mathbf{G} = \mathbf{V}$. Accordingly,

$$\begin{aligned}
&[(\mathbf{D_G})_{ii} + (\mathbf{D_V})_{ii}]^2 \geq 4(\mathbf{D_G})_{ii}(\mathbf{D_V})_{ii} \\
\Longrightarrow\ &\frac{(\mathbf{D_G})_{ii} + (\mathbf{D_V})_{ii}}{(\mathbf{D_G})_{ii}(\mathbf{D_V})_{ii}} \geq \frac{4}{(\mathbf{D_G})_{ii} + (\mathbf{D_V})_{ii}}
\end{aligned}$$

$$\Longrightarrow \frac{1}{(\mathbf{D_G})_{ii}+(\mathbf{D_V})_{ii}} \leq \frac{1}{4}\left[\frac{1}{(\mathbf{D_G})_{ii}}+\frac{1}{(\mathbf{D_V})_{ii}}\right]. \tag{7.15}$$

Applying this result in Eq. (7.14), we have

$$\begin{aligned}
(\mathbf{G}+\mathbf{V})^{-1} &\leq \mathbf{R}\begin{bmatrix} \frac{1}{4}\left[\frac{1}{(\mathbf{D_G})_{11}}+\frac{1}{(\mathbf{D_V})_{11}}\right] & & \\ & \ddots & \\ & & \frac{1}{4}\left[\frac{1}{(\mathbf{D_G})_{MM}}+\frac{1}{(\mathbf{D_V})_{MM}}\right] \end{bmatrix}\mathbf{R}^{\dagger} \\
&= \frac{1}{4}\mathbf{R}\left\{\begin{bmatrix} \frac{1}{(\mathbf{D_G})_{11}} & & \\ & \ddots & \\ & & \frac{1}{(\mathbf{D_G})_{MM}} \end{bmatrix}+\begin{bmatrix} \frac{1}{(\mathbf{D_V})_{11}} & & \\ & \ddots & \\ & & \frac{1}{(\mathbf{D_V})_{MM}} \end{bmatrix}\right\}\mathbf{R}^{\dagger} \\
&= \frac{1}{4}\mathbf{R}\left(\mathbf{D_G}^{-1}+\mathbf{D_V}^{-1}\right)\mathbf{R}^{\dagger} \\
&= \frac{1}{4}\left(\mathbf{R}\mathbf{D_G}^{-1}\mathbf{R}^{\dagger}+\mathbf{R}\mathbf{D_V}^{-1}\mathbf{R}^{\dagger}\right) \\
&= \frac{1}{4}\left(\mathbf{G}^{-1}+\mathbf{V}^{-1}\right). \qquad (7.16)
\end{aligned}$$

■

Corollary 1 *Let the square Hermitian matrix* $\mathbf{Y}(i)$ *be positive definite, where* $i \in [1,\infty)$ *and* $\mathbf{Y}(i)$ *has same order for all* i*. Then*

$$\left(\sum_{i=1}^{\infty}\mathbf{Y}(i)\right)^{-1} \leq \sum_{i=1}^{\infty}\frac{1}{4^i}\mathbf{Y}^{-1}(i), \tag{7.17}$$

with equality if and only if $\mathbf{Y}(i)=\sum_{k=i+1}^{\infty}\mathbf{Y}(k)\ \forall\, i \geq 1$.

Proof: In Lemma 3, put $\mathbf{G}=\mathbf{Y}(i)$, $\mathbf{V}=\sum_{k=i+1}^{\infty}\mathbf{Y}(k)$, and the result follows. ■

From Eq. (7.11) and Corollary 1, we obtain

$$R_j \leq \frac{1}{9}\log_2\det\left[\mathbf{I}_M+PE_{\mathbf{H}}[\mathbf{H}_j(0)\mathbf{H}_j^{\dagger}(0)]\left(\frac{1}{4\sigma_{\mathbf{z}}^2}\mathbf{I}_M+\frac{1}{P}\sum_{i\geq 1}\frac{1}{4^{i+1}}E_{\mathbf{H}}\left\{[\mathbf{H}_j(i)\mathbf{H}_j^{\dagger}(i)]^{-1}\right\}\right)\right]. \tag{7.18}$$

7.2.1 Data Signal Strength Computation

Because $\mathbf{H}_j(0)$ is a $M \times S_0$ matrix with iid zero mean unit variance entries, then we arrive at

$$E_{\mathbf{H}}[\mathbf{H}_j(0)\mathbf{H}_j^{\dagger}(0)] = \begin{bmatrix} E_h\left[\sum_{s=1}^{S_0-1} h_{1s,j}(0)h_{1s,j}^*(0)\right] & 0 & \cdots & 0 \\ 0 & E_h\left[\sum_{s=1}^{S_0-1} h_{2s,j}(0)h_{2s,j}^*(0)\right] & \cdots & 0 \\ \vdots & \vdots & \ddots & \vdots \\ 0 & 0 & \cdots & E_h\left[\sum_{s=1}^{S_0-1} h_{Ms,j}(0)h_{Ms,j}^*(0)\right] \end{bmatrix}. \tag{7.19}$$

Because the distance between the transmit antenna from any other node and each receiving antenna in node j is assumed to be the same, we have

$$\begin{aligned} E_h\left[\sum_{s=1}^{S_0-1} h_{ms,j}(0)h_{ms,j}^*(0)\right] &= E_{S,\phi,r}\left[\sum_{s=1}^{S_0-1} \frac{\phi_{ms,j}(0)\phi_{ms,j}^*(0)}{(1+r_{s,j}(0))^{2\alpha}}\right] \\ &= E_{S,r}\left[\sum_{s=1}^{S_0-1} \frac{1}{(1+r_{s,j}(0))^{2\alpha}}\right], \end{aligned} \tag{7.20}$$

for $1 \leq m \leq M$.

Therefore, we obtain

$$E_{\mathbf{H}}[\mathbf{H}_j(0)\mathbf{H}_j^{\dagger}(0)] = E_{S,r}\left[\sum_{s=1}^{S_0-1} \frac{1}{(1+r_{s,j}(0))^{2\alpha}}\right]\mathbf{I}_M. \tag{7.21}$$

Lemma 4 *For the uniform mobility model,*

$$E_{S,r}\left[\sum_{s=1}^{S_0-1} \frac{1}{(1+r_{s,j}(0))^{2\alpha}}\right] = \left(\rho\, a_{cell} + e^{-\rho\, a_{cell}} - 1\right) g(a_{cell}, \alpha), \tag{7.22}$$

where $g(a_{cell}, \alpha) = \frac{1}{a_{cell}}\left[\frac{(1+\sqrt{2a_{cell}})^{2\alpha-1} - 1 - \sqrt{2a_{cell}}(2\alpha-1)}{(2\alpha-2)(2\alpha-1)(1+\sqrt{2a_{cell}})^{2\alpha-1}}\right]$.

Proof: Because the steady state node distribution is uniform, the distances between the nodes in cell 0 and node j are iid distributed. Therefore,

$$E_{S,r}\left[\sum_{s=1}^{S_0-1}\frac{1}{(1+r_{s,j}(0))^{2\alpha}}\right]=\sum_{S_0=2}^{\infty}(S_0-1)\mathbb{P}\{S=S_0\}\int_0^{r_m}\frac{f_R(r)dr}{(1+r)^{2\alpha}}, \tag{7.23}$$

where $f_R(r)$ is the probability density function for the distance between a sender node and node j in cell 0, and r_m is their maximum distance. For a uniform node distribution and considering node j located at the center of cell 0 (for a circular cell shape), we have that [36]

$$f_R(r)=\begin{cases}\dfrac{2r}{r_m^2} & \text{if } 0\le r\le r_m\\ 0 & \text{otherwise.}\end{cases} \tag{7.24}$$

This assumption is justified by observing that the cell arrangement in Fig. 7.1 can be moved for the purpose of capacity computation. Besides, the analytical results will be contrasted with Monte-Carlo simulations for the actual ergodic capacity. Noting that the maximum possible distance inside a cell between two nodes is $r_m=\sqrt{2a_{cell}}$, we obtain the following result

$$\begin{aligned}\int_0^{r_m}\frac{2rdr}{r_m^2\,(1+r)^{2\alpha}} &= \frac{1}{a_{cell}}\int_0^{\sqrt{2a_{cell}}}\frac{rdr}{(1+r)^{2\alpha}}\\ &= \frac{1}{a_{cell}}\left[\frac{\left(1+\sqrt{2a_{cell}}\right)^{2\alpha-1}-1-\sqrt{2a_{cell}}\,(2\alpha-1)}{(2\alpha-2)(2\alpha-1)\left(1+\sqrt{2a_{cell}}\right)^{2\alpha-1}}\right].\end{aligned} \tag{7.25}$$

Now, from (3.6), the summation term in (7.23) becomes

$$\begin{aligned}\sum_{S_0=2}^{\infty}(S_0-1)\,\mathbb{P}\{S=S_0\} &= \sum_{S_0=2}^{\infty}(S_0-1)\,\frac{1}{S_0!}\,(\rho\,a_{cell})^{S_0}\,e^{-\rho\,a_{cell}}\\ &= e^{-\rho\,a_{cell}}\sum_{k=1}^{\infty}\frac{k}{(k+1)!}\,(\rho\,a_{cell})^{k+1}\\ &= \rho\,a_{cell}+e^{-\rho\,a_{cell}}-1\,.\end{aligned} \tag{7.26}$$

Combining (7.23), (7.25) and (7.26) it results that

$$E_{S,r}\left[\sum_{s=1}^{S_0-1}\frac{1}{(1+r_{s,j}(0))^{2\alpha}}\right]=\frac{1}{a_{cell}}\left[\frac{\left(1+\sqrt{2a_{cell}}\right)^{2\alpha-1}-1-\sqrt{2a_{cell}}(2\alpha-1)}{(2\alpha-2)(2\alpha-1)\left(1+\sqrt{2a_{cell}}\right)^{2\alpha-1}}\right]\left(\rho\, a_{cell}+e^{-\rho\, a_{cell}}-1\right). \tag{7.27}$$

■

7.2.2 Interference Computation

To simplify the derivations, we assume that the distance between the receiver node j in cell 0 and the interferer in cell i is on average the distance from center to center of these two cells. Accordingly, due to the cell arrangement illustrated in Fig. 7.1, the path loss from each interfering cell using the same frequency band ΔW as j can be written by [2]

$$\begin{aligned}\frac{1}{(1+r_j(i))^{\alpha}} &= \frac{1}{\left(1+\sqrt{(3\sqrt{a_{cell}}\,k_i)^2+(3\sqrt{a_{cell}}\,\ell_i)^2}\right)^{\alpha}}\\ &= \frac{1}{\left(1+3\sqrt{a_{cell}}\sqrt{k_i^2+\ell_i^2}\right)^{\alpha}},\end{aligned} \tag{7.28}$$

where $(3\sqrt{a_{cell}}\,k_i, 3\sqrt{a_{cell}}\,\ell_i)$ are the coordinates of cell i with respect to cell 0 (i.e., cell 0 is taken as the origin for the coordinates), in which $k_i \in \mathbb{Z}$ and $\ell_i \in \mathbb{Z}$, and both k_i and ℓ_i cannot be zero simultaneously. Consequently,

$$\begin{aligned}\mathbf{H}_j(i)\mathbf{H}_j^{\dagger}(i) &= \frac{1}{(1+r_j(i))^{2\alpha}}\mathbf{\Phi}_j(i)\mathbf{\Phi}_j^{\dagger}(i)\\ &= \frac{1}{\left(1+3\sqrt{a_{cell}}\sqrt{k_i^2+\ell_i^2}\right)^{2\alpha}}\mathbf{\Phi}_j(i)\mathbf{\Phi}_j^{\dagger}(i).\end{aligned} \tag{7.29}$$

The following lemma is used to compute interference in Eq. (7.18).

[2] In this case, $r_j(i)$ is the distance between the center of cell i and the center of the cell in which j is currently located (i.e., cell 0).

Lemma 5 *Let* $\mathbf{G}\mathbf{G}^{\dagger} \sim \mathcal{W}_p(\mathbf{\Psi}, q)$. *Then, for* $q - p > 0$

$$E_{\mathbf{G}}[(\mathbf{G}\mathbf{G}^{\dagger})^{-1}] = \frac{1}{q-p}\,\mathbf{\Psi}^{-1}. \tag{7.30}$$

Proof: See [60] and [29] considering the complex Wishart distribution given in Eq. (7.8).

Thus, from Eq. (7.29) and Lemma 5, the term associated with the total interference in Eq. (7.18) is given by

$$\begin{aligned}
\sum_{i\geq 1} \frac{1}{4^{i+1}} E_{\mathbf{H}}\Big\{ [\mathbf{H}_j(i)\mathbf{H}_j^{\dagger}(i)]^{-1} \Big\} &= \sum_{i\geq 1} \frac{1}{4^{i+1}} E_{\mathbf{\Phi}}\left\{ \left[\frac{1}{(1+r_j(i))^{2\alpha}} \mathbf{\Phi}_j(i)\mathbf{\Phi}_j^{\dagger}(i) \right]^{-1} \right\} \\
&= \sum_{i\geq 1} \frac{(1+r_j(i))^{2\alpha}}{4^{i+1}} E_S\left[\frac{1}{S_i - M} \right] \mathbf{\Psi}_j^{-1}(i) \\
&= \underbrace{\frac{(\rho a_{cell})^{M+1}\, {}_2F_2(1,1;2,M+2;\rho a_{cell})}{\Gamma(M+1)\, e^{\rho a_{cell}}}}_{\zeta(a_{cell},\rho,M)} \\
&\qquad \cdot \underbrace{\sum_{k_i\in\mathbb{Z}} \sum_{\ell_i\in\mathbb{Z}} \frac{\left(1+3\sqrt{a_{cell}}\sqrt{k_i^2+\ell_i^2}\right)^{2\alpha}}{4^{i+1}}}_{u(a_{cell},\alpha)} \mathbf{I}_M \\
&= \zeta(a_{cell},\rho,M) u(a_{cell},\alpha),
\end{aligned} \tag{7.31}$$

where we used the fact that $\mathbf{\Psi}_j(i) = \mathbf{I}_M \; \forall (i,j)$, and

$$\begin{aligned}
\zeta(a_{cell},\rho,M) &:= E_S\left[\frac{1}{S_i - M} \right] \\
&= \sum_{S_i=M+1}^{\infty} \frac{1}{S_i - M} \mathbb{P}\{S = S_i\} \\
&= \sum_{S_i=M+1}^{\infty} \frac{1}{S_i - M} \frac{1}{S_i!} (\rho\, a_{cell})^{S_i} e^{-\rho\, a_{cell}} \\
&= \frac{(\rho a_{cell})^{M+1}\, {}_2F_2(1,1;2,M+2;\rho a_{cell})}{\Gamma(M+1)\, e^{\rho a_{cell}}},
\end{aligned} \tag{7.32}$$

in which ${}_2F_2(\cdot,\cdot;\cdot,\cdot;\cdot)$ is the generalized hypergeometric function [33], [19].

For practical computation of the interference, it is important to observe that the function $u(a_{cell},\alpha)$ in Eq. (7.31) converges very fast. As illustrated in Fig. 7.4, $u(a_{cell},\alpha)$ attains convergence for the eight closest interfering cells (i.e., $i = 8$). This result demonstrate that only adjacent interfering cells are dominant, which is commonly considered for MAC protocol design [63]. By inspecting Fig. 7.4, we observe that the four adjacent interfering nodes for cell 5 in the center of Fig. 7.1 are located in symmetry, i.e., same distance. Therefore, the channel matrix associated to these interfering cells are equivalent on the average, for a uniform distribution of the nodes. We also show this by comparing our analytical results with Monte-Carlo simulation of (7.9) to demonstrate the tightness of capacity upper-bound.

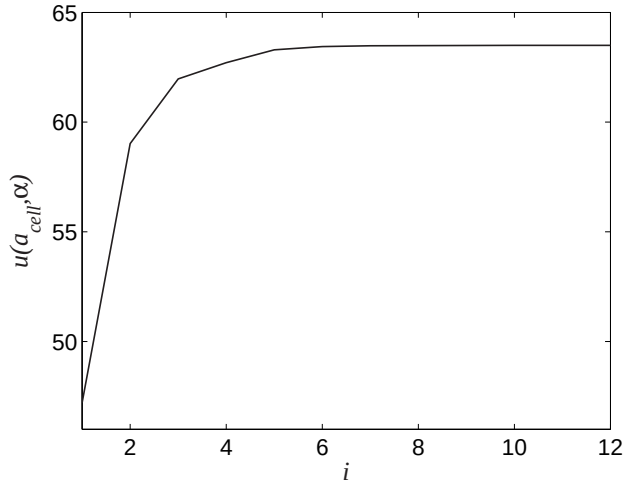

Figure 7.4: Convergence of $u(a_{cell},\alpha)$ as a function of cell i, for $a_{cell} = 2\,m^2$ and $\alpha = 2$.

7.2.3 Capacity

The ergodic capacity of a node j follows from Eqs. (7.18) and (7.21), Lemma 4, and Eq. (7.31). Hence,

$$R_j \leq \frac{1}{9}\log_2 \det\left\{\left[1+P\left(\rho\, a_{cell}+e^{-\rho\, a_{cell}}-1\right) g(a_{cell},\alpha)\left(\tfrac{1}{4\sigma_{\mathbf{z}}^2}+\tfrac{\zeta(a_{cell},\rho,M)u(a_{cell},\alpha)}{P}\right)\right]\mathbf{I}_M\right\}$$
$$= \frac{M}{9}\log\left[1+P\left(\rho\, a_{cell}+e^{-\rho\, a_{cell}}-1\right) g(a_{cell},\alpha)\left(\tfrac{1}{4\sigma_{\mathbf{z}}^2}+\tfrac{\zeta(a_{cell},\rho,M)u(a_{cell},\alpha)}{P}\right)\right]. \tag{7.33}$$

For the case of no interference, the upper-bound capacity is obtained from Eqs. (7.11) and (7.33) where the term associated with interference is ignored. Accordingly, we have

$$R_j \leq \frac{M}{9}\log_2\left[1+\tfrac{P}{\sigma_{\mathbf{z}}^2}\left(\rho\, a_{cell}+e^{-\rho\, a_{cell}}-1\right) g(a_{cell},\alpha)\right]. \tag{7.34}$$

On the other hand, if interference is strong, the term associated with noise is neglected. Consequently, we obtain

$$R_j \leq \frac{M}{9}\log_2\left[1+4\left(\rho\, a_{cell}+e^{-\rho\, a_{cell}}-1\right) g(a_{cell},\alpha)\zeta(a_{cell},\rho,M)u(a_{cell},\alpha)\right]. \tag{7.35}$$

Therefore, from Eqs. (7.33), (7.34) and (7.35), the node capacity grows with the number of receiving antennas M. Furthermore, because the terms in these equations do not depend on n, the node capacity does not decrease with n, which contrasts with the decreasing node capacity obtained in [13]. Note that our channel matrix $\mathbf{H}_j(i)$ incorporates the decay with distance, i.e., $\frac{1}{(1+r_j(i))^{\alpha}}$, which is the large scale representation of the channel.

This result shows that the ergodic upper-bound capacity for a node increases with power P, as in Eqs. (7.33) and (7.34), up to a point where it remains constant and there can

be no gain in capacity, as in Eq. (7.35), by increasing P.

Moreover, for the intermediate case, from Eq. (7.33), the capacity upper-bound increase with power P is the direct result of using cooperation among nodes and reducing destructive effect of interference in the network. Besides, our approach utilizes the strong interference that exists inside a cell.

7.3 Numerical and Simulation Results

The numerical and simulation results presented here were obtained considering that the maximum number of nodes allowed to communicate in a cell is $\mathcal{A}$ (as said in Section 7.1.1).

Fig. 7.5 shows the resultant node capacity upper-bound indicated by the solid line as a function of the transmit power P, obtained by considering the lower-part curve from the intersection of the three curves given by (7.33), (7.34) and (7.35). We observe that the ergodic capacity increases with the increase of the power up to a point where interference is dominant such that no increase in capacity is possible by increasing P. In this figure, we also demonstrate the Monte-Carlo simulation of (7.9) by averaging over 5000 random network topologies. Unlike our analytical model that interfering nodes are assumed to be located in the center of each interfering cell, the nodes are distributed randomly and uniformly in the simulation area. The result clearly shows that our upper-bound is close to the simulation. The intuition behind it is based on the fact that it is commonly known that the major portion of interference is caused by two adjacent hops in wireless ad hoc networks [63]. However, in our approach, the adjacent hops are utilizing different frequencies for communication. Our

proposed cooperation allows nodes inside a cell to cooperate and no longer compete, by employing a distributed MIMO concept. Also, note that the first interfering cells are in the same symmetric distance for any given cell. Therefore, the Wishart matrices for these channels, on average, are equivalent which makes Lemma 3 a reasonable approach for computation of the capacity.

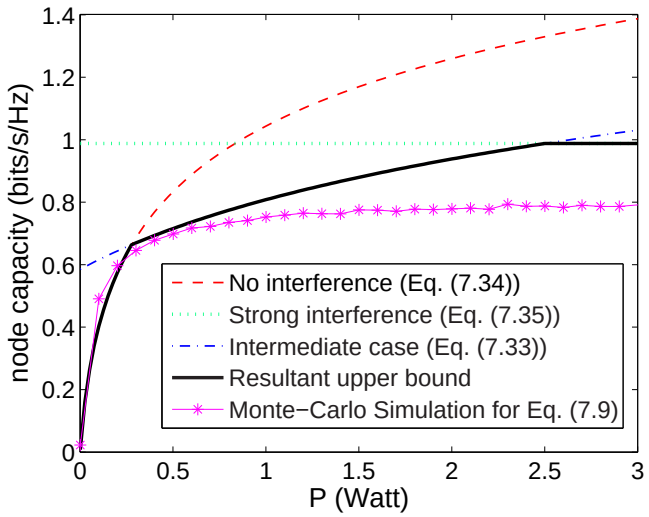

Figure 7.5: Ergodic node capacity as function of power (P) for $M = 2$, $a_{cell} = 2m^2$, $\rho = 3\,nodes/m^2$, $\sigma_{\mathbf{z}}^2 = 0.01$, $\alpha = 2$, and $\mathcal{A} = 4$.

7.4 Conclusions

In this chapter, we have shown that the ergodic capacity of MIMO mobile ad hoc network can be upper-bounded. This upper-bound does not decrease with the increase in the number of nodes in the network. Another important aspect of these results is the use of the new communication scheme (called opportunistic cooperation) that allows multiple nodes in a cell to communicate concurrently with other nodes in the same cell. This approach inhibits

the destructive effects of interference. As shown, the capacity of each node increases when the transmit power P of every node increases up to a point where interference becomes dominant and then no more increase in capacity is possible. Perhaps, the most significant result of this chapter is the demonstration that with cooperation among nodes, the capacity of the ad hoc networks increases by increasing the transmit power of the nodes for some practical values of P.

Chapter 8

Conclusion and Future Work

8.1 Conclusion

In this thesis, we have studied the performance of wireless ad hoc networks in the context of mobility, capacity, and delay. We summarized the work related to our research and by utilizing Information Theory concepts we proposed new designs and analyses for wireless networks improving their overall behavior.

We first proposed a multi-copy forwarding scheme of packets, such that the delivery delay is substantially reduced without changing the order of the capacity of the network. Using the results of random occupancy, we provided a mathematical formula for computation of the node throughput as a function of the network parameters. The delay analysis was corroborated by simulation results showing the exponential delay reduction obtained. We also showed that interference can be overcome if transmission is restricted among close neighbors, where an analytical method for computation of the interference was presented.

Then we presented a study on mobility-capacity-delay trade-off for wireless ad hoc networks. By restricting the movements of the nodes inside a cell, we showed that mobility is an entity that can be exchanged with capacity and delay. We employed two different schemes for such analysis. In the first case, the area of the cells in the network is a function of the total number of nodes n. We found that a throughput gain of $\Theta(\log(n))$ is obtained, compared to the case of Gupta and Kumar [28], where a penalty in delay is the cost for such an improvement. In the second case, we assumed the area of the cells to be independent of n. We showed that a constant asymptotic throughput is obtained and that our results are a generalizations of the results by Grossglauser and Tse [26]. In addition, we observed that by changing the physical layer properties of the wireless network (e.g., using directional antennas) the throughput or delay performance can be improved and the result obtained agrees with previous work which employs network flow analysis.

Another important contribution of our work is to present a new communication technique for MANETs, called opportunistic cooperation. In this novel approach, we propose a simultaneous many-to-many framework for node communication, where nodes collaborate with each other in order to relay and deliver packets. Because multiple concurrent transmissions are allowed, multi-copies of the same packet can be relayed which reduces the delivery delay in ad hoc networks. We introduced a channel access scheme for neighbors discovery and provided a protocol for distribution of codes and frequency such that reuse of code and frequency is possible. We provided two examples of how opportunistic cooperation can be implemented. The former case uses FDMA combined with CDMA in which nodes performs multiuser detection with successive interference cancellation. We obtained the link's Shannon

capacity, the per source-destination throughput and delay, and compared the increased performance obtained with previous schemes. The later case employs FDMA with MIMO where we assume that nodes are endowed with multiple antennas for communication. We computed an upper bound for the ergodic capacity and showed that it is possible to have increase in capacity for practical increasing values of transmit power.

8.2 Future Work

The simulation results presented in Chapter 3 suggests that by having a mobility model in which nodes tend to be clustered, like in the random waypoint model, it helps to reduce delivery delay in mobile ad hoc networks. Therefore, a interesting line of investigation would consider other models for node mobility where nodes tend to move forming clusters and try to analyze which model would provide the lower average delivery delay. Following this direction, the use of controlled mobility can also result in further delay reduction if some information regarding node location can be propagated in the network which helps to guide a relay node in the path to the destination, for example. In addition, it would be very useful to try to directly relate the analogous random loading balancing results [4], [38] with the delay reduction observed for the multi-copy relaying. Furthermore, the search for the exact solution for the delay behavior in the multi-copy forwarding strategy is very important. However, the approximation presented in Chapter 3, i.e., Eqs. (3.29)-(3.40), provided practical information because simulation of MANETs have shown that these approximations are close to simulation results.

For the mobility-capacity-delay trade-off, one can try to modify Scheme 1 to be

further improved and obtain a better gain in capacity. In this case, the communication regions may be changed and the delay analysis must be recomputed. On the other hand, the idea of multiple concurrent transmissions can be carried out for the case of directional antennas if a node can be assumed to have multiple directional antennas positioned to distinct neighbors simultaneously. Therefore, capacity may be further increased for this case.

In the context of opportunistic cooperation implemented with FDMA/CDMA, power control can be considered since it can result in further interference reduction. The strategies used to obtain the throughput lower-bound in Theorem 5 and in [51] assume that each node transmits at constant power and its packets follow the minimum distance path to the destination. However, it was also shown by Negi and Rajeswaran [51] that, if transmission power control is allowed, then a minimum power route to destination can be obtained (not necessarily equal to the minimum distance path) which provides an upper-bound for the throughput. Hence, it is interesting to allow power control in such analysis and investigate the associated behavior of the throughput and bandwidth expansion considering CDMA and SIC.

For the FDMA/MIMO implementation, the lower-bound capacity is also of high significance, because together with the upper-bound capacity obtained in Chapter 7, it will provide the gap between these both bounds. This gap will establish an important performance limit range for MIMO mobile ad hoc networks. Moreover, one can explore the inherent diversity of MIMO systems and try to apply space-time codes with opportunistic cooperation and study the associated performance. Another direction of analysis can assume that each node also uses multiple antennas for transmission, instead of just one antenna. This approach tends to add more complexity in the system; however, it may present better performance.

Besides, other multiuser detection schemes can also be considered for opportunistic cooperation. For example, the orthogonal frequency division multiplex (OFDM) technique is a natural candidate for such implementation, and its analysis for capacity bounds is also of interest.

Bibliography

[1] *RFR3300 RF-to-IF Receiver*, QUALCOMM Inc., August 2004.

[2] A. Agarwal and P. R. Kumar, "Capacity bounds for ad hoc and hybrid wireless networks," *ACM SIGCOMM Computer Communications Review*, vol. 34, no. 3, pp. 71–81, July 2004.

[3] J. G. Andrews, "Interference cancellation for cellular systems: A contemporary overview," *IEEE Wireless Communications Magazine*, pp. 19–29, April 2005.

[4] Y. Azar, A. Z. Broder, A. R. Karlin, and E. Upfal, "Balanced allocations," in *Proc. of ACM STOC*, Montreal, Canada, May 1994.

[5] N. Bansal and Z. Liu, "Capacity, delay and mobility in wireless ad-hoc networks," in *Proc. of IEEE Infocom*, San Francisco, California, March 2003.

[6] L. Bao and J. J. Garcia-Luna-Aceves, "Transmission scheduling in ad hoc networks with directional antennas," in *Proc. of ACM Mobicom*, Atlanta, Georgia, September 2002.

[7] L. Bao and J. J. Garcia-Luna-Aceves, "Hybrid channel access scheduling in ad hoc networks," in *Proc. of IEEE ICNP*, Paris, France, November 2002.

[8] P. D. L. Beasley, A. G. Stove, B. J. Reits, and B.-O. As, "Solving the problems of a single antenna frequency modulated cw radar," *Record of the IEEE 1990 International Radar Conference*, pp. 391–395, May 1990.

[9] C. Bettstetter, H. Hartenstein, and X. Pérez-Costa, "Stochastic properties of the random waypoint mobility model: epoch length, direction distribution, and cell change rate," in *Proc. of ACM MSWiM*, Atlanta, Georgia, September 2002.

[10] R. Blum, "MIMO capacity with interference," *IEEE Journal on Selected Areas in Communications*, vol. 21, no. 5, pp. 793–801, June 2003.

[11] A. R. Calderbank, G. Pottie, and N. Seshadri, "Cochannel interference suppression

through time/space diversity," *IEEE Transactions on Information Theory*, vol. 46, no. 3, pp. 922–932, May 2000.

[12] T. Camp, J. Boleng, and V. Davies, "A survey of mobility models for ad hoc network research," *Wireless Communication & Mobile Computing (WCMC): Special issue on Mobile Ad Hoc Networking: Research, Trends and Applications*, vol. 2, no. 5, pp. 483–502, 2002.

[13] B. Chen and M. J. Gans, "Limiting throughput of MIMO ad hoc networks," in *Proc. of IEEE International Conference on Acoustics, Speech, and Signal Processing*, Philadelphia, PA, March 2005.

[14] R. R. Choudhuri, X. Yang, R. Ramanathan, and N. H. Vaidya, "Using directional antennas for medium access control in ad hoc networks," in *Proc. of ACM Mobicom*, Atlanta, Georgia, September 2002.

[15] T. M. Cover and J. A. Thomas, *Elements of Information Theory*. John Wiley & Sons, 1991.

[16] S. N. Diggavi, M. Grossgaluser, and D. Tse, "Even one-dimensional mobility increases ad hoc wireless capacity," in *Proc. of IEEE ISIT*, Laussane, Switzerland, June 2002.

[17] O. Dousse, P. Thiran, and M. Hasler, "Connectivity in ad-hoc and hybrid networks," in *Proc. of IEEE Infocom*, New York, New York, June 2002.

[18] T. Eng and L. B. Milstein, "Capacities of hybrid FDMA/CDMA systems in multipath fading," in *Proc. of IEEE MILCOM*, Boston, Massachusetts, October 1993.

[19] H. Exton, *Handbook of Hypergeometric Integrals: Theory, Applications, Tables, Computer Programs*. Chichester, England: Ellis Horwood, 1978.

[20] G. J. Foschini, "Layered space-time architecture for wireless communication in a fading environment when using multi-element antennas," *Bell Labs Technical Journal*, vol. 2, no. 2, pp. 41–59, Autumn 1996.

[21] G. J. Foschini and M. J. Gans, "On limits of wireless communications in a fading environment when using multiple antennas," *Wireless Personal Communications, Kluwer Academic Press*, no. 6, pp. 311–355, 1998.

[22] M. Franceschetti, O. Dousse, D. Tse, and P. Tiran, "Closing the gap in the capacity of random wireless networks," in *Proc. of IEEE ISIT*, Chicago, Illinois, June 2004.

[23] A. E. Gamal, J. Mammen, B. Prabhakar, and D. Shah, "Throughput-delay trade-off in wireless networks," in *Proc. of IEEE Infocom*, Hong Kong, March 2004.

[24] S. Ghez, S. Verdu, and S. Schwartz, "Optimal decentralized control in the random access multipacket channel," *IEEE Transactions on Automatic Control*, vol. 34, no. 11, pp. 1153–1163, November 1989.

[25] A. J. Goldsmith, S. A. Jafar, N. Jindal, and S. Vishwanath, "Capacity limits of mimo channels," *IEEE Journal on Selected Areas in Communications*, vol. 21, no. 5, pp. 684–702, June 2003.

[26] M. Grossglauser and D. Tse, "Mobility increases the capacity of wireless ad-hoc networks," in *Proc. of IEEE Infocom*, Anchorage, Alaska, March 2001.

[27] M. Grossglauser and D. Tse, "Mobility increases the capacity of wireless ad hoc networks," *IEEE/ACM Transactions on Networking*, vol. 10, no. 4, pp. 477–486, August 2002.

[28] P. Gupta and P. R. Kumar, "The capacity of wireless networks," *IEEE Transactions on Information Theory*, vol. 46, no. 2, pp. 388–404, March 2000.

[29] L. R. Haff, "An identity for the wishart distribution with applications," *Journal of Multivariate Analysis*, vol. 9, pp. 531–544, 1979.

[30] B. Hajek, A. Krishna, and R. O. LaMaire, "On the capture probability for a large number of stations," *IEEE Transactions on Communications*, vol. 45, no. 2, pp. 254–260, February 1997.

[31] L. Hanzo, L.-L. Yang, E.-L. Kuan, and K. Yen, *Single- and Multi-Carrier DS-CDMA Multi-User Detection, Space-Time Spreading, Synchronisation, Networking and Standards*. John Wiley & Sons, 2003.

[32] A. Hasan, K. Yang, and J. G. Andrews, "High-capacity CDMA ad hoc networks without closed-loop power control," in *Proc. of IEEE MILCOM*, Boston, Massachusetts, October 2003.

[33] A. T. James, "Distributions of matrix variates and latent roots derived from normal samples," *Annals of Mathematical Statistics*, vol. 35, no. 2, pp. 475–501, June 1964.

[34] A. Jovičić, P. Viswanath, and S. R. Kulkarni, "Upper bounds to transport capacity of wireless networks," *IEEE Transactions on Information Theory*, vol. 50, no. 11, pp. 2555–2565, November 2004.

[35] R. Knopp and P. A. Humblet, "Information capacity and power control in single-cell multiuser communications," in *Proc. of IEEE ICC*, Seattle, Washington, June 1995.

[36] C. T. Lau and C. Leung, "Capture models for mobile packet radio networks," *IEEE Transactions on Communications*, vol. 40, no. 5, pp. 917–925, May 1992.

[37] B. Liu, Z. Liu, and D. Towsley, "On the capacity of hybrid wireless networks," in *Proc. of IEEE Infocom*, San Francisco, California, March 2003.

[38] M. Mitzenmacher, "The power of two choices in randomized load balancing," *IEEE Transactions on Parallel and Distributed Systems*, vol. 12, no. 10, pp. 1094–1104, October 2001.

[39] R. M. de Moraes, H. R. Sadjadpour, and J. J. Garcia-Luna-Aceves, "Throughput-delay analysis of mobile ad-hoc networks with a multi-copy relaying strategy," in *Proc. of IEEE SECON*, Santa Clara, California, October 2004.

[40] R. M. de Moraes, H. R. Sadjadpour, and J. J. Garcia-Luna-Aceves, "On mobility-capacity-delay trade-off in wireless ad hoc networks," in *Proc. of IEEE/ACM MASCOTS*, Volendam, The Netherlands, October 2004.

[41] R. M. de Moraes, H. R. Sadjadpour, and J. J. Garcia-Luna-Aceves, "Making ad hoc networks scale using mobility and multi-Copy forwarding," in *Proc. of IEEE Globecom*, Dallas, Texas, November 2004.

[42] R. M. de Moraes, H. R. Sadjadpour, and J. J. Garcia-Luna-Aceves, "A study on mobility-capacity-delay trade-off in wireless ad hoc networks," in *Proc. of IEEE Globecom Wireless Ad Hoc and Sensor Networks Workshop*, Dallas, Texas, November 2004.

[43] R. M. de Moraes, H. R. Sadjadpour, and J. J. Garcia-Luna-Aceves, "Reducing delay while maintaining capacity in mobile ad-hoc networks using multiple random routes," in *Proc. of Asilomar Conference on Signals, Systems, and Computers*, Pacific Grove, California, November 2004.

[44] R. M. de Moraes, H. R. Sadjadpour, and J. J. Garcia-Luna-Aceves, "Mobility-capacity-delay trade-off in wireless ad hoc networks," *Accepted for Elsevier Ad Hoc Networks Journal*, 2005.

[45] R. M. de Moraes, H. R. Sadjadpour, and J. J. Garcia-Luna-Aceves, "A new communication scheme for MANETs," in *Proc. of IEEE WirelessCom (Symposium on Information Theory)*, Maui, Hawaii, June 2005.

[46] R. M. de Moraes, H. R. Sadjadpour, and J. J. Garcia-Luna-Aceves, "Opportunistic cooperations: a new communication approach for MANETs," in *Proc. of Asilomar Conference on Signals, Systems, and Computers*, Pacific Grove, California, November 2005.

[47] R. Motwani and P. Raghavan, *Randomized Algorithms*. Cambridge Univ. Press, 1995.

[48] A. Muqattash and M. Krunz, "CDMA-based MAC protocol for wireless ad hoc networks," in *Proc. of ACM MobiHoc*, Annapolis, Maryland, June 2003.

[49] D. Nain, N. Petigara, and H. Balakrishnan, "Integrated routing and storage for messaging applications in mobile ad hoc networks," in *Proc. of WiOpt*, Antipolis, France, March 2003.

[50] M. J. Neely and E. Modiano, "Improving delay in ad-hoc mobile networks via redundant packet transfers," in *Proc. of Conference on Information Sciences and Systems*, Baltimore, Maryland, March 2003.

[51] R. Negi and A. Rajeswaran, "Capacity of power constrained ad-hoc networks," in *Proc. of IEEE Infocom*, Hong Kong, March 2004.

[52] A. V. Oppenheim, A. S. Willsky, and S. H. Nawab, *Signals and Systems*. Prentice-Hall, 1996.

[53] B. W. Parkingson and J. J. Spilker, *Global Positioning System: Theory and Applications Vol. I*. American Institute of Aeronautics and Astronautics, Inc., 1996.

[54] P. Patel and J. Holtzman, "Analysis of a simple successive interference cancellation scheme in a DS/CDMA system," *IEEE Journal on Selected Areas in Communications*, vol. 12, no. 5, pp. 796–807, June 1994.

[55] C. Peraki and S. D. Servetto, "On the maximum stable throughput problem in random networks with directional antennas," in *Proc. of ACM MobiHoc*, Annapolis, Maryland, June 2003.

[56] E. Perevalov and R. Blum, "Delay limited capacity of ad hoc networks: asymptotically optimal transmission and relaying strategy," in *Proc. of IEEE Infocom*, San Francisco, California, March 2003.

[57] E. Perevalov and R. Blum, "Delay-limited throughput of ad hoc networks," *IEEE Transactions on Communications*, vol. 52, no. 11, pp. 1957–1968, November 2004.

[58] T. S. Rappaport, *Wireless Communications: Principles and Practice*. Prentice Hall, 2002.

[59] V. Rodoplu and T. H. Meng, "Position based CDMA with multiuser detection (P-CDMA/MUD) for wireless ad hoc networks," in *Proc. of IEEE Int. Symp. on Spread-Spectrum Tech. & Appli.*, New Jersey, September 2000.

[60] D. V. Rosen, "Moments for the inverted wishart distribution," *Scandinavian Journal of Statistics*, vol. 15, pp. 97–109, 1988.

[61] T. J. Shepard, "A channel access scheme for large dense packet radio networks," in *Proc. of ACM SigComm*, San Francisco, California, August 1996.

[62] E. Telatar, "Capacity of multi-antenna gaussian channels," *European Transactions on Telecommunications*, vol. 10, no. 6, pp. 585–595, November 1999.

[63] F. Tobagi and L. Kleinrock, “Packet switching in radio channels: Part II - the hidden terminal problem in carrier sense multiple-access and the busy-tone solution,” *IEEE Transactions on Communications*, Vol. COM-23, No. 12, pp. 1417-1433, December 1975.

[64] L. Tong, Q. Zhao, and G. Mergen, “Multipacket reception in random access wireless networks: From signal processing to optimal medium access control,” *IEEE Communications Magazine*, pp. 108–112, November 2001.

[65] S. Toumpis and A. J. Goldsmith, “Capacity regions for wireless ad hoc networks,” *IEEE Transactions on Wireless Communications*, vol. 2, no. 4, pp. 736–748, July 2003.

[66] S. Toumpis and A. J. Goldsmith, “Large wireless networks under fading, mobility, and delay constraints,” in *Proc. of IEEE Infocom*, Hong Kong, March 2004.

[67] C. de Waal and M. Gerharz, “Bonnmotion: A mobility scenario generation and analysis tool,” http://www.cs.uni-bonn.de/IV/BonnMotion/, 2003.

[68] L. Xie and P. R. Kumar, “A network information theory for wireless communications: Scaling laws and optimal operation,” *IEEE Transactions on Information Theory*, vol. 50, no. 5, pp. 748–767, May 2004.

[69] K. Yamazaki, S. Aly, and D. Falconer, “Convergence behaviour of a jointly adaptive transversal and memory-based echo canceller,” *IEE Proceedings F Radar and Signal Processing*, vol. 138, no. 4, pp. 361–370, August 1991.

[70] S. Yi, Y. Pei, and S. Kalyanaraman, “On the capacity improvement of ad hoc wireless networks using directional antennas,” in *Proc. of ACM MobiHoc*, Annapolis, Maryland, June 2003.

[71] X. Yu, R. M. de Moraes, H. R. Sadjadpour, and J. J. Garcia-Luna-Aceves, “Capacity of MIMO mobile wireless ad hoc networks,” in *Proc. of IEEE WirelessCom (Symposium on Information Theory)*, Maui, Hawaii, June 2005.

[72] W. Yuen, R. Yates, and S.-C. Mau, “Exploiting data diversity and multiuser diversity in noncoperative mobile infostation networks,” in *Proc. of IEEE Infocom*, San Francisco, California, March 2003.

[73] F. Zhang, *Matrix Theory*. Springer-Verlag, 1999.